Journal
of
The Franklin Institute

EDITOR, HENRY BUTLER ALLEN, MET.E., D.SC.
ASSISTANT EDITOR, JOHN FRAZER, PH.D.

Associate Editors:

WILDER D. BANCROFT, PH.D. — C. B. BAZZONI, PH.D. — ARTHUR L. DAY, SC.D. — R. EKSERGIAN, PH.D. — A. S. EVE, F.R.S. — PAUL D. FOOTE, PH.D. — W. J. HUMPHREYS, PH.D. — C. E. K. MEES, D.SC. — WILLIAM B. MELDRUM, PH.D. — HENRY C. SHERMAN, SC.D. — W. F. G. SWANN, D.SC. — HUGH S. TAYLOR, D.SC. — A. F. ZAHM, PH.D. — JOHN ZELENY, PH.D.

Committee on Publications:

G. H. CLAMER, CHAIRMAN — RICHARD HOWSON — C. L. JORDAN — LIONEL F. LEVY — MALCOLM LLOYD, JR. — HIRAM S. LUKENS — RICHARD H. OPPERMANN — WINTHROP R. WRIGHT

Vol. 244 — **NOVEMBER, 1947** — **No. 5**

CONTENTS

Some Notes on the Design of Magnetic Amplifiers ..... ALAN S. FITZGERALD 323

Erosion in Vent Plugs, the Effect of Vent Diameter, Part II ..... JAMES H. WIEGAND 363

The Dynamics of Nuclear Reactions ..... C. E. MANDEVILLE 385

Notes from the National Bureau of Standards 401

The Franklin Institute Notes 407

Notes from the Biochemical Research Foundation 410

Monochromatic Light Absorption by Chicken Erythrocytes—A Correction. J. O. ELY AND M. H. ROSS

Book Reviews 411

Publications Received 413

Current Topics 400, 406

Published by
THE FRANKLIN INSTITUTE OF THE STATE OF PENNSYLVANIA
Prince and Lemon Streets, Lancaster, Penna.; and
Benjamin Franklin Parkway at Twentieth St., Philadelphia 3, Penna.

SIX DOLLARS PER YEAR (Foreign Postage Additional) **SINGLE NUMBERS, SIXTY CENTS**

Indexes to the semi-annual volumes of the JOURNAL are published with the June and December numbers

Journal
of
The Franklin Institute
Devoted to Science and the Mechanic Arts

Vol. 244 NOVEMBER, 1947 No. 5

SOME NOTES ON THE DESIGN OF MAGNETIC AMPLIFIERS.

BY

ALAN S. FITZGERALD.

GENERAL.

In a previous paper [1] the circuit arrangements and connections for combining a number of saturating reactors to form a multi-stage amplifier were discussed. The present paper will deal briefly with some of the factors to be taken into consideration in designing such amplifiers, as, for example: the magnetic design of the individual saturating reactors so that each stage is properly related to the other stages; and the procedure for determining the proper coil windings.

However, before going into these aspects of the problem it is necessary to consider some first principles in respect of the performance of the saturating reactor. In the case of such apparatus as generators, motors, transformers, etc., the technique and procedure, given the structural dimensions and characteristics of the materials used, for calculating output, efficiency, regulation and the like, are well established.

Although, as shown by the references in the previous paper, the saturating reactor is by no means a recent development, there seems to be no generally understood or acknowledged procedure for computing the performance of a saturating reactor when used as an amplifier. Accordingly, it may be desirable first to consider this aspect of the design of magnetic amplifiers.

This subject will be discussed for the most part, in relation to amplifiers of the neutral type, primarily because these arrangements are the simplest. However, many of the principles formulated are equally pertinent to the design of amplifiers of other types.

[1] Alan S. FitzGerald, J. FRANKLIN INST., 244, 249 (1947).

(Note—The Franklin Institute is not responsible for the statements and opinions advanced by contributors in the JOURNAL.)

OUTPUT OF A SATURATING REACTOR.

In developing magnetic amplifiers it is necessary to study quantitatively the performance of a single saturating reactor which may constitute a stage in such an amplifier.

We must know, specifically, the magnitudes of the input and output power, the ratio of which we will call the "Gain."

The input may readily be computed; if the input winding has a resistance of r ohms, and receives a current of i amperes, then the input is i^2r.

The measurement of the output is more involved. Each stage in a magnetic amplifier, as, for example, the type shown in Fig. 1, delivers

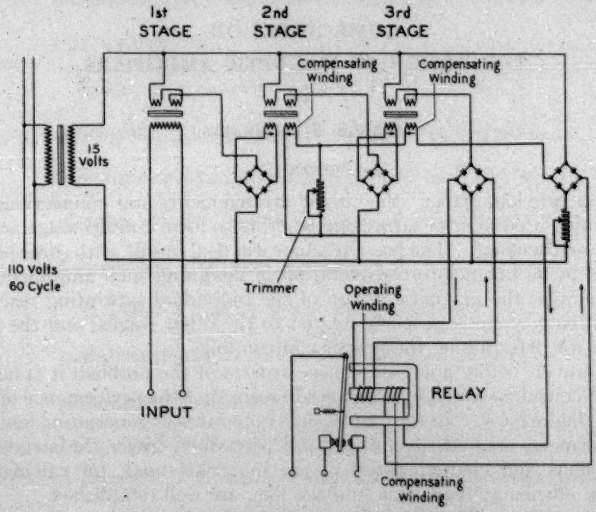

FIG. 1. Three-stage neutral type magnetic amplifier.

a rectified output current which has a definite magnitude, which we will call I_o, when there is no input, and which increases to the value I_s when the current i flows in the saturating winding.

These currents, I_o and I_s, flow in an output circuit, which, in a magnetic amplifier, may be the input winding of the next stage, or the winding of a relay or other control device.

In the practical use of the saturating reactor circuit as an amplifier it is normally only the difference current $(I_s - I_o)$ which is effective in producing useful output since the effect of the current I_o is suppressed or compensated for in one way or another so as to bring this condition about.

Thus the result of the increased current I_s, flowing in a circuit which embodies such a compensating feature, is the same as that which would be due to a current of the value $(I_s - I_o)$ in a simple circuit having no such compensating arrangement.

It follows, therefore, that if the output circuit has a resistance R the effective output power is:

$$(I_s - I_o)^2 R.$$

In the type of magnetic amplifier which we will consider principally in this paper, all of the stages, other than the first, have a compensating winding for annulling the effect of I_o, so that the net excitation applied to the next stage is due to the *excess* of I_s over I_o.

The power expended in the compensating winding is derived directly from the source from which the amplifier is supplied; it is not interstage power and it is not therefore to be taken into account in computing output or gain.

If the input winding of the second stage has N turns, the excitation applied to the second stage, when there is no input to the first stage, will be NI_o ampere-turns. The current in the compensating winding will be adjusted so as to produce likewise NI_o ampere-turns opposing the excitation in the input winding. The net excitation, therefore, to the second stage, under this condition, will be zero.

If, now, an input be received by the first stage, the output current of the first stage will increase from I_o to I_s and the second stage will be saturated to an extent which is due to a DC excitation of $N(I_s - I_o)$ ampere-turns only.

Now, suppose the first stage be taken away entirely and that at the same time the compensating winding of the second stage be eliminated, the second stage being now treated as an initial stage. Clearly, if the saturating effect applied to this stage is to remain exactly as it was, that is, if it is still to be $N(I_s - I_o)$ ampere-turns, there must flow in the input winding a current of value $(I_s - I_o)$.

If it should now be desired to compute the gain developed in the originally designated *second* stage, the quotient in this calculation, is the input to this stage. Obviously, the input power delivered thereto, when the stage receives a DC excitation of $N(I_s - I_o)$ ampere-turns, and when this effect is produced by the presence of a single current, in a single winding, of value $(I_s - I_o)$, is $(I_s - I_o)^2 R$.

The gain of this stage may be calculated upon this basis.

It is equally clear that if, instead, this excitation, of $N(I_s - I_o)$ ampere-turns, be produced by the excess of I_s over I_o, the effect of I_o being nullified by the compensating winding, it does not affect the gain of the second stage.

Thus the effective input to the second stage is $(I_s - I_o)^2 R$, and this is likewise the correct way of expressing the output of the first stage.

EFFECT OF OPERATING CONDITIONS UPON GAIN.

The output and gain characteristics of a single stage in a magnetic amplifier are, basically, functions of the incremental permeability curve[2] of the core material. Gain and output curves may be determined experimentally with a circuit arrangement such as that illustrated in Fig. 7 of the author's previous paper, to be found on page 257 of the JOURNAL, in which provision is made for varying the AC supply voltage as well as the resistance of the load or output circuit.

The impedance of the AC winding of the saturating reactor will be almost entirely reactive, and will be a function of the permeability of

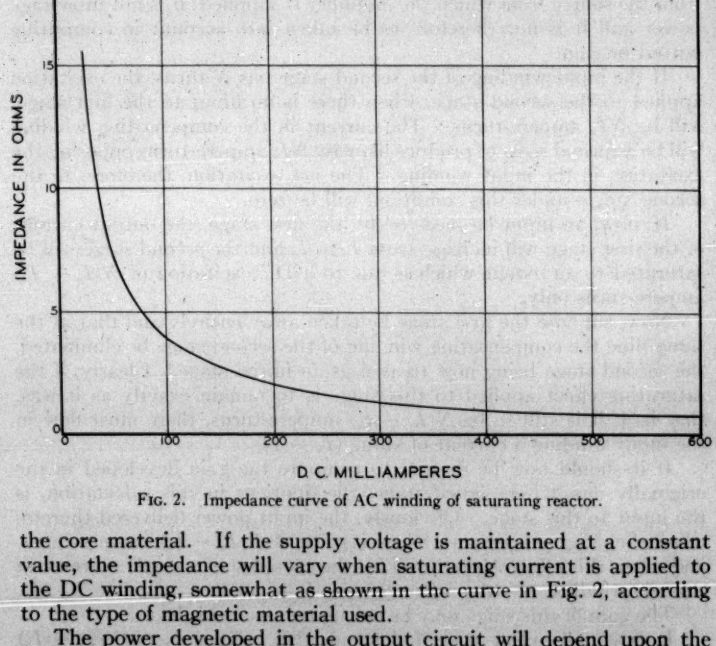

FIG. 2. Impedance curve of AC winding of saturating reactor.

the core material. If the supply voltage is maintained at a constant value, the impedance will vary when saturating current is applied to the DC winding, somewhat as shown in the curve in Fig. 2, according to the type of magnetic material used.

The power developed in the output circuit will depend upon the relation between the resistance of the output circuit and the impedance of the AC winding. For relatively high values of DC excitation, such that I_s is very much greater than I_o, maximum power will be developed when matched impedance conditions obtain; that is, if the output re-

[2] *Magnetic Core Materials Practice*, Allegheny Steel Company.

sistance, in ohms, is equal to the impedance of the AC winding. However, in practice, a more complex relation exists, and it is necessary to take into account both I_s and I_o.

Fig. 3 shows, in a typical saturating reactor, how the effective output power, computed as above, that is to say, $(I_s - I_o)^2R$, varies with the circuit resistance, for various values of input current.

Likewise, there is an optimum value of AC voltage, E, at which, with given input, and given resistance, the difference between I_s and I_o is a maximum.

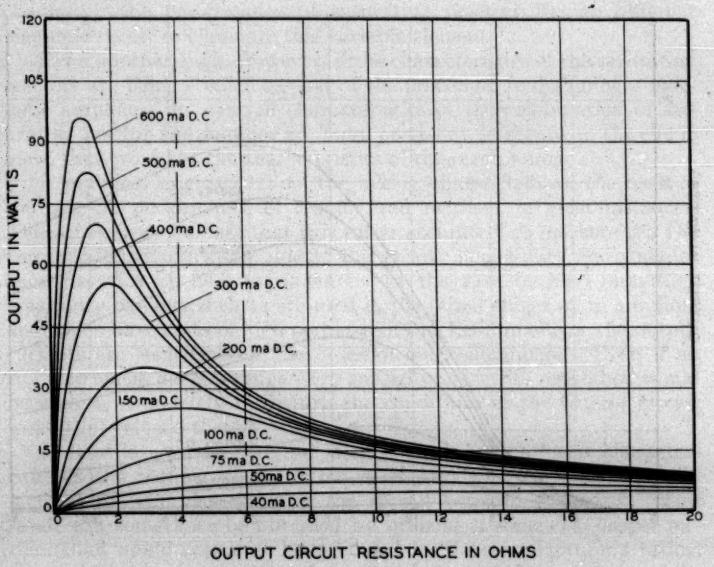

FIG. 3. Relation between output power and output circuit resistance.

Fig. 4 shows how the effective output varies with the supply voltage, for various values of DC input. In these curves the circuit resistance is adjusted, for all values of voltage and DC current, to give maximum effective output power.

In the development of magnetic amplifiers a major consideration is naturally the magnetic structure of the saturating reactor—that is to say, the proportions, the dimensions, and the magnetic characteristics of the core material—and the relation between this structure and the output. In studying the comparative effectiveness of different cores, it is important to point out that in comparing the performance of two

different cores when subjected to the same input, the comparison of the two outputs is meaningless unless, at the same time, the load resistance and the voltage be taken into consideration.

In practice, therefore, figures giving the relative output and gain of a number of different reactors are not strictly comparable unless taken both at optimum resistance and at optimum voltage.

Due to these circumstances the acquisition of performance data, relating to gain and output of saturating reactors, is excessively time-consuming and tedious.

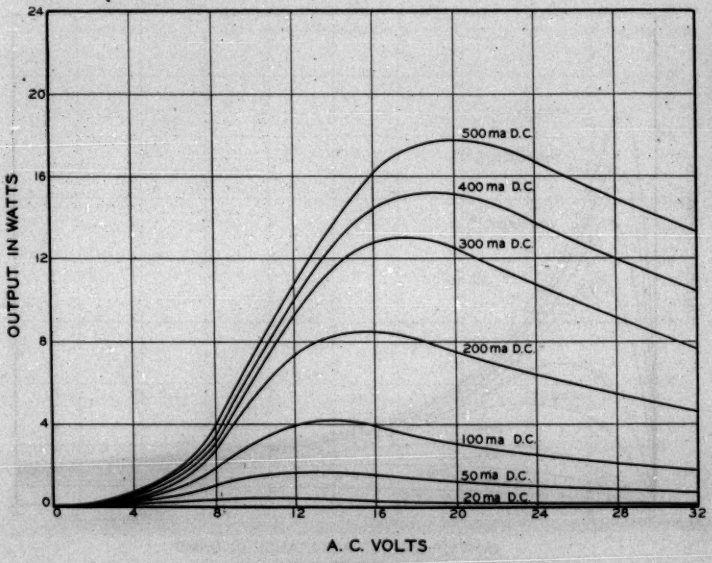

FIG. 4. Relation between output power and AC voltage.

The output, as stated, is $(I_s - I_o)^2R$. In the procedure for determining this quantity from a single saturating reactor, no direct indication of this function can be discerned by the observation of instrument readings. The output is known only when the above function has, by arithmetical difference, squaring and multiplying, been calculated.

The optimum values of R and E, therefore, cannot be determined by observation, but only by the expenditure of time required to compute the output a considerable number of times with different values of R and different values of E, the maximum value being arrived at by selection.

The author has devised an arrangement for furnishing a pointer in-

dication proportional to the quantity $(I_i - I_o)^2R$. With this apparatus the output power can be maximalized visually as the parameters E and R are varied.

RECTIFIER CHARACTERISTICS.

One component in the resulting figures for the gain and output is the performance of the rectifier used. The rectifier is a device having non-linear characteristics which result in variable resistance and variable efficiency in rectification. Clearly it would be very desirable, in comparing the performance of saturating reactors having different magnetic cores, to eliminate this variable element.

From another angle, however, if the characteristics of the saturating reactors are being studied as part of the procedure in designing a magnetic amplifier, the over-all characteristics of the combination of saturating reactor and rectifier are more pertinent, in regard to the end in view, than would be the characteristics of the reactor alone.

A practical exigency favors the taking of test data on the basis of the over-all performance of reactor and rectifier, in most instances. This arises from the fact that it is easier accurately to measure the DC current after rectification, due to the greater availability and superior characteristics of DC instruments. In the case of high-gain, high sensitivity reactors such as are used in the initial stages of an amplifier and which have cores of high permeability nickel-iron alloys, the output currents are sometimes of the order of one milliampere. Even if an AC instrument of this range were specially made, its resistance would be such as completely to disturb the conditions of the reactor circuit were it introduced therein.

It is of interest to note, in passing, that the non-linear characteristics of the rectifier, if the latter is selected with care, can actually increase the gain, by widening the spread between I_i and I_o. This result can sometimes be obtained by utilizing a somewhat larger rectifier than would appear to be indicated by the manufacturer's rating. By working at a low rectifier plate current density the resistance of the rectifier may be substantially higher for I_o than it is for I_i.

Accordingly, data relating to different saturating reactors, in order to be comparable, should be taken with rectifiers chosen so that, as far as is reasonably possible, there is no substantial difference in the efficiency of rectification.

METHOD OF COLLATING DATA.

The performance data of a single saturating reactor magnetic core, inclusive of rectification, may conveniently be presented in the form shown in the curve Fig. 5, which shows both the output and the gain plotted against the input.

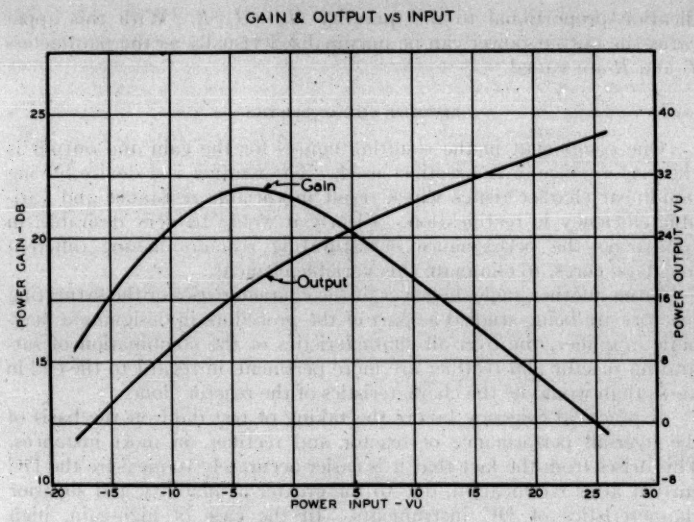

FIG. 5. General characteristic curves of EI-3A silicon steel core.

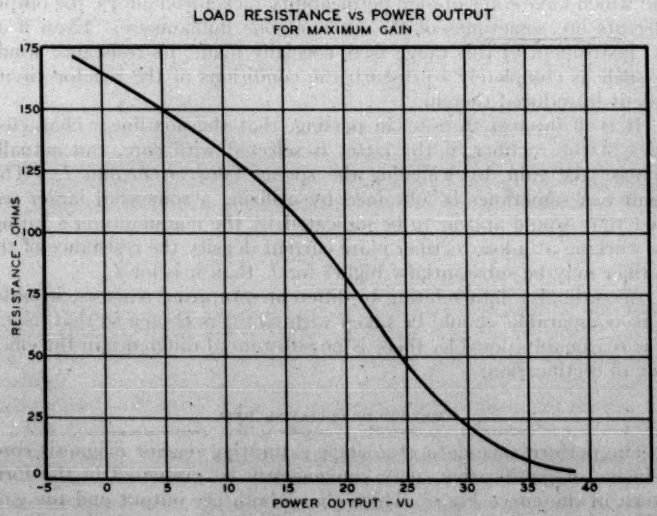

FIG. 11. Output resistance characteristic of EI-3A silicon steel core with 15 volt winding.

As explained above,

the input power is: i^2r,

the output power is: $(I_s - I_o)^2R$

and the gain is: $\dfrac{(I_s - I_o)^2R}{i^2r}$.

The input power levels involved in studying the performance of saturating reactors of the types and dimensions utilized in magnetic amplifiers vary between small fractions of a microwatt and several watts. Because of this range of magnitude it has been found more convenient to plot both input and output in VU.*

While the gain of a single stage does not cover such a wide dimensional range it is convenient to plot this also logarithmically since the gain, shown in DB, is the difference between the input and output VU.

Both in the output and gain curves, each point plotted represents the maximum figure selected from a number of readings taken at different values of the load resistance R. Similarly, for each point taken, there is selected, from the relatively few rectifier plate sizes available, the size which gives the highest gain.

It would be desirable, in order to obtain a curve of completely general applicability, also to maximalize the AC voltage for each point plotted. Whether this is worth the additional work involved is open to question. By way of compromise, in the gain and output curves included in this paper, the AC voltage is maintained at a constant value for all readings. This value is that at which maximum output is given at the value of input at which the peak of the gain curve occurs. Comparison of curves, of different types of reactor, taken in this manner would appear to be valid.

It is to be pointed out, however, that, if the curves are obtained in this manner at constant voltage, in accordance with the characteristics shown in Fig. 4, for high values of power input some increase in gain over that indicated in Fig. 5 may be obtained by increasing the voltage. Likewise, in some cases, increase in gain at very low inputs may be possible at a lower voltage.

EFFECT OF DIFFERENT MAGNETIC CORE MATERIALS.

The curves shown in Fig. 5 refer to a core made up of EI-3A[3] punchings of silicon steel stacked to give a square center section. Fig. 6 gives the dimensions of this lamination.

Curves in Fig. 7 give like data for a similar core stacked with No. 4750 alloy.

---

* Volume unit = number of DB above one milliwatt reference level. Cf. Table VI.

[3] Allegheny-Ludlum Steel Corporation lamination type.

Similar data for mumetal are given in Fig.8.

The value of this data is more strikingly evident if the gain curves for these three core materials be plotted together as shown in Fig. 9. The comparative performance of the three materials are more clearly presented by plotting the linear values of gain rather than the DB figures.

PROPORTIONAL GAIN.

These gain and output curves, while they are relevant and factual, fail to bring out what is perhaps the most significant factor in the design of magnetic amplifiers. This is the relation between the input and the ratio of I_o and I_s. The importance, indeed the necessity, of the various

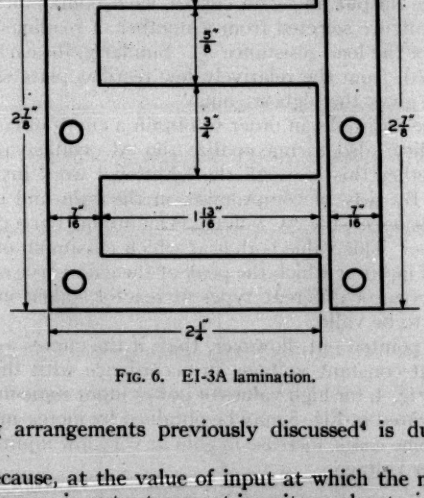

FIG. 6. EI-3A lamination.

compensating arrangements previously discussed[4] is due entirely to this relation.

This is because, at the value of input at which the maximum gain occurs, the increase in output current is quite moderate. In most cases the increment due to the input is less than 100 per cent. That is to say, at maximum gain I_s is less than twice the value of I_o.

Clearly, with such a ratio, the operation of a multi-stage magnetic amplifier without some method of compensating for the value of I_o would be impossible. If it be desired to dispense with compensating arrangements, obviously I_s must very substantially exceed I_o. It is, therefore, particularly important to note that for values of input at

[4] Alan S. FitzGerald, J. FRANKLIN INST., 244, 249 (1947).

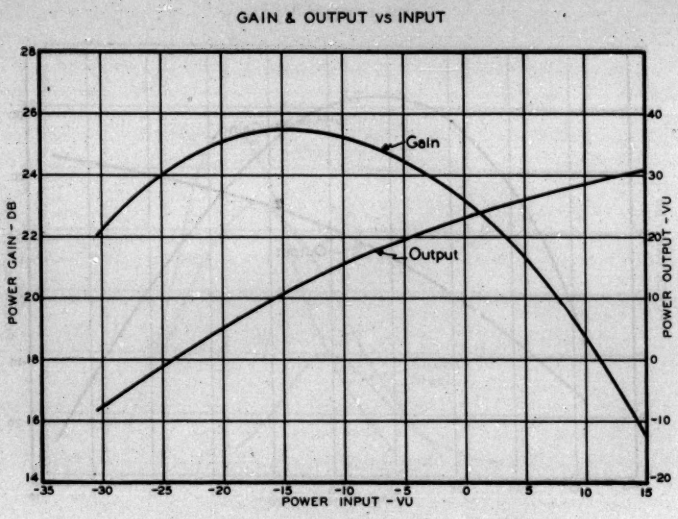

FIG. 7. General characteristic curves of EI-3A No. 4750 alloy core.

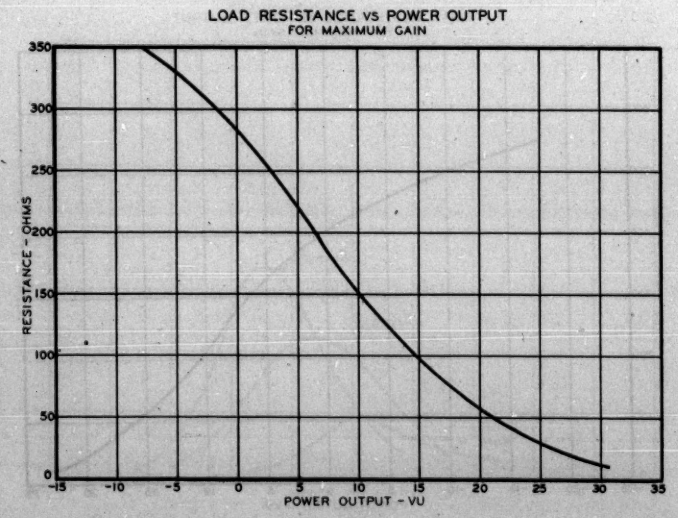

FIG. 12. Output resistance characteristic of EI-3A No. 4750 alloy core with 7 volt winding.

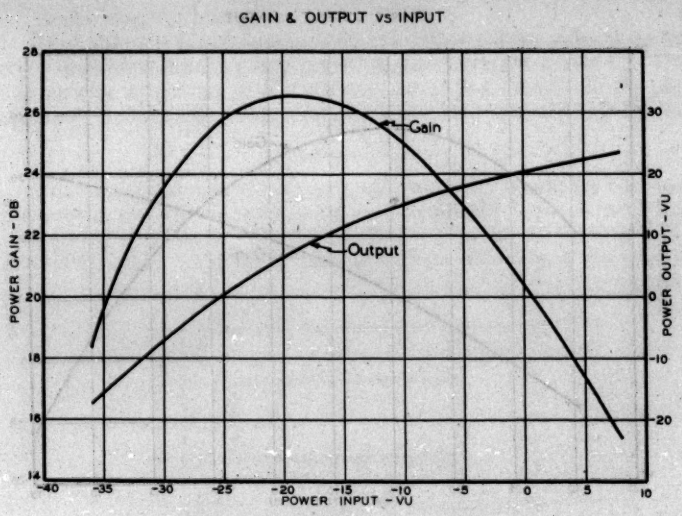

FIG. 8. General characteristic curves of EI-3A mumetal core.

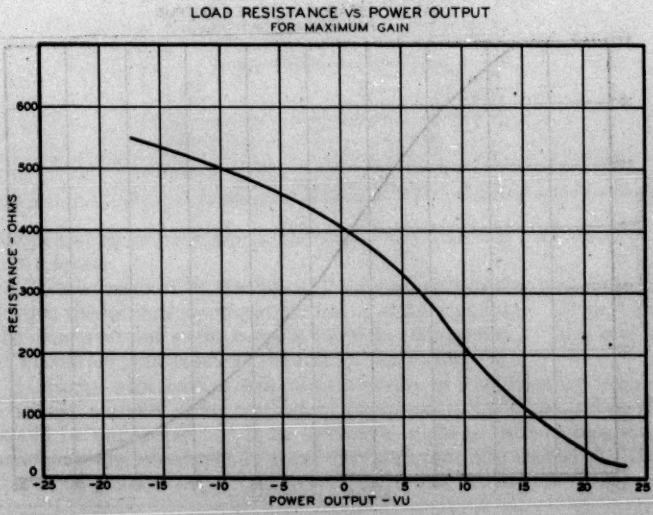

FIG. 13. Output resistance characteristic of EI-3A mumetal core with 5 volt winding.

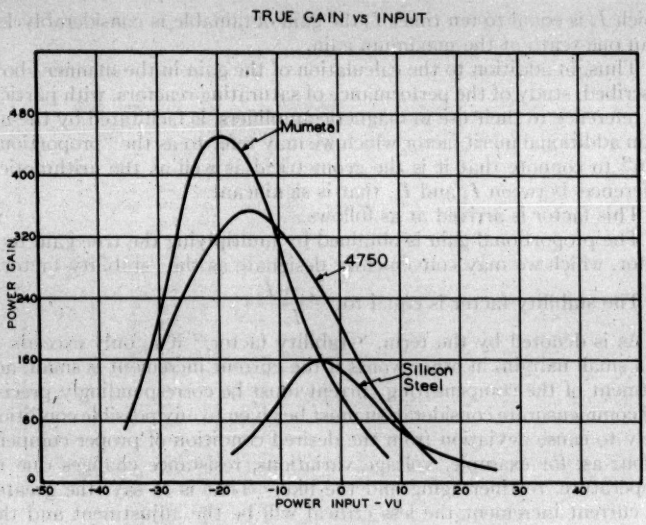

FIG. 9. Gain curves of three different core materials.

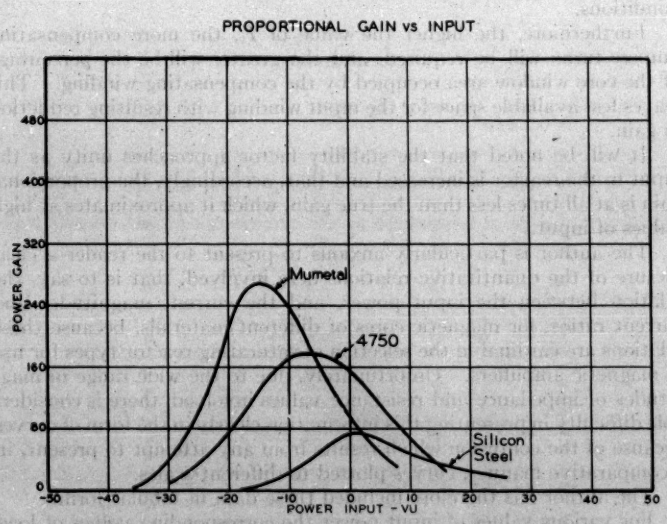

FIG. 10. Proportional gain curves of three different core materials.

which I_s is equal to ten times I_o the gain obtainable is considerably less than one-tenth of the maximum gain.

Thus, in addition to the calculation of the gain in the manner above described, study of the performance of saturating reactors, with particular reference to their use in magnetic amplifiers, is facilitated by the use of an additional merit factor which we may refer to as the "proportional gain" to connote that it is the geometrical as well as the arithmetical difference, between I_s and I_o, that is significant.

This factor is arrived at as follows.

The proportional gain is obtained by multiplying the true gain by a factor, which we may conveniently designate as the "stability factor."

The stability factor is equal to: $\frac{I_s - I_o}{I_s}$.

As is denoted by the term, "stability factor," if I_s only exceeds I_o by a small margin, in other words if the current increment is small, adjustment of the compensating current must be correspondingly precise and commensurate consideration must be given to any possible condition likely to cause deviation from the desired condition of proper compensation; as, for example, voltage variations, resistance changes due to temperature, rectifier aging and the like. That is to say, the greater the current increment the less critical will be the adjustment and the greater the ability of the amplifier to withstand varying or disturbing conditions.

Furthermore, the higher the value of I_o, the more compensating ampere-turns will be required, and the greater will be the percentage of the core window area occupied by the compensating winding. This leaves less available space for the input winding with resulting reduction in gain.

It will be noted that the stability factor approaches unity as the input to the reactor is increased and that, accordingly, the proportional gain is at all times less than the true gain, which it approximates at high values of input.

The author is particularly anxious to present to the reader a clear picture of the quantitative relations here involved, that is to say, the relation between the input power, and the current magnitudes and current ratios, for magnetic cores of different materials, because these relations are cardinal in the selection of saturating reactor types for use in magnetic amplifiers. Unfortunately, due to the wide range in magnitudes of impedance and resistance values involved, there is considerable difficulty in presenting this information clearly in the form of curves because of the confusion which results from any attempt to present, in a comparative manner, curves plotted to different scales.

The author has therefore included these data in tabular form.

For various values of input power the corresponding values of load resistance, current, power output, gain, and proportional gain, are given

TABLE I

E1-3A SILICON STEEL

INPUT VU	OUTPUT CIRCUIT OHMS	I_0 MA	I_s MA	$I_s - I_0$ MA	OUTPUT POWER WATTS	VU	TRUE GAIN LINEAR	DB	PROP'L GAIN $\frac{I_s - I_0}{I_s}$	LINEAR
-18	172	30.0	31.8	1.8	0.6×10^{-3}	-2.5	35.4	15.5	0.06	2.0
-16	160	32.0	34.8	2.8	1.3	1.0	50.1	17.0	0.08	3.1
-14	152	34.0	38.2	4.2	2.7	4.3	67.6	18.3	0.11	7.4
-12	142	35.0	41.3	6.3	5.6	7.5	89.1	19.5	0.15	13.6
-10	132	37.0	46.1	9.1	11.0	10.4	111.0	20.4	0.20	22.0
- 8	120	38.0	51.2	13.2	20.9	13.2	132.0	21.2	0.26	34.1
- 6	107	40.0	58.9 *	18.9	38.0	15.8	151.0	21.8	0.32	50.1
- 4	95	42.0	70.8	28.8	63.1	18.0	158.0	22.0	0.41	64.2
- 2	83	45.0	79.3	34.3	97.5	19.9	155.0	21.9	0.43	67.2
0	70	48.0	93.3	45.3	144.0	21.6	144.0	21.6	0.49	70.0
2	60	53.0	115.8	62.8	209.0	23.2	132.0	21.2	0.54	71.8
4	50	58.0	133.1	75.1	282.0	24.5	112.0	20.5	0.56	63.2
6	42	63.0	158.2	95.2	380.0	25.8	95.4	19.8	0.60	57.4
8	35	67.0	188.0	121.0	513.0	27.1	81.3	19.1	0.64	52.3
10	29	72.0	225.0	153.0	676.0	28.3	67.6	18.3	0.68	45.8
12	23	80.0	279.0	199.0	911.0×10^{-3}	29.6	57.5	17.6	0.71	41.0
14	19	85.0	337.0	252.0	1.20 WATTS	30.8	47.8	16.8	0.75	35.8
16	15	90.0	419.0	329.0	1.62	32.1	40.7	16.1	0.79	32.0
18	12	95.0	518.0	423.0	2.14	33.3	33.9	15.3	0.82	27.6
20	9	100.0	694.0	594.0	2.82	34.5	28.2	14.5	0.86	24.1
22	7	100.0	829.0	729.0	3.72	35.7	23.4	13.7	0.88	20.6
24	5	100.0	1080.0	980.0	4.78	36.8	19.0	12.8	0.91	17.2
26	4	100.0	1360.0	1260.0	6.31	38.0	15.8	12.0	0.93	14.6

TABLE II

E1-3A 4750

INPUT VU	OUTPUT CIRCUIT OHMS	I_0 MA	I_s MA	$I_s - I_0$ MA	OUTPUT POWER WATTS	VU	TRUE GAIN LINEAR	DB	PROP'L GAIN $\frac{I_s - I_0}{I_s}$	LINEAR
-30	350	9.8	10.5	0.7	0.2×10^{-3}	- 7.8	166	22.2	0.07	11
-28	330	10.0	11.0	1.0	0.3	- 5.0	199	23.0	0.09	18
-26	305	10.7	12.1	1.4	0.6	- 2.3	234	23.7	0.12	27
-24	280	11.1	13.1	2.0	1.1	0.3	269	24.3	0.15	41
-22	250	11.7	14.4	2.7	1.9	2.7	295	24.7	0.19	56
-20	220	12.4	16.2	3.8	3.2	5.1	324	25.1	0.24	76
-18	185	13.3	18.7	5.4	5.4	7.4	342	25.4	0.29	99
-16	155	14.7	22.3	7.6	8.9	9.5	354	25.5	0.34	121
-14	135	15.5	25.5	10.2	14.1	11.5	364	26.5	0.40	142
-12	115	16.5	30.3	13.8	21.9	13.4	366	25.4	0.46	157
-10	95	18.3	37.1	18.8	33.5	15.3	335	25.3	0.51	170
- 8	80	20.0	45.1	25.1	50.1	17.0	316	25.0	0.56	176
- 6	65	22.5	56.1	33.6	73.2	18.7	292	24.7	0.60	175
- 4	55	23.5	67.4	43.9	106.0	20.3	246	24.3	0.65	173
- 2	45	25.0	82.8	57.8	150.0	21.7	237	23.8	0.70	166
0	40	26.0	98.3	72.3	209.0	23.2	209	23.2	0.74	154
2	30	31.0	128.4	97.4	285.0	24.6	180	22.6	0.76	137
4	25	32.0	155.0	123.0	375.0	25.8	150	21.8	0.79	119
6	20	33.0	188.0	155.0	478.0	26.8	120	20.8	0.82	99
8	18	34.0	217.0	183.0	602.0	27.8	96	19.8	0.84	81
10	15	35.0	257.0	222.0	741.0	28.7	75	18.7	0.86	64
12	12	35.0	307.0	272.0	891.0×10^{-3}	29.5	56	17.5	0.89	56
14	10	35.0	358.0	320.0	1.02 WATTS	30.1	41	16.1	0.90	37
16	10	35.0	385.0	350.0	1.12 WATTS	30.5	29	14.5	0.91	26

in Table I for the silicon steel core of which the gain and output curves are given in Fig. 5.

Table II and Table III respectively show the corresponding figures for the No. 4750 alloy and mumetal.

Fig. 10 shows the proportional gain of the three cores in a similar manner to the way in which the gain curves are shown in Fig. 9.

TABLE III

E1-3A MUMETAL

INPUT VU	OUTPUT CIRCUIT Ohms	I_0 MA	I_s MA	$I_s - I_0$ MA	OUTPUT WATTS	POWER VU	TRUE GAIN LINEAR	GAIN DB	PROP'L $\frac{I_s - I_0}{I_s}$	GAIN LINEAR
-36	950	2.9	3.1	0.2	17.8×10^{-6}	-17.5	71	18.5	0.06	4
-34	825	3.0	3.3	0.3	44.7	-13.5	112	20.5	0.09	10
-32	500	3.1	3.6	0.5	107.2	- 9.7	170	22.3	0.13	22
-30	475	3.2	3.9	0.7	224.0	- 6.5	224	23.5	0.18	40
-28	450	3.3	4.3	1.0	457.0	- 3.4	288	24.6	0.23	67
-26	425	3.4	4.8	1.4	873.0×10^{-6}	- 0.6	346	25.4	0.33	113
-24	375	3.7	5.8	2.1	1.6×10^{-3}	2.0	398	26.0	0.36	168
-22	350	4.0	6.8	2.8	2.8	4.4	436	26.4	0.41	180
-20	300	4.4	8.3	3.9	4.5	6.6	452	26.6	0.47	198
-18	250	4.5	9.8	5.3	7.1	8.5	446	26.5	0.54	242
-16	200	4.8	12.2	7.4	11.0	10.4	436	26.4	0.61	265
-14	165	5.0	15.0	10.0	16.4	12.1	407	26.1	0.67	271
-12	135	5.5	18.5	13.0	22.9	13.6	363	25.6	0.70	255
-10	110	6.0	23.0	17.0	31.6	15.0	316	25.0	0.74	234
- 8	100	6.0	26.6	20.6	42.7	16.3	269	24.3	0.77	209
- 6	75	6.5	33.6	27.1	54.9	17.4	218	23.4	0.81	176
- 4	65	7.0	40.0	33.0	70.8	18.5	178	22.5	0.83	147
- 2	50	7.5	49.8	42.3	89.1	19.5	141	21.5	0.86	121
0	40	7.5	59.9	52.4	110.0	20.4	110	20.4	0.88	96
2	35	8.0	69.4	61.4	132.0	21.2	83	19.2	0.89	74
4	30	8.0	80.7	72.7	158.5	22.0	63	18.0	0.99	57
6	30	8.0	86.9	78.9	186.0	22.7	47	16.7	0.91	43
8	25	8.0	101.4	93.4	218.0	23.4	35	15.4	0.92	32
10	20	8.0	123.0	115.0	263.0×10^{-3}	24.2	26	14.2	0.93	24

VALUE OF CURVE DATA.

We may now consider the significance and utility of the various curves shown in the foregoing figures, especially from the point of view of the selection of saturating reactor cores in accordance with the power values in various stages in a magnetic amplifier.

The first thing that is clearly apparent from these curves is that, due to the impedance match relationship, high values of gain are definitely associated with limited ranges of power values. Simple magnetic amplifier circuits of the type dealt with in the present paper, therefore, are not to be expected to furnish any substantial degree of linear or proportional response.

Linear response magnetic amplifiers are available, however, and will be discussed in another paper.

Three important limiting values may be obtained from these curves. These figures represent definite indices by means of which different

magnetic cores may be compared, with particular reference to their suitability for employment in any particular stage, or at any given power level, in a magnetic amplifier.

These are:

(*a*) Maximum gain.
(*b*) Sensitivity, or minimum input.
(*c*) Maximum output.

MAXIMUM GAIN.

The value of power input at which the maximum proportional gain occurs indicates clearly the power level at which any given magnetic core furnishes best performance.

The relative merits of different magnetic cores are well signalized by calculating and tabulating the following factors based upon the maximum proportional gain:

(1) Gain per pound,
(2) Gain per dollar,

computed from the weight of the magnetic core and the cost of this weight of the specified core material, as for example, silicon steel, No. 4750, or mumetal.

SENSITIVITY.

For any given magnetic core there is a threshold value of input power below which there is no response whatever.

However, for practical purposes it is more convenient to set some arbitrary and more significant minimum value for purposes of comparison.

For example, the sensitivity or minimum input value may be taken on the basis of a given value of proportional gain, such, as, say, ten.

Or the sensitivity may be taken to be the value of input power which produces a given percentage increase in the current in the output circuit. The exact value of the lowest increment which it is practical to use depends upon factors related to the particular application involved and having reference to the question of stability, such as, for example, variation in the supply voltage, frequency, ambient temperature, etc.

A satisfactory value for minimum input power is that at which the current increment is ten per cent. That is to say, I_s is ten per cent. greater than I_o.

MAXIMUM OUTPUT.

It will be seen on referring to Figs. 5, 7, and 8 that, due to the essential saturating principle, all of the output curves tend towards limiting maximum values irrespective of the extent to which the input power may be increased.

It is clear, therefore, that for any given magnetic core there is a definite maximum power level beyond which the output cannot be in-

creased with any magnitude of input no matter how great. However, since this limiting output level is approached asymptotically, it is impracticable to determine this value.

Accordingly, here again it is convenient to employ some arbitrary factor. It will be noted on referring to the curves of Figs. 5, 7, and 8 that the gain falls off rapidly for high values of input. A convenient figure having reference to the maximum power for which any given magnetic core is suitable, is the value of power input at which the gain is decreased to one-tenth of the maximum gain; or, if desired, the maximum power may be taken as the value at which the gain is decreased to a given value, such as ten, for example.

In the curves presented in this paper the sensitivity value is taken as the value giving an increment of ten per cent., the maximum power output is taken as the value giving one-tenth of the maximum gain, and the curves in Figs. 5 through 10 embrace these limits.

It will be clear from the foregoing that all these curves are of a type such that the data they present may be described as general characteristic curves for any given lamination, stacking, and core material, at any given frequency. They represent limiting values, not specific values, and are valid for different voltages and windings on the basis of substantially equivalent DC coil space factors.

All data included in the present paper refer to a frequency of 60 cycles.

For reasons which have been previously explained these curves include a factor involving rectifier characteristics. It is to be pointed out that exactly similar curves based upon alternating current output instead of rectified output are entirely possible if their value, in that the data furnished refer exclusively to magnetic characteristics, is sufficient to off-set any difficulty in instrumentation.

These general characteristic curves must be distinguished from the gain and output curves which would be obtained with a constant load resistance. This is a less generalized condition and is the one under which a magnetic amplifier in fact operates. The characteristics obtained with a given AC winding, and AC supply voltage, and with a fixed load resistance, may be designated the specific characteristics.

Thus, the general characteristic is of great use in determining the initial elements in the design of a magnetic amplifier. The specific characteristic curve is applicable for the purposes of determining the performance of a given stage in a magnetic amplifier when it has been designed.

It will be noted that the general characteristic curve is the envelope of an infinite number of specific characteristic curves for different output resistances. The use of the specific characteristic curves will be referred to later in connection with the design procedure with particular reference to coil windings.

It is perhaps desirable to point out the relation between the proportional gain curves shown in Fig. 10 and the true gain curves of Fig. 9. It should not be inferred that the proportional gain curves completely take the place of the curves in Fig. 9. Both are helpful.

The specific utility of the proportional gain curves in Fig. 10 lies in the fact that these curves indicate clearly which type of core, or core material, should be selected for any given range of input power level.

On referring to Fig. 10 it is immediately apparent, at first glance, that the useful range of the silicon steel core is restricted to power levels greater than 14 VU. Likewise, it is equally evident that below -6 the mumetal is better than the No. 4750 core. The useful range of the No. 4750 material lies approximately within these limits.

The significance of the true gain curves of Fig. 9, on the other hand, is that they refer to actual performance.

That is to say, while the curves of Fig. 10 are clearly highly instructive, they do not represent real physical quantities. The curves in Fig. 9 relate to actual power levels developed in the output circuit. This is not the case with the proportional gain curves.

Similar curves may be drawn to scales showing gain per pound and/or gain per dollar and these are of even more direct value in determining the most economic design for a magnetic amplifier.

It may appear at first sight that the proportional gain curves of Fig. 10 do not very materially differ in general configuration and character from the curves of true gain in Fig. 9.

However it is pointed out that the above curves refer to a frequency of 60 cycles. The value of an approach to the problem of magnetic amplifier design through consideration of the factor of proportional gain becomes much more apparent and is of greatly increased interest when higher frequencies are contemplated. This is due to the fact that whereas the true gain increases as the frequency is raised, the ratio $(I_s - I_o)/I_s$ varies in the opposite sense, and decreases as the frequency is increased.

One further comment is pertinent with reference to the procedure outlined above for computing gain and output, and to the use of proportional gain as a merit factor. The usefulness of this treatment is not restricted to magnetic amplifier circuits of the type shown in Fig. 1 in which compensating windings are employed.

In a previous paper,[5] various other circuit arrangements and networks were presented in which means other than compensating windings, for accomplishing the same result, were described. The relations discussed on page 336 with reference to the "stability factor" have some degree of pertinence to these circuits also.

Moreover, these bridge or network type circuits are subject to inherent internal loss or attenuation of interstage power. The higher the

[5] Alan S. FitzGerald, J. FRANKLIN INST., 244, 249 (1947).

value of I_o which is to be annulled, since the impedance values of the network will be a function of the value of I_o, the greater the attenuation may be expected to be. Thus, for a given value of $I_s - I_o$, the lower the value of I_o the higher the gain is likely to be.

The salient properties and relative merits of the three core materials referred to in Figs. 5, 7 and 8, with particular respect to their use in magnetic amplifiers, are very clearly and briefly brought out in Table

TABLE IV

EI-3A LAMINATION

PROPERTIES OF STACK HAVING SQUARE CENTRE SECTION

Material	Silicon Steel	#4750	Mumetal
Weight of core lbs.	1.11	1.23	1.29
Cost of core material per lb.	$0.37	$2.13	$3.18
Cost of core	$0.41	$2.62	$4.11
Minimum Input microwatts	25	1.5	0.4
Maximum Gain	150	350	450
Maximum Gain per lb.	135	284	349
Maximum Gain per dollar	356	134	109
Maximum Output watts	6.30	1.20	0.20
Maximum Output, watts, per lb.	5.67	0.98	0.16
Maximum output, watts, per dollar	15.3	0.46	0.05

IV in which a number of limiting values and other significant quantitative relations are tabulated.

Having thus equipped ourselves with some yard-sticks for evaluating the quantitative performance of magnetic amplifiers, we are now in a position to deal with the question of how to determine the structure necessary to meet any given performance requirement.

It is not the author's purpose to treat comprehensively and in detail, at this time, of the design of magnetic amplifiers. Rather, it is intended in the present paper to adumbrate some of the salient elements involved.

CONNECTION OF AC WINDINGS.

It is an essential principle of the AC winding structure that there be no inductive relation between the AC and DC windings. Various AC winding arrangements were shown diagrammatically in a previous paper.[6] It will be noted that the AC windings may be connected either in series or in parallel.

It has just been implied that there is no transformer action between AC and DC windings. This requires more particular definition. There is, in fact, in a saturating reactor no transformer action between the DC winding and the external circuit connecting with the AC winding. Under certain circumstances, however, there is inductive action in respect of the individual sections of the AC winding.

If these windings are series connected there is no inductive action at the fundamental or supply frequency. There is, however, inevitably a certain amount of distortion of wave form resulting in induced harmonic voltages, some of them even harmonics. Since the AC windings are connected for phase opposition at the fundamental frequency, the second harmonic components are additive. Accordingly, a double frequency voltage of a relatively low order of magnitude is set up in the DC winding.[7]

The degree to which the double frequency component may be considered other than negligible depends on several factors. In the first place, it depends upon the source from which the DC winding is supplied. If there is no unilaterally conducting element in the circuit from which the saturating winding is supplied, the harmonic effect can in general be ignored. However, in magnetic amplifier circuits it may be assumed that the DC winding is supplied by a rectifier. As will be again referred to later on in connection with the design of DC windings, if there be present in the DC output circuit of a 4-leg or bridge type rectifier, an alternating EMF, even though the AC connections of the rectifier be open, the rectifier will function as a half-wave rectifier. Thus to the extent that this double frequency transformer EMF results in the presence of direct current in the saturating winding, it has to be taken into consideration. Only in a very few instances has the author found this effect present in a magnitude requiring consideration in the design of an amplifier. This has occurred when a relatively large reactor such as may be used in the last stage of an amplifier is operated at somewhat less than usual power level. As a rule the last stage, and those immediately preceding the last stage, are operated at power levels at which the magnitude of the output rather than the maximum gain, is the predominant consideration. Under such conditions the input thereto is of a magnitude such that any second harmonic effect is entirely negligible. If such a last stage reactor be operated under con-

[6] Alan S. FitzGerald, J. FRANKLIN INST., **244**, 249 (1947), Figs. 1 and 2.

[7] Boyajian, *A. I. E. E. Transactions*, 1924.

ditions giving relatively high gain, the input level will be correspondingly lower. The second harmonic effect, in comparison with this lower input, may now be of significant magnitude.

If the pair of AC coils be connected in parallel the phase relation of the harmonic components will be in opposition in respect of the external circuit, but will be cumulative as regards the closed circuit which the two parallel connected coils now constitute. Accordingly, the double frequency component will be absorbed by circulation and will give rise to no rectified current in the DC winding.

However, a serious disadvantage arises from the use of the parallel connected arrangement. While there is still no transformer action between the DC winding and the external circuit connected to the AC windings, there is neverthless, an inductive relation between the DC winding and the closed loop circuit formed by the two parallel connected AC windings.

A result of this relation is that transient short circuit currents proportional to the rate of change of the current in the DC winding, are set up in this closed loop, which oppose the build-up of the saturating flux and prolong its decay.

The rate of response of a magnetic amplifier having parallel connected AC coils, therefore, is slower than if the AC windings are connected in series.

The author has found it possible and preferable to use the series connection in all but a very few special cases.

NUMBER OF AC TURNS.

We may now consider the procedure for arriving at the number of turns for the AC winding.

If the windings are connected in parallel, obviously the turns per coil will be double the number appropriate for series connection.

The AC turns are subject to quite definite determining conditions and there is no very wide latitude of selection.

There is of course a direct relation between the number of AC turns and the AC voltage from which the stage is supplied. This arises from the incremental permeability curve of the core material and is clearly brought out by the curves in Fig. 4 which show that for any given number of AC turns there is an optimum AC voltage. Another way of expressing this relation is to say that for any given voltage there is an optimum number of turns. It is, of course, the voltage per turn that determines the point upon the permeability curve at which the core operates.

The AC voltage from which a given magnetic amplifier stage operates is the resultant of the AC voltage across the winding and the AC voltage across the rectifier. In accordance with the impedance match relations indicated by the curves in Fig. 3, the coil and rectifier voltages are of the same order of magnitude and are substantially in quadrature. In

view of the fact that the wave shapes are not strictly sinusoidal any reference to the quantitative and vector relations is necessarily approximate.

Bearing in mind, then, the above finite relationship between the AC turns and the voltage at which the stage operates, it is important to note that the operating voltage cannot, as a general rule, be selected at random, or a standard supply voltage used, and the circuit constants of the amplifier be determined accordingly. In most cases it works the other way round. The exigencies of the magnetic amplifier design tend to determine the order of magnitude of the AC voltage.

The AC voltage and the AC winding are determined primarily by the output power level of the stage. This quantity determines two other entities which latter in turn set definite limits to the turns and voltage. These are:

(*a*) The DC winding of the derivative, or following, stage.
(*b*) The rectifier.

Unfortunately for clarity of exposition these two elements cannot be discussed separately. They are directly inter-related and jointly affect the conclusion. They must therefore be considered together although this may involve a certain amount of unclearness. If the reader will re-peruse this portion of the text after the section dealing with the DC winding design has been read, and the curves in Figs. 11, 12 and 13 have been noted, it is hoped it may be more readily followed.

Considering first the DC winding, we may again note the curves shown in Fig. 3 which refer to the impedance match relationship between the AC winding impedance and the resistance of the output circuit which is energized through the rectifier by the current in the AC winding.

As will be discussed more completely in connection with the DC coil design, the resistance of the input coil in the derivative stage is a definite function of the impedance of the AC winding. It depends upon the dimensions of the core, the magnetic material of which it is constructed, and it is proportional to the square of the number of turns.

If we refer now to Fig. 10 it is immediately apparent that the type of magnetic material to be used in any given core is directly determined by the power level. That is to say, if the power level is substantial, ordinary transformer material such as silicon steel will be used for the core. If the power level is low, a material of greater permeability will be employed. Due to the great difference in the magnetic properties of these materials, the turns of the AC winding for any given AC voltage would be different, and since the permeability is also different there is a very substantial difference between the reactance values of the AC coils with the different magnetic alloys. Accordingly, as shown in Tables I, II and III the proper resistance values of the DC coil are

widely different for the different materials. Thus, since the power level determines the material it also determines the DC coil resistance.

Where the power level is very low, as for example in a first stage of a high sensitivity amplifier, in which a core of mumetal might be employed, if the AC turns exceed a moderate value it will have the result that the resistance value thus prescribed for the DC coil of the derivative stage would be so high as to require that this coil be wound with a very fine conductor size; also the value of the current would be very low.

Both from the standpoints of cost and reliability and ruggedness of apparatus the use of very fine wire where avoidable is unattractive. The turns of the AC winding therefore may desirably not exceed the number which would result in a DC coil conductor size any finer than, say, No. 30.

Furthermore, with high permeability alloys, the magnetizing ampere-turns involved are of a very low order of magnitude; as a result, unless the AC turns are of a moderate order, the current values involved will be quite small.

This brings us now to the subject of the rectifier characteristics. The rectifier contributes to the upper limit for the AC turns already discussed in that, if the current value is very low, the rectifier situation is likely to be unsatisfactory for one reason or another, associated either with performance, uniformity, procurability or reliability.

The rectifier itself definitely sets the lower limit for the AC turns. Clearly the AC voltage from which the stage operates must not only exceed the minimum voltage at which the rectifier commences to conduct but must be high enough for the rectifier to operate at its most efficient voltage and current density.

This latter point is of interest in connection with the choice of rectifiers of different types as, for example, copper oxide or selenium. Since the minimum voltage at which efficient rectification is possible is substantially higher for selenium than is the case with copper, it follows that in a high sensitivity or low input stage with a mumetal core the derivative DC coil would have to be wound with much finer wire if selenium be used than would be necessary with copper oxide.

It is clear from the above that for the initial stages in a magnetic amplifier, where the power levels involved are relatively low, rectifiers having only a single plate in series per leg are indicated. The use of multiple plates in series per leg would require higher AC voltages, more AC turns, and would result in a fine wire DC winding in the derivative stage.

However, in stages where the power levels are more substantial, as for example in an output or penultimate stage, should these be operated at the same voltage as the earlier stages, substantially higher current values may be reached which would require rectifiers of commensurate aggregate plate area such as might be provided by the use of rectifiers

having multiple plates in parallel. Possibly also the resistance and current values predicated for the DC coil might be so low as to require an inconveniently heavy conductor. For such stages, if desired, therefore, higher AC voltages may be used so that lower current values are involved, permitting the use of a more flexible, easily wound conductor for the DC coil. A rectifier of correspondingly higher voltage rating with the plates stacked in series in each leg instead of in multiple, may then be used.

To sum up then, the AC turns should not be such as will involve unsuitable conductor sizes for DC coils, and are otherwise predicated upon the rectifier characteristics. Accordingly, the basis for deciding the AC turns and the AC voltage from which the stage operates may very largely be based on costs and availability of rectifier types.

Since the price listings of rectifiers of different plate diameters and series and parallel plate stackings for different voltage and current ratings, may in some cases be rather arbitrary, the AC turns are somewhat likely to be determined on a fortuitous and random rather than a theoretical basis.

Thus, subject to DC wire size, the AC voltage and turns should be that at which the rectifier costs are lowest. The arrangement of series or parallel plate stackings is likewise determined on this basis. It is to be noted that the rectifier is selected for maximum efficiency of rectification rather than in accordance with the manufacturer's current loading or temperature rating. This is because the efficiency of rectification is a direct component of the gain.

It will be apparent from the foregoing that, as in the case of electronic amplifiers, the conditions which obtain tend to favor an increase in the stage operating voltage with increase of power levels, so that, in like manner, the more remote a given stage is from the input or first stage, the higher will be the most appropriate voltage. Thus magnetic amplifiers for operation at ordinary supply voltages may be expected to include a step-down transformer for supplying such voltages as are required for the several stages.

Because of the above relations the author has found that the silicon steel core referred to in Fig. 5 and Table I may desirably have a winding suitable for operating from a 15 volt AC circuit. On the other hand, 5 is found to be a better voltage for the mumetal core while the No. 4750 core gives better results with 7 volts. The figures given in the tables refer to these voltages. It is apparent from the current and resistance values shown in these tables why these different voltage values are preferable.

DC WINDINGS.

Little need be said on the subject of the design of direct current windings other than that, obviously, the space factor is a component in the gain obtained. That is to say, the output depends upon the

DC ampere-turns, and the more completely the lamination window area is filled up, the lower will be the power input by means of which the DC ampere-turns may be furnished.

As has been indicated previously, in reference to Fig. 3, the resistance of the DC coil should in some degree match the impedance of the previous AC winding. There is no high order of precision to be taken into consideration in this respect in view of the fact that the ohms-per-pound of two adjacent wire sizes have a ratio of the order of 60 per cent. It is necessary to choose one or another wire size and fill up the space available for the input winding. There is nothing to be gained by leaving any portion of the window area unfilled in order to produce a particular value of resistance for matching purposes.

Suitable AC windings having been decided upon, a curve of the type shown in Fig. 11, showing the relation between optimum load resistance in ohms and power output in VU, may be drawn.

Fig. 11 refers to a 15 volt AC winding for the silicon steel core of Fig. 5. Similar curves for 7 volt windings for the No. 4750 core of Fig. 7 and 5 volt windings for the mumetal core of Fig. 8 are given in Figs. 12 and 13.

While these curves may readily be used in conjunction with gain and output curves such as those shown in Figs. 5, 7 and 8 it is important to distinguish the difference between these two types of curves. Figs. 5, 7 and 8, as explained above, are general characteristic curves referring to the magnetic core. Figs. 11, 12, and 13 refer specifically to a particular AC winding, and have no value or significance with respect to any other windings.

It would be possible to plot curves of the type of Figs. 11, 12, and 13, with power input, instead of power output, as the independent variable; in many cases, they are handier to use this way. However, output circuit resistance curves if plotted against power input are inapplicable if a feed-back winding is used, since the degree of saturation produced results from the sum of the ampere-turns contributed by the input winding and the feed-back winding, and it is difficult to evaluate the latter. When the resistance is plotted against the power output it is valid for the degree of saturation by means of which the said power output is produced, irrespective of the arrangement by means of which this excitation is brought about.

COMPENSATING WINDINGS.

A minimum of comment is called for in reference to these windings since the problem is the entirely conventional one, in electrical technology, of designing a winding to furnish given ampere-turns from a given source of supply.

The number of ampere-turns required may, initially, be taken to be the product of the value of I_o which flows in the DC input winding, of

known resistance, and the number of turns of the input winding. Moreover, as shown in Fig. 1, arrangements of resistors may be included in the compensating winding supply circuit to determine the value of current which flows.

The only features in the determination of this winding which may possibly be peculiar to this particular problem are as follows. First, unlike the relation between the DC and AC windings in a saturating reactor, the input winding and the compensating winding are in inductive relation. The compensating winding is supplied through a rectifier; accordingly, there is a double-frequency ripple component in the compensating current. As a result, there will appear in the input winding a double frequency EMF of no very considerable magnitude, but, nevertheless, not to be entirely ignored. As previously discussed in connection with series or parallel AC windings, since the input winding is supplied from a rectifier, this double frequency EMF, through the half-wave rectifying action of the rectifier, sets up a certain amount of rectified current in the input winding; this component has the effect of increasing the apparent value of I_o by a small increment seldom reaching as much as 10 per cent.

This effect should be distinguished from the second harmonic which results from the series connection of the AC coils, as it has nothing whatever to do with the alternating current winding.

This parasitic rectified current emanating from the compensating current ripple may readily be eliminated by filtering the compensating winding supply. But there is no advantage in doing this. The only practical result of this phenomenon is an apparent value of I_o somewhat higher than anticipated. It may be compensated for; just as the value of I_o is compensated for, by merely setting the value of the compensating current slightly higher than would be required if the ripple be filtered out.

In other words, the only way in which this double frequency parasitic effect need be taken into consideration is that, in designing the compensating winding, it is well to figure on about 10 per cent. more compensating ampere-turns than the value arrived at on the basis of I_o alone.

Space for the compensating winding is provided for by incompletely filling the window area with the input winding. Unlike the input winding, the power necessary to deliver the necessary ampere-turns in the compensating winding is not a component in the gain; it is drawn directly from the source. Therefore, the amount of power necessary to furnish the required ampere-turns is of no significance. Because of this the compensating winding may be wound over the input winding; the increased mean length of turn is of no consequence. However, sufficient window area for the compensating winding must be provided

for to furnish a winding which will deliver the requisite ampere-turns without substantial temperature rise.

It is desirable, in designing compensating arrangements, especially in connection with the output of a first stage where the sensitivity is relatively high, to see that the over-all temperature co-efficient, inclusive of coil, rectifier, and any other current determining elements, is the same for the compensating winding as it is for the saturating winding. Since both of these circuits include elements having a temperature effect and also elements that are not responsive to temperature, it is possible to arrange that both circuits include such elements in the proper proportion. This will avoid any temperature effects in the operation of the amplifier due to ambient temperature change; or as a result of the effect of heat losses in the coils, rectifiers, resistors, etc., which might otherwise cause a difference between the response characteristics when the amplifier is put into service initially at room temperature, and the performance following the warming up period, when the structure has attained final steady operating internal temperature conditions.

MULTI-STAGE AMPLIFIERS.

As mentioned previously, and as is evident from the various curves, magnetic amplifiers of the type discussed in the present paper have only a limited range within which high gain may be obtained.

The procedure for designing a multi-stage magnetic amplifier is entirely straightforward, use being made of the various characteristic curves already presented in Figs. 5 through 13.

If we restrict our consideration, for the present, and by way of example, to magnetic cores of the same lamination size and stacking for which curves are included in this paper, the procedure in designing a multi-stage magnetic amplifier may be somewhat as follows.

Suppose we assume that the input power level applied to the first stage is to be 2 microwatts. This is − 27 VU. On referring to the proportional gain curves of Fig. 10 we see that at this input power level the mumetal core is clearly preferable and accordingly the mumetal core of Fig. 8 may be selected for the first stage.

The first stage DC winding design is actually unrelated to the design of the magnetic amplifier per se. The DC coil will consist of a winding which completely fills the lamination window space, less AC winding. The weight of a substantially full DC coil for this lamination will in general be known from previous winding experience; it can be computed if necessary.

The resistance of the first, or input, stage winding will be prescribed in accordance with the application for which the amplifier is required on exactly the same basis as in the case of a relay or any other control device. The resistance required will be a function of the internal resistance of the circuit or source from which the input is to be energized.

Accordingly, the wire size selected for the input coil will be that of which the ohms-per-pound multiplied by the full coil weight comes nearest to the value of resistance desired.

AC coil designs for each type of magnetic core material being determined, and the curves of Figs. 11, 12, and 13 being available, we refer to Fig. 8 from which we note that with an input of − 27 VU the corresponding output will be − 2.5 VU.

Referring now to Fig. 13, at this output power level we see that the optimum output circuit resistance is approximately 440 ohms. We therefore select a wire size for the second stage input DC coil such that the ohms-per-pound multiplied by the weight of the coil approaches this figure.

There is this difference between the design of the second stage DC coil and the first stage input coil. In the first stage, the DC winding completely fills up the window area with the exception of that portion occupied by the AC coil. The second stage DC coil also includes the compensating winding; thus there is less space available for the input winding. However, in the case of a first stage of mumetal the compensating excitation required is of the order of one ampere-turn or less; thus the compensating winding will probably consist of no more than one layer. This diminution of available winding space is negligible.

On referring again to Fig. 10 it is seen that, the output power level of the first stage being −2.5 VU and this power level being applied to the second stage, the proportional gain obtainable with a core of No. 4750 alloy is better than that obtainable with either mumetal or silicon steel. Accordingly, this core material is appropriate for the second stage.

From Fig. 7 we see that with an input of −2.5 VU we may expect an output of about +21.5 VU. On referring this last value to Fig. 12 a value of resistance for the third stage of about 50 ohms is indicated.

The third stage wire size is accordingly determined in a somewhat similar manner to the procedure outlined for the second stage. In this case, however, the compensating winding may comprise a number of layers and allowance may be made for this fact.

Referring again to Fig. 10, the second stage output power being 21.5 VU, it is noted that at this power level silicon steel gives a higher proportional gain than No. 4750 alloy. Accordingly, silicon steel may be the material used for the core of the third stage.

On referring to Figs. 5 and 11 we note that with an input of 21.5 VU we may expect an output for the third stage of 35.2 VU and that maximum power will be delivered by the third stage if it feeds into a resistance of about 8 ohms, which fact may be taken note of in selecting the winding of the relay or other load device which is to be energized by the amplifier output.

The procedure outlined above was indicated in reference to cores

of the same size merely because curves for these cores are included in this paper. In designing amplifiers in general especially if it be desired to build up the output power level to a higher value than that for which the core in Fig. 5 is suitable, curves similar to those included in this paper, for other and larger cores may be made use of in exactly the same way.

OVER-ALL CHARACTERISTICS.

The over-all characteristic, that is to say, the relation between the power input to the first stage and the output power of the last stage will depend to a considerable extent upon the relation, in each of the stages, between the resistance of each DC coil and the characteristics of the preceding AC winding. In other words, upon just where this resistance value lies, on a curve such as those shown in Figs. 11, 12 and 13, in relation to the power level. The curves show what the resistance should be for maximum gain. If the resistance be more, or be less than, the value shown in the curve for any given power level, the gain will be less; but the over-all characteristic of the magnetic amplifier will be different, according to whether the resistance value be higher or lower than the value prescribed for maximum gain. If it be lower the gain will increase as the input power is increased. If it be higher the gain will increase as the power level decreases. It is to be noted that, in view of the ohms-per-pound figures for the standard wire sizes, the matching of DC coil resistances with the circuit characteristics can, in any event, be only approximate.

These conditions are indicated by curves of the type referred to on page 340 as specific characteristics. Figs. 14 and 15 show curves of this type for the No. 4750 core of which the general characteristic curve is shown in Fig. 7.

In Figs. 14 and 15 curves of output VU and true gain in DB are plotted, against input VU, for three different values of output circuit resistance. That is to say, whereas in Fig. 7 the resistance value was varied for different input values so that the output power was maximalized throughout the curve, in Figs. 14 and 15 the curves are plotted for constant values of resistance.

These resistance values are chosen as follows, the curves being identified by corresponding legends.

A. The resistance value giving maximum output at lowest input power plotted.
B. The resistance value giving maximum output at the value of power input at which maximum gain occurs.
C. The resistance value giving maximum output at the highest input power plotted.

To avoid confusion, curves of output versus input are shown in Fig. 15, and curves of gain versus input are shown in Fig. 14.

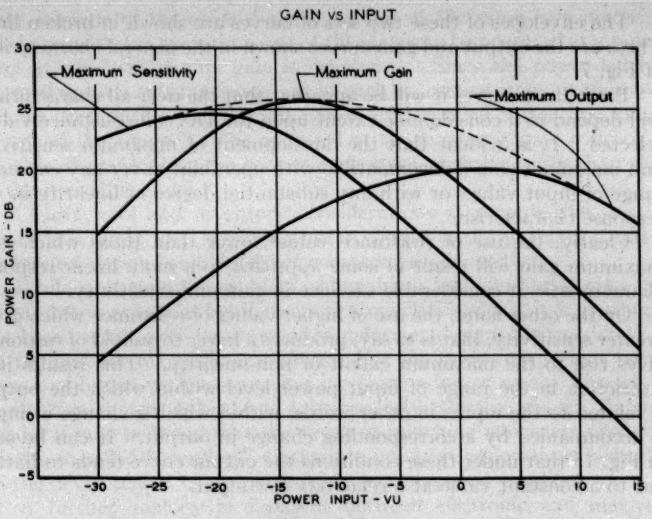

FIG. 14. Gain curves of EI-3A No. 4750 alloy core for three different values of output resistance.

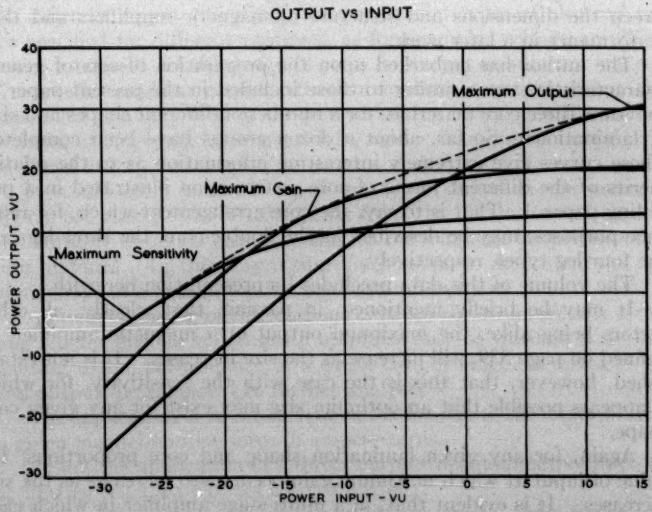

FIG. 15. Output curves of EI-3A No. 4750 alloy core for three different values of output resistance.

The envelopes of these two sets of curves are shown in broken lines. These are the output and gain curves shown in the general characteristic of Fig. 7.

From these curves it will be apparent that the over-all characteristic will depend to a considerable extent upon the DC coil resistance values selected. It is evident that the development of maximum sensitivity and maximum gain is incompatible with operability over any extended range of input values or with any substantial degree of linearity in the response characteristic.

Clearly, the use of resistance values lower than those which give maximum gain will result in some approach to a more linear response characteristic at considerable sacrifice in gain and sensitivity.

On the other hand, the use of higher values of resistance which gives greater sensitivity, that is to say, produces a lower threshold of response, gives rise to the maximum extent of non-linearity. This results in a restriction in the range of input power level within which the output is related to the input; in other words, within which a change in input is accompanied by a corresponding change in output. It can be seen in Fig. 15 that under these conditions the output curve tends to flatten out to a constant value at a relatively low input.

CORE DESIGN.

It is hoped to discuss in a more complete manner the relations between the dimensions and structure of magnetic amplifiers and their performance in a later work.

The author has embarked upon the preparation of sets of general characteristic curves similar to those included in the present paper, in the same three core materials, for a number of different shapes and sizes of laminations. So far, about a dozen groups have been completed. These curves give extremely interesting information as to the relative merits of the different forms of core construction illustrated in a preceding paper. [8] That is to say, the core arrangement which, for reference purposes, may be described as the double-core, the three-leg, and the four-leg types, respectively.

The volume of this data precludes its presentation herewith.

It may be briefly mentioned, in passing, that, clearly, all other factors being alike, the maximum output of a magnetic amplifier, as defined on page 339, will increase as the size increases. It is not established, however, that this is the case with the sensitivity, for which it appears possible that an optimum size may exist for any given core shape.

Again, for any given lamination shape and core proportions, the value of input at which maximum gain occurs also increases as the size increases. It is evident that, in a multi-stage amplifier in which each

[8] Alan S. FitzGerald, J. FRANKLIN INST., 244, 249 (1947), Fig. 1.

stage is made of the same dimensions and of the same core material, it is impossible for more than one of the stages to be operated at a power level at which maximum gain is developed. Since the power level is stepped up to a substantial extent in each successive stage, it therefore follows that, with a given input power level applied to the first stage, if each of the stages is to be operated at the maximum gain which it is capable of developing, the core of each stage must be larger than that of the preceding stage.

Clearly, tool and inventory considerations as regards dies, laminations, coil forms, etc., are somewhat in conflict with this relation and in a practical design some degree of compromise is expedient.

While mentioning the subject of punchings and lamination sizes it is of interest to note that laminations of proportions which, it is presumed, are based upon considerations of transformer design, are not likely to be the best for magnetic amplifiers. For the same core weight better gain is obtained with a somewhat increased window area. The EI-3A lamination shown in Fig. 6 is a particularly effective shape. In particular it may be noted that the types of punching which are produced by the so-called "scrapless" method do not have proportions favorable to the development of maximum gain in a magnetic amplifier.

A further analogy is apparent between electronic and magnetic amplifiers. We have seen in connection with the design of the AC winding that there are conditions tending to prescribe different voltages in the different stages. Similarly, just as special types of electron tube are specified for different purposes, as for example, voltage amplifiers, power tubes, etc., in the design of cores for output or adjacent stages in a magnetic amplifier considerations of maximum output rather than maximum gain may well be the predominating factor. In like manner in an input stage maximum sensitivity rather than maximum gain may be aimed at.

It would seem that curves of the types shown in the preceding figures are susceptible of calculation from the dimensions of the core and suitably obtained data referring to the magnetic properties of the core material. In this way it appears possible to determine the optimum shape of a lamination for any required purpose.

An understanding of the relations between the structure of a saturating reactor and its action as an amplifier may be clarified if the data relating to the performance of a single core or stage, in terms of gain and output, be subjected to further analysis.

The application of direct current excitation due to the input produces a given magnetomotive force in ampere-turns.

Again, the application of a direct current magnetomotive force to a saturating reactor produces a given output.

Thus, the gain of a single stage of a magnetic amplifier may be

divided into two contributing components:

(*a*) the ampere-turns per watt of input, or NI/p,
(*b*) the output in watts per ampere-turn, or P/NI.

The product $NI/p \times P/NI$ is P/p which is the gain.

The first term NI/p may be designated by some such descriptive expression as the saturation component; because it is a measure of the amount of saturation produced by any given input power.

The second term P/NI we may refer to as the reactance component; since it refers to the amount of reactive power to which any given degree of saturation gives rise.

Clearly, the saturation component is entirely a simple function of the window area of the punching, the mean length of turn of the DC coil, and the space factor of this coil.

The reactance component, on the other hand, is a function of the cross-sectional area of the AC magnetic path, the length of this magnetic path, and the magnetic qualities of the core material.

SATURATION COMPONENT.

This component is a function of the physical dimensions solely. The magnetic property of a core material enters only into the reactance component.

Thus, the saturation component is independent of the core material, and for any given punching and stacking is equally applicable, for example, to silicon steel, mumetal, or any other alloy.

Since the resistance of the AC winding enters to a negligible extent into the performance of a magnetic amplifier, unless the input value very greatly exceeds that at which maximum gain is obtained, the space occupied by the AC winding is a relatively minor portion of the window area and a fixed percentage allowance may be made therefor.

While the saturation component itself is not a constant, it includes a constant term. The ampere-turns are proportional to the square-root of the input power. For any given coil, the constant term consists of the turns divided by the square-root of the resistance. Thus, the saturation component is obtained by dividing this constant term by the square-root of the power. This constant term varies within a relatively narrow range of magnitude for ordinary wire sizes. For example, for coils of the paper-layer-wound type, fitting square-center-section cores of the lamination shown in Fig. 6, the value of $N/\sqrt{R}$ varies between about 330 for No. 38 conductor to approximately 360 for No. 18.

REACTANCE COMPONENT.

This component, on the other hand, refers specifically to the magnetic performance; it is a function of the incremental permeability

curve of the core material. Accordingly, the only practicable method of presentation is in the form of a curve.

For any given magnetic core, therefore, a curve may be drawn which shows the relation between the output power and the DC ampere-turns. However, due to the wide range of magnitudes involved, such a curve is not very serviceable unless the power be expressed in VU and the ampere-turns be plotted to a log scale. It then has the same general form as an output curve of the type shown in Fig. 7 in which output is plotted against VU input. This is because there is a linear relation between the VU power scale and a log NI scale. This relation includes a factor of two, because of the square function, plus the constant term $N/\sqrt{R}$. The input power and consequently the gain can therefore readily be arrived at from a curve showing the relation between the output and the DC excitation in ampere-turns.

The relations between the saturation and reactance components and the limiting values referred to previously on pages 339 and 340 are of interest. For example, it is to be noted that, for any given material, the sensitivity, or minimum input, depends more upon the saturation component than it does upon any other single factor. On the other hand, the maximum output, as previously defined, is principally a function of the reactance component; the density at which the core material saturates and the cross-section of the AC magnetic circuit are clearly the predominant elements involved.

SOME PRACTICAL DETAILS.

In practical laboratory work in connection with the development and design of magnetic amplifiers, time and effort can frequently be saved by an approach based upon the consideration of these two separate saturation and reactance components.

It is clear that, in the construction of an amplifier for service and use, unless the DC coil substantially fills the punching window area, the amplifier will not develop the full gain of which the magnetic core is capable.

On the other hand, on any occasion when it is merely required to test a single stage of a magnetic amplifier to determine its performance, the question of space factor is entirely immaterial. That is to say, any magnetic core having the proper AC winding can be tested in a completely valid manner with any DC coil with which it happens to be stacked. By referring the performance to an ampere-turn basis all necessary information may be obtained. The gain can at all times be computed from the saturation component.

This means that in the laboratory any existing core with the proper AC coil, whether or not it be stacked with any DC coil, can be studied effectively by threading one or more turns of DC excitation through

the core and furnishing the necessary ampere-turns in the form of a relatively high current flowing in a small number of turns.

In general, therefore, in any developmental activity in which a study of the performance of the magnetic core per se is the objective, it is not necessary to stack the core specially with the particular DC coil that it is finally intended to use. Tests may be made entirely on a DC ampere-turn basis either with any particular DC coil that happens to be stacked; or with a few turns of wire threaded on.

The pertinence of this technique may be illustrated by supposing that we have two similar magnetic amplifier units which, to outward appearance are the same, but which do not give the same gain. Possibly the DC coils may be different; or perhaps the number of DC turns may be unknown. Readers experienced in the development of small devices involving magnetic cores will be familiar with the fact that laminations of widely different magnetic properties are often not distinguishable by their appearance.

In such a postulated situation a single turn can nearly always be threaded through the core for furnishing DC excitation when it will be immediately apparent whether the difference in gain is to be attributed to the saturation component or to the reactance component.

The above remarks relating to testing procedure on a DC ampere-turn basis are somewhat obvious and the author trusts he may be pardoned for their inclusion. There has, however, in the past, especially during the war, at times been procurement difficulties associated with high permeability core material of which there has not always been a sufficient quantity on hand in the laboratory to provide simultaneously for all investigations in progress. Occasions can be recalled when magnetic amplifiers have had to be stacked with laminations borrowed from some other project.

Moreover, as is well known, the performance of magnetic amplifiers is so much more effective at frequencies above 60 cycles that it is very evident that the more important future developments will be associated with substantially higher frequencies. At such frequencies very thin laminations are necessary. Those readers who have ever personally stacked up a magnetic amplifier core with three-mil laminations will not require to be reminded of the desirability of avoiding an unnecessary repetition of this tiresome task. Indeed it appears more than probable that employment of very thin laminations will lead to the use of jointless cores with threaded-on windings with reference to which the foregoing comments may be even more in point.

While referring to practical methods it may be of interest to mention one rather important precaution that it is advisable to take in testing magnetic amplifiers.

It is, as a general rule, undesirable to open and close the input circuit of a high sensitivity magnetic amplifier stage in a test set-up, made for measurement purposes.

Bearing in mind that the electrical quantities involved are often associated with micro-volts and micro-amperes, it is both convenient and desirable to apply the input by means of a shunt of a relatively low and even value of resistance, as for example 1 ohm or 0.1 ohm, the input winding being energized by the voltage developed across the shunt by a current of measured magnitude flowing therein.

This avoids opening the magnetic amplifier input circuit when applying and withdrawing the input signal. Furthermore, this procedure additionally recommends itself in that it eliminates the necessity of providing instruments of very low current ranges such as must be used if the input current is read directly.

The importance of not opening the input circuit applies principally to magnetic amplifiers of the polarized type to be described in a later paper. It is, however, pertinent in reference to any magnetic amplifier which has a feed-back winding. In this case, due to the presence of the double frequency rectifier ripple, a transformer EMF will be present in the input winding. The opening and closing of the input circuit, if this be supplied, through an interrupting switch, from a source, will cause a change in the output current. This is susceptible of being inadvertently attributed to the input excitation and being interpreted as a gain; whereas in fact this phenomenon occurs entirely due to the switching action and will occur even though no DC excitation be applied.

The advisability of avoiding interruption of the DC input circuit, as a general rule, arises from the fact that in the event of a defective AC winding having unequal turns on the two coils, or a short-circuited turn, a transformer EMF will be set up in the input winding in which case closing the switch supplying the input circuit will cause an increase in the output current, and opening the switch will cause the output current to decrease, entirely irrespective of the presence or absence of any DC input. Such a coil defect is therefore susceptible of inadvertent interpretation as gain; or the apparent existence of a value of gain higher than that which is actually the true figure.

The author has included in Tables V and VI two numerical compilations which have been found to be time saving aids in magnetic amplifier work.

Because of the wide range of power levels involved, in the slide rule computation of power levels from current and resistance values, close attention is necessary in order to keep track at all times of the exact decimal magnitude. Table V enables the decimal point to be instantly checked at a glance.

The author has found that cognition at all times of the magnitude of power levels is facilitated by restricting use of the decimal exponent to multiples of three, in accordance with the practice in the writing and printing of numbers, of separating each group of three decades by commas.

The convenience of this procedure is apparent in Table VI.

TABLE V.

POWER TABLE

MICROAMPS

MICROAMPS	OHMS	10	20	30	50	70	100	200	300	500	700	1000
1		10	20	30	50	70	100	200	300	500	700	1.0
2		40	80	120	200	280	400	800	1.2	2.0	2.8	4.0
3		90	180	270	450	630	900	1.8	2.7	4.5	6.3	9.0
4		160	320	480	800	1.12	1.6	3.2	4.8	8.0	11.2	16.0
5		250	500	750	1.25	1.75	2.5	5.0	7.5	12.5	17.5	25.0
6		360	720	1.08	1.80	2.52	3.6	7.2	10.8	18.0	25.2	36.0
7		490	980	1.47	2.45	3.43	4.9	9.8	14.7	24.5	34.3	49.0
8		640	1.28	1.92	3.20	4.48	6.4	12.8	19.2	32.0	44.8	64.0
9		810	1.62	2.43	4.05	5.67	8.1	16.2	24.3	40.5	56.7	81.0
10		1.0	2	3	5	7	10	20	30	50	70	100
20		4.0	8	12	20	28	40	80	120	200	280	400
30		9.0	18	27	45	63	90	180	270	450	630	900
40		16.0	32	48	80	112	160	320	480	800	1120	1.6
50		25.0	50	75	125	175	250	500	750	1250	1750	2.5
60		36.0	72	108	180	252	360	720	1080	1800	2.52	3.6
70		49.0	98	147	245	343	490	980	1470	2.45	3.43	4.9
80		64.0	128	192	320	448	640	1280	1.92	3.20	4.48	6.4
90		81.0	162	243	405	567	810	1.62	2.43	4.05	5.67	8.1
100		100	200	300	500	700	1.0	2	3	5	7	10
200		400	800	1.2	2.0	2.8	4.0	8	12	20	28	40
300		900	1.8	2.7	4.5	6.3	9.0	18	27	45	63	90
400		1.6	3.2	4.8	8.0	11.2	16	32	48	80	112	160
500		2.5	5.0	7.5	12.5	17.5	25	50	75	125	175	250
600		3.6	7.2	10.8	18.0	25.2	36	72	108	180	252	360
700		4.9	9.8	14.7	24.5	34.3	49	98	147	245	343	490
800		6.4	12.8	19.2	32.0	44.8	64	128	192	320	448	640
900		8.1	16.2	24.3	40.5	56.7	81	162	243	405	567	810
1000		10.0	20	30	50	70	100	200	300	500	700	1000

WATTS X 10^{-12}

WATTS X 10^{-9}

MICROWATTS

POWER TABLE

MILLIAMPS

MILLIAMPS	OHMS	10	20	30	50	70	100	200	300	500	700	1000
1		10	20	30	50	70	100	200	300	500	700	1.0
2		40	80	120	200	280	400	800	1.2	2.0	2.8	4.0
3		90	180	270	450	630	900	1.8	2.7	4.5	6.3	9.0
4		160	320	480	800	1.12	1.6	3.2	4.8	8.0	11.2	16.0
5		250	500	750	1.25	1.75	2.5	5.0	7.5	12.5	17.5	25.0
6		360	720	1.08	1.80	2.52	3.6	7.2	10.8	18.0	25.2	36.0
7		490	980	1.47	2.45	3.43	4.9	9.8	14.7	24.5	34.3	49.0
8		640	1.28	1.92	3.20	4.48	6.4	12.8	19.2	32.0	44.8	64.0
9		810	1.62	2.43	4.05	5.67	8.1	16.2	24.3	40.5	56.7	81.0
10		1.0	2	3	5	7	10	20	30	50	70	100
20		4.0	8	12	20	28	40	80	120	200	280	400
30		9.0	18	27	45	63	90	180	270	450	630	900
40		16.0	32	48	80	112	160	320	480	800	1120	1.6
50		25.0	50	75	125	175	250	500	750	1250	1750	2.5
60		36.0	72	108	180	252	360	720	1080	1800	2.52	3.6
70		49.0	98	147	245	343	490	980	1470	2.45	3.43	4.9
80		64.0	128	192	320	448	640	1280	1.92	3.20	4.48	6.4
90		81.0	162	243	405	567	810	1.62	2.43	4.05	5.67	8.1
100		100	200	300	500	700	1.0	2	3	5	7	10
200		400	800	1.2	2.0	2.8	4.0	8	12	20	28	40
300		900	1.8	2.7	4.5	6.3	9.0	18	27	45	63	90
400		1.6	3.2	4.8	8.0	11.2	16	32	48	80	112	160
500		2.5	5.0	7.5	12.5	17.5	25	50	75	125	175	250
600		3.6	7.2	10.8	18.0	25.2	36	72	108	180	252	360
700		4.9	9.8	14.7	24.5	34.3	49	98	147	245	343	490
800		6.4	12.8	19.2	32.0	44.8	64	128	192	320	448	640
900		8.1	16.2	24.3	40.5	56.7	81	162	243	405	567	810
1000		10.0	20	30	50	70	100	200	300	500	700	1000

MILLIWATTS

WATTS

Table VI.

WATTS TO VU

VU = NUMBER OF DB ABOVE 1 MILLIWATT REFERENCE LEVEL
VU = DB(6MW = 0) + 7.782 DB(6MW = 0) = VU - 7.782

MILLIWATTS = WATTS X 10^{-3} MILLI-MICROWATTS = WATTS X 10^{-9}
MICROWATTS = WATTS X 10^{-6} MICRO-MICROWATTS = WATTS X 10^{-12}

WATTS X 10^{-3}	VU	WATTS X 10^{-6}	VU	WATTS X 10^{-9}	VU	WATTS X 10^{-12}	VU
1	0	1	-30.000	1	-60.000	1	-90.000
2	3.010	2	-26.990	2	-56.990	2	-86.990
3	4.771	3	-25.224	3	-55.224	3	-85.224
4	6.021	4	-23.979	4	-53.979	4	-83.979
5	6.990	5	-23.070	5	-53.070	5	-83.070
6	7.782	6	-22.218	6	-52.218	6	-82.218
7	8.451	7	-20.458	7	-50.458	7	-80.458
8	9.031	8	-20.969	8	-50.969	8	-80.969
9	9.452	9	-20.458	9	-50.458	9	-80.458
10	10.000	10	-20.000	10	-50.000	10	-80.000
20	13.010	20	-16.990	20	-46.990	20	-76.990
30	14.771	30	-15.224	30	-45.224	30	-75.224
40	16.021	40	-13.979	40	-43.979	40	-73.979
50	16.990	50	-13.070	50	-43.070	50	-73.070
60	17.782	60	-12.218	60	-42.218	60	-72.218
70	18.451	70	-11.549	70	-41.549	70	-71.549
80	19.031	80	-10.969	80	-40.969	80	-70.969
90	19.452	90	-10.458	90	-40.458	90	-70.458
100	20.000	100	-10.000	100	-40.000	100	-70.000
200	23.010	200	-6.990	200	-36.990	200	-66.990
300	24.771	300	-5.224	300	-35.224	300	-65.224
400	26.021	400	-3.979	400	-33.979	400	-63.979
500	26.990	500	-3.010	500	-33.010	500	-63.010
600	27.782	600	-2.218	600	-32.218	600	-62.218
700	28.451	700	-1.549	700	-31.549	700	-61.549
800	29.031	800	-0.969	800	-30.969	800	-60.969
900	29.452	900	-0.458	900	-30.458	900	-60.458
1000	30.000	1000	+0.000	1000	-30.000	1000	-60.000

VU TO WATTS

VU = NUMBER OF DB ABOVE 1 MILLIWATT REFERENCE LEVEL
VU = DB(6MW = 0) + 7.782 DB(6MW = 0) = VU - 7.782

MILLIWATTS = WATTS X 10^{-3} MILLI-MICROWATTS = WATTS X 10^{-9}
MICROWATTS = WATTS X 10^{-6} MICRO-MICROWATTS = WATTS X 10^{-12}

VU	WATTS X 10^{-3}	VU	WATTS X 10^{-6}	VU	WATTS X 10^{-9}	VU	WATTS X 10^{-12}
0	1.0000	0	1000.00	-30	1000.00	-60	1000.00
1	1.2589	-1	794.33	-31	794.33	-61	794.33
2	1.5849	-2	630.95	-32	630.95	-62	630.95
3	1.9953	-3	501.18	-33	501.18	-63	501.18
4	2.5119	-4	398.10	-34	398.10	-64	398.10
5	3.1623	-5	316.22	-35	316.22	-65	316.22
6	3.9811	-6	251.18	-36	251.18	-66	251.18
7	5.0119	-7	199.52	-37	199.52	-67	199.52
8	6.3096	-8	158.48	-38	158.48	-68	158.48
9	7.9433	-9	125.89	-39	125.89	-69	125.89
10	10.000	-10	100.00	-40	100.00	-70	100.00
11	12.589	-11	79.433	-41	79.433	-71	79.433
12	15.849	-12	63.095	-42	63.095	-72	63.096
13	19.953	-13	50.118	-43	50.118	-73	50.118
14	25.119	-14	39.810	-44	39.810	-74	39.810
15	31.623	-15	31.622	-45	31.622	-75	31.622
16	39.811	-16	25.118	-46	25.118	-76	25.148
17	50.119	-17	19.952	-47	19.952	-77	19.952
18	63.096	-18	15.848	-48	15.848	-78	15.848
19	79.43	-19	12.589	-49	12.589	-79	12.589
20	100.00	-20	10.000	-50	10.000	-80	10.000
21	125.89	-21	7.9433	-51	7.9433	-81	7.9433
22	158.49	-22	6.3095	-52	6.3095	-82	6.3095
23	199.53	-23	5.0118	-53	5.0118	-83	5.0118
24	251.19	-24	3.9810	-54	3.9810	-84	3.9810
25	316.23	-25	3.1622	-55	3.1622	-85	3.1622
26	398.11	-26	2.5118	-56	2.5118	-86	2.5118
27	501.19	-27	1.9952	-57	1.9952	-87	1.9952
28	630.96	-28	1.5848	-58	1.5848	-88	1.5848
29	794.33	-29	1.2589	-59	1.2589	-89	1.2589
30	1000.00	-30	1.0000	-60	1.0000	-90	1.0000

CONCLUSION.

The author would like again to point out that the general approach to, and treatment of, magnetic amplifiers in these notes is not intended to be restricted to the specific type of circuit which is shown, by way of example only, in Fig. 1.

With the exception of pages 348 and 349 it is believed that the foregoing subject matter applies, in some degree, to any type of magnetic amplifier circuit.

It is possible that the most significant feature of the foregoing notes may be the direction of attention to the relation between the comparative magnitudes of I_s and I_o and the performance of a magnetic amplifier; and to the use of the quantity proportional gain as a merit factor which embraces both the true gain and the relation between the values of I_s and I_o.

EROSION IN VENT PLUGS, THE EFFECT OF VENT DIAMETER.

BY

JAMES H. WIEGAND, Ph.D.[1]

PART II.

EXPERIMENTAL WORK.

The previous work shows that for a given chamber, powder, and vent size, the weight eroded, W, will be related to the charge by an equation of the type $W = K(C - C_0)$. The present experiments were directed at establishing first, the relation of W to the powder type and the vent size for charges above the value C_0; second, the relation of C_0 to these variables; and third, the relation of W to C in the region of charges below C_0. The first two of these deal with the conditions for melting of the vent surface, while the last deals with the conditions for chemical reaction between the hot gases and the vent surface. The experimental work was divided, therefore, into two parts; the first part dealt with a study of the melting region, and the second with experiments in the chemical region.

TABLE III.

Descriptions of Powders Used.

Army Lot No. or G. A. R. Code	Type of Powder	Grain Dimensions					
		Length, in.	Outer Dia., in.	Hole Dia., in.	Web, in.	No. of Holes	T_0 ° K.
8108	37 mm. gun	0.2449	0.0691	0.0089	0.0301	1	3430
		2500	682	88	297	1	
4173	60 mm. mortar ignition	0.0026	0.0352			0	3810
		30	0.035			0	
6912	60 mm. mortar ignition	0.0028	0.0328			0	3810
		—	—				
10952	2.36" rocket powder	4.761	0.3734	0.0630		1	3830
		4.77	375	525		1	
2	SR 4759 duPont	0.0593	0.0488	0.0176	0.0156	0	3060
		—	—	—	—		
MD							3170
RDB							3170
Charge A							3120
Charge B							3020
Charge C							2970
Charge D							2870
NCT							2770
Charge E							2570
Charge F							2370
Charge G							2320

[1] Capt., Ordnance Department, A.U.S., Ballistic Research Laboratory, Aberdeen Proving Ground, Md. Present address, Box N160, NOTS, Inyokern, Calif.

The Melting Region.

The intitial studies used the single straight erosion vent. The first powder used was Lot 8108 for the 37 mm. gun, double base powder whose description is given in Table III. Ignition was accomplished by means of a primer containing 54 grains of Al black powder, U. S. Army Specification No. 50–14-1B. A series of firings were performed at charges increasing in steps of 7.5 grams. The results were plotted

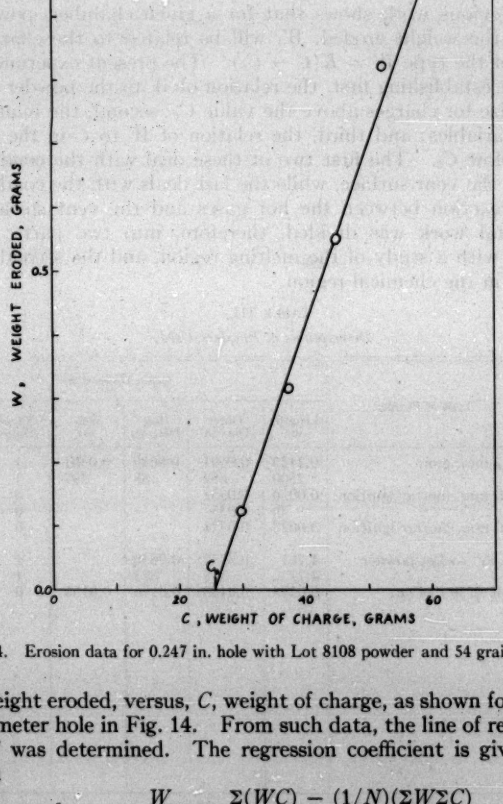

FIG. 14. Erosion data for 0.247 in. hole with Lot 8108 powder and 54 grain primer.

as W, weight eroded, versus, C, weight of charge, as shown for the 0.247 inch diameter hole in Fig. 14. From such data, the line of regression of W on C was determined. The regression coefficient is given by the equation

$$b_{WC} = \frac{W}{C - C_0} = \frac{\Sigma(WC) - (1/N)(\Sigma W \Sigma C)}{\Sigma(C^2) - (1/N)(\Sigma C)^2} \qquad (1)$$

and the intercept, C_0, is given by the equation

$$C_0 = \frac{\Sigma C}{N} - \frac{\Sigma W}{N}\left[\frac{1}{W/(C - C_0)}\right], \qquad (2)$$

using the value of $W/(C - C_0)$ as determined by Eq. 1. The regression coefficient, $W/(C - C_0)$, and the intercept on the C axis, C_0, were then plotted as functions of the diameter of the hole in the vent plug as

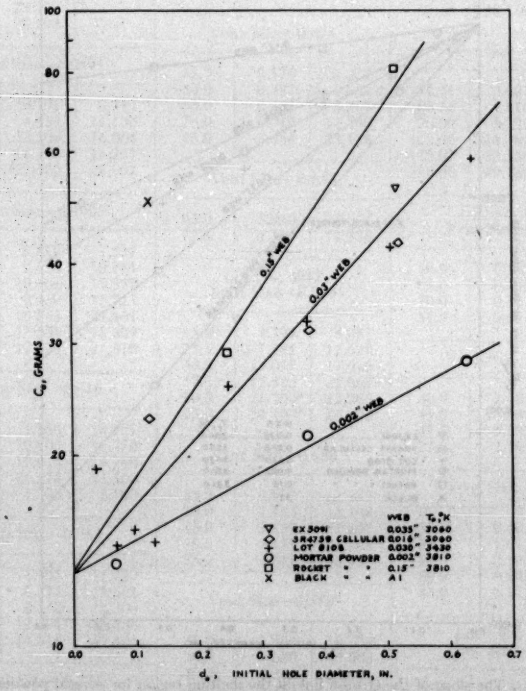

FIG. 15. The minimum charge to produce melting as a function of hole diameter for several powders.

shown in Figs. 15 and 16. The results shown there are all for SAEX1020 cold rolled steel vents.

After a complete study had been made for the Lot 8108 powder, several other powders were studied. Since there was no trap to prevent powder grains from blowing out, the question arose as to loss of powder

from this cause. Therefore, tests were made with 60 mm. mortar ignition powders Lot 4173 and Lot 6912 (descriptions are given in Table III) which are extremely fast, and following this, a very large web of powder was used in the form of $\frac{3}{8}'' \times \frac{1}{16}''$ rocket powder. With this large web, a trap was necessary for large vents and this was made from a piece of one inch standard iron pipe with a cover welded on, and with a

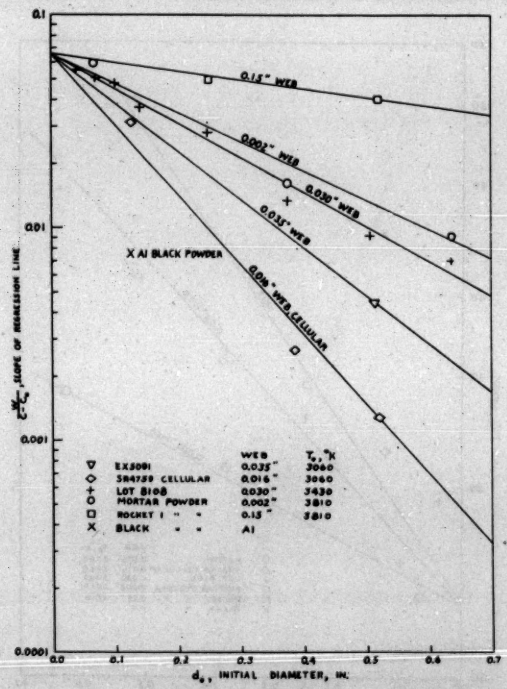

FIG. 16. The slope of the erosion line in the melting region for several powders.

large number of $\frac{1}{8}''$ holes drilled in the pipe and cover. This trap was held in place by a shoulder fitting the recess into which the vent plug was placed.

The necessity of the trap for the large web powder when used with large vents was demonstrated by several shots fired without the trap using a $\frac{5}{8}$ inch vent. A board, about $\frac{3}{4}$ inch thick, was placed a few feet from the vent and after the firing, large pieces of powder were found

TABLE IV.

Summary of Results on Single Erosion Vents.
All tests used primer containing 54 grains of black powder.

Lot No. 8108
Vent Size—0.070

Charge	Erosion	Press.
15.0	1.668	8,168
22.5	6.686	11,757
30.0	12.287	16,899
37.5	19.071	21,388
45.0	22.179	
45.0	25.892	

Vent Size—0.0995

15.0	0.191	6,443
22.5	4.459	11,100
30.0	12.200	16,064
37.5	14.799	14,257
45.0	22.489	25,907

Vent Size—0.1405

15.0	0.819	7,527
22.5	2.950	10,284
30.0	10.361	15,557
37.5	9.459	15,713
45.0	16.585	21,461
35.0	12.334	18,809
40.0	17.623	21,810

Vent Size—0.040

22.5	1.860	10,927
30.0	10.103	15,370
37.5	17.613	19,740
45.0	21.523	25,500
20.0	1.305	8,700

Vent Size—0.250

30.0	1.931	11,429
37.5	4.875	16,654
45.0	8.550	15,306
52.0	12.694	24,886
60.0	14.818	30,502

Vent Size—0.375

30.0	0.205	7,875
37.5	1.092	11,420
45.0	2.753	21,033
52.5	4.206	19,906
60.0	5.928	25,109

Lot No. 8108 *Continued*
Vent Size—0.504

Charge	Erosion	Press.
45.0	0.520	9,733
52.5	1.245	12,748
60.0	2.567	16,407
70.0	3.984	20,887

Vent Size—0.625

52.5	0.176	6,337
60.0	0.387	no record
60.0	0.157	8,307
70.0	0.910	12,468
85.0	3.336	23,148

Vent Size—0.638

95.0	3.910	23,074
77.5	1.182	14,388

Lot No. 6912
Vent Size—0.070

15.0	2.799	8,027
22.5	7.551	12,625
30.0	13.077	17,649
37.5	22.542	22,067
40.0	25.700*	22,965
45.0	29.190*	26,602

Vent Size—0.628

35.0	0.990	12,139
40.0	1.753	14,108
45.0	2.157	21,297
50.0	3.179	23,168
55.0	3.841	26,957

Vent Size—0.378*

35.0	1.492	19,508
30.0	1.630	15,603
40.0	3.300	22,121
45.0	5.152	no record
50.0	6.523	28,173
40.0	6.571	21,763

Lot No. 10978
Vent Size—0.250

Charge	Erosion	Press.
31.70	1.179	6,390
40.51	8.510	8,979
46.67	15.210	13,444
54.93	19.264	15,682
66.44	28.158	22,898

Vent Size—0.520

77.31	0.607	2,988
88.35	4.646	5,105
90.00	5.299	4,991
102.56	14.364	9,377
115.02	22.166	13,799
128.00	29.739	18,286

Lot No. 4759
Vent Size—0.517

50.0	0.107	18,077
65.0	0.438	27,266
70.0	0.523	27,149
57.5	0.352	22,206

Vent Size—0.125

30.0	2.483	14,361
45.0	10.808	22,935
37.5	6.582	18,356
27.0	2.705	13,100

Vent Size—0.375

35.0	0.403	13,905
55.0	1.034	25,096
40.0	0.103	17,542
50.0	0.892	22,567
45.0	0.342	no record

Lot—Ex. 5091
Vent Size—0.517

65.0	0.519	17,680
75.0	1.436	21,458
57.5	0.256	13,386
70.0	1.067	18,882

Lot—Al Black Pdr.
Vent Size—0.125

60.0	1.675	8,884
90.0	4.461	15,350
120.0	8.415	20,327
150.0	12.356	28,081

* Cartridge case retainer.

embedded in the wood, several having gone nearly through. This was not observed with the small web powders, such as Lot 8108, except for rounds with maximum pressures less than 5–10,000 p.s.i. For these reasons the trap was used with the large web rocket powder only.

Difficulty was experienced with the 60 mm. mortar ignition powder firings, the speed of burning being so rapid that the mouth of the cartridge case would fold inward. This would result in a deposit of brass

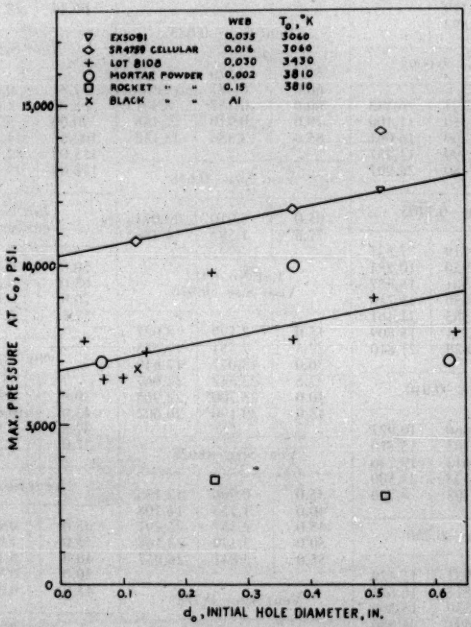

FIG. 17. Maximum pressure during a shot corresponding to the minimum charge to produce melting.

on the vent plug, apparently due to melting of the folded mouth. This difficulty was eliminated by the insertion of a close-fitting steel ring into the mouth of the cartridge case, which held the case in shape. The ring was kept in place by a shoulder fitting into the vent plug recess.

The results for all powders are given in Figs. 15 and 16, and a complete tabulation of the data is given in Table IV. The lines drawn on these figures are empirical. The convergence of all lines to a point

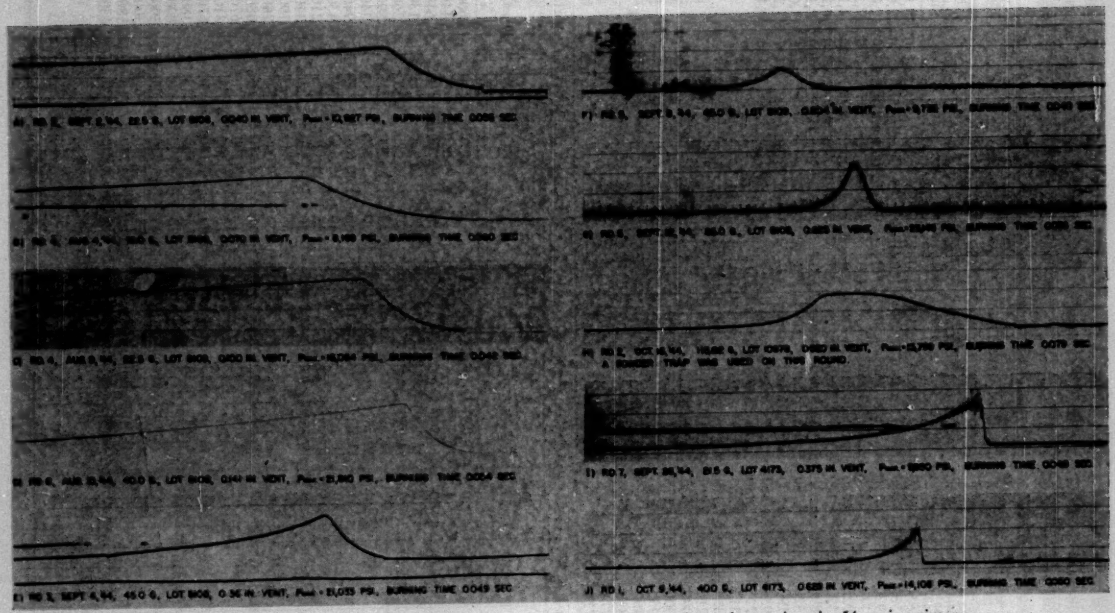

FIG. 18. Sample records taken with several sizes of vents and several powders, using the 54-grain primer.

TABLE V.

Pressure-time Value for Typical Rounds.

Time from $P_{max.}$, ms.	Pressure, p.s.i.											
	0.375 in. Vent						0.50 in. Vent			0.625 in. Vent		
	C = 15 g. Lot 4173	C = 37.5 g. Lot 8108	C = 45.0 g. Lot 4173	C = 52.5 g. Lot 8108	C = 52.5 g. Lot 4173	C = 60.0 g. Lot 8108	C = 45.0 g. Lot 8108	C = 52.5 g. Lot 8108	C = 60.0 g. Lot 8108	C = 77.5 g. Lot 8108	C = 85.0 g. Lot 8108	C = 95.0 g. Lot 8108
0	6,830	11,420	19,900	19,910	29,030	25,110	9,730	12,750	16,410	14,390	23,150	23,830
1	6,580	11,300	17,380	18,880	25,360	24,050	9,440	10,460	13,020	11,300	19,880	22,000
2	5,920	9,460	14,110	15,290	21,760	19,500	7,090	7,400	9,200	6,870	13,380	12,080
3	4,740	7,670	11,720	12,720	16,780	15,730	5,410	5,590	6,720	4,305	7,050	7,260
4	4,020	6,310	9,880	10,580	14,010	13,310	4,310	4,270	5,210	2,810	4,540	4,740
5	3,370	5,350	8,100	8,610	11,860	10,890	3,450	3,250	4,000	1,933	3,020	3,250
6	2,890	4,520	6,330	7,160	10,080	9,060	2,770	2,710	3,090	1,371	2,260	2,430
7	2,520	3,870	5,780	5,880	8,640	7,800	2,250	2,410	2,360	934	1,731	1,685
8	2,190	3,270	4,900	5,020	7,480	6,350	1,960	2,110	1,937	684	1,427	1,277
9	1,934	2,800	4,350	4,250	6,680	5,380	1,667	1,924	1,574		1,123	1,142
10	1,725	2,440	3,740	3,570	5,780	4,510	1,521	1,684	1,271		820	
11	1,517	2,200	3,260	3,050	5,160	3,930	1,374	1,503	1,150		744	
12	1,354	1,785	2,710	2,800	4,530	3,160	1,300	1,383	968			
13	1,215	1,666	2,240	2,370	3,910	2,770	1,154	1,323	968			
14	1,099	1,368	2,030	2,110	3,370	2,480		1,323				
15	1,006	1,131	1,828	1,962	3,100	2,290		1,082				
16	960			1,685		2,090		1,022				
17	890			1,600		1,898						
18	820			1,514		1,800						
19	774			1,429		1,610						
20	728			1,343		1,414						

C = 30.0 g., Lot 8108		C = 35.0 g., Lot 4173		C = 37.5 g., Lot 8108		C = 37.5 g., Lot 4173		C = 45.0 g., Lot 4173	
Time after $P_{max.}$, ms.	P, p.s.i.	Time after $P_{max.}$, ms.	P, p.s.i.	Time after $P_{max.}$, ms.	P, p.s.i.	Time after $P_{max.}$, ms.	P, p.s.i.	Time after $P_{max.}$, ms.	P, p.s.i.
0	16,890	0	18,030	0	21,390	0	22,070	0	26,600
		5	16,900	1	21,010	5	19,660	5	23,440
6	16,250	10	15,860	6	22,660	10	18,200	10	21,640
		15	15,120	11	18,790	15	16,960	15	20,130
12	14,920	20	14,080	16	17,650	20	16,080	20	18,260
		25	13,340	26	14,910	25	14,700	25	16,890
16	14,200	30	12,430	36	12,860	30	13,820	30	15,240
		35	11,820	46	10,930	35	13,090	35	13,940
21	13,420	40	10,910	56	9,620	40	11,630	40	12,430
		45	10,300	66	8,360	45	11,120	45	11,210
26	12,660	50	9,650	76	7,280	50	10,320	50	10,340
		55	8,830	86	6,420	55	9,440	55	9,190
31	11,650	60	8,350	96	5,460	60	9,000	60	8,260
		65	7,790	106	4,950	65	8,710	65	7,680
41	10,420	70	7,260	116	4,260	70	8,200	70	6,670
		75	6,790	126	3,810	75	7,400	75	6,310
51	9,100	80	6,310	136	3,580	80	7,180	80	5,670
		85	6,000	146	3,070	85	6,590	85	5,380
61	8,070	90	5,480	156	2,900	90	5,790	90	4,800
		95	5,180	166	2,690	95	5,720	95	4,590
71	7,130	100	4,960	176	2,440	100	5,350	100	4,300
		110	4,310	186	2,440	110	4,770	110	3,580
81	6,290	130	3,310			130	3,890	130	2,430
91	6,130								
101	5,090								
111	4,650								
121	4,290								

at zero hold diameter is roughly indicated, but since these figures have a vertical logarithmic scale, small differences do not show up. Consideration of these figures shows that both web and composition of the powder are important. The hotter powders give a greater rate of increase of melting with charge and a lower minimum charge to start the melting. However a larger web causes this minimum charge to be increased.

Another method of showing the beginning of melting is given by Fig. 17. In this figure are plotted the values of the pressure, P_0, corresponding to the minimum charge, C_0, as a function of hole diameter.

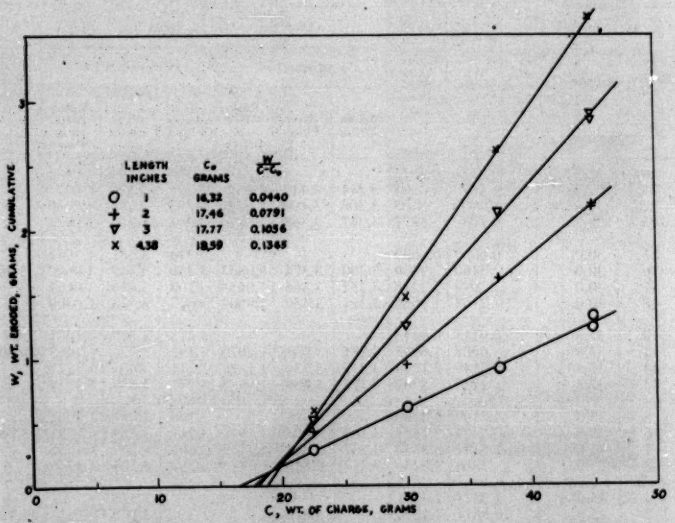

FIG. 19. Original data for the multiple erosion blocks in the melting region, with Lot 8108 powder and 54 grain primer.

Comparison of Fig. 17 with Fig. 15 shows that P_0 increases one-third over the range of vent diameters while C_0 increases from two to ten times depending on the powder. Also, as the web increases the maximum pressure corresponding to V_0 goes down. With this decrease in maximum pressure goes an increase in discharge time. This is shown for the Lot 8108 powder in Figs. 18A to 18F. A typical pressure-time curve for the large webbed rocket powder is shown in Fig. 18H; for the 60 mm. mortar powder in Figs. 18I and 18J. The burning times given in Fig. 18 are the time from ignition to maximum pressure. Typical time pressure discharge data are given in Table V.

The next step was to determine the effect of length on the rate of melting. The multiple erosion vent shown in Fig. 12 was used, together with Lot 8108 powder and 54 grain primer. Fig. 19 shows the original data for the four sections and these data are tabulated in Table VI. In the data taken in the melting region, the last section was $1\frac{3}{8}''$ long, as compared with one inch for the other three sections, so the results for this fourth section appear somewhat high in comparison.

TABLE VI.

Summary of Results on Multiple Erosion Blocks.

Section No.	Charge, g.	Length of Sect., in.	Wt. Loss, g.	Cumulative Wt. Loss, g.	Diameter of Holes at Ends, mm.						$P_{max.}$, p.s.i.
					Upstream End			Downstream End			
					Before Firing	After Firing	Ratio After to Before	Before Firing	After Firing	Ratio After to Before	
20	22.5	1	0.2811	0.2811	—	—	—	3.268	3.440	1.0526	
21	22.5	1	0.1390	4201	3.244	3.447	1.0626	3.224	3.377	1.0474	—
22	22.5	1	0.0907	5108	3.308	3.490	1.0550	3.283	3.296	1.0040	
23	22.5	$1\frac{3}{8}$	0.769	5877	3.247	3.368	1.0373	3.264	3.272	1.0024	
15	30.0	1	0.6009	0.6009	—	—	—	3.216	3.552	1.1044	
16	30.0	1	3460	9469	3.290	3.574	1.0863	3.250	3.445	1.0600	3,900
17	30.0	1	3049	1.2518	3.252	3.466	1.0658	3.208	3.420	1.0661	
18	30.0	$1\frac{3}{8}$	2168	1.4686	3.254	3.450	1.0602	3.275	3.373	1.0300	
10	37.5	1	0.9113	0.9113	—	—	—	3.275	3.819	1.1661	
11	37.5	1	6982	1.6095	3.281	3.963	1.2079	3.193	3.724	1.1663	19,600
12	37.5	1	5149	2.1244	3.215	3.736	1.1621	3.214	3.605	1.1217	
13	37.5	$1\frac{3}{8}$	4743	2.5987	3.375	3.489	1.0338	3.271	3.650	1.1159	
5	45.0	1	1.2169	1.2169	—	—	—	3.196	3.857	1.2068	
6	45.0	1	0.9484	2.1653	3.267	3.893	1.1916	3.241	3.789	1.1691	18,980
7	45.0	1	7197	2.8850	3.337	3.824	1.1459	3.261	3.769	1.1558	
8	45.0	$1\frac{3}{8}$	7386	3.6236	3.217	3.810	1.1843	3.262	3.701	1.1346	
1	45.0	1	1.3221	1.3221	—	—	—	—	3.876	—	
2	45.0	1	0.8671	2.1892	—	3.873	—	—	3.762	—	23,650
3	45.0	1	6594	2.8486	—	3.756	—	—	3.639	—	
4	45.0	$1\frac{3}{8}$	0.0039	2.8447	—	3.639	—	—	3.673	—	

The effect of contracting taper on erosion has been shown by Figs. 5 and 6 from the Greaves, Abram, and Rees data. A contrasting series was run with the multiple erosion assembly using an expanding taper in the third section, of $\frac{1}{8}''$ initial diameter, for the first two sections to final diameters of $\frac{3}{16}''$, $\frac{1}{4}''$, $\frac{5}{16}''$, and $\frac{3}{8}''$, for the last of the four sections. After the firings, the tapered sections were cut in two lengthwise. Fig. 20 shows pictures of these four tapered sections and the weight losses of all sections are given in Table VII.

The weights actually lost by the tapered sections do not tell the whole story, however. A close examination of Fig. 20 will reveal that

all except the $\frac{1}{16}$"taper section are eroded for only a part of their length. Also, the diameter at the end of the eroded portion is nearly the same in all cases, indicating that when a certain expansion is reached, the erosion stops. If the weights lost are divided by the length eroded,

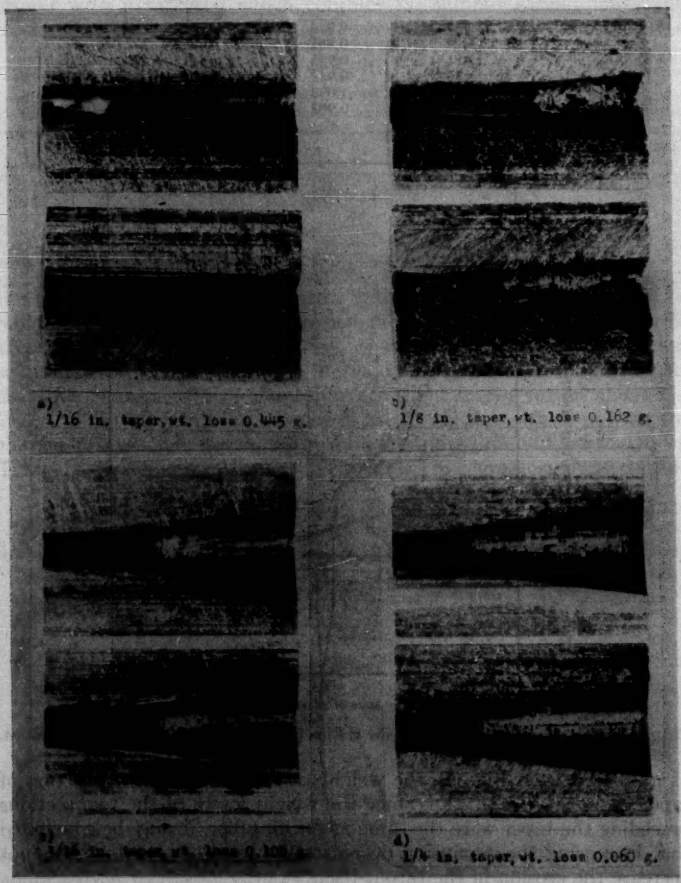

FIG. 20. Third sections of $\frac{1}{4}$ in. multiple erosion vents showing effect of increasing taper in one inch length. Each was preceded by two $\frac{1}{4}$ in. straight sections and followed by one straight section of the larger diameter. The direction of gas flow was from left to right. The charge was 45 g. of Lot No. 8108 powder ignited by 54-grain primer.

A18415

TABLE VII.

Results on Tapered Section Tests.

Final Dia., in.	Weight Loss of Individual Sections, Grams			
	1	2	3 Tapered	4
1/2	1.217	0.948	0.720	0.739
1/4	1.322	0.867	0.659	—
3/16	1.181	0.985	0.445	0.005
1/8	1.187	0.942	0.162	0.001
5/16	1.218	1.093	0.100	0.003 gain
3/8	1.120	0.902	0.060	0.001 gain

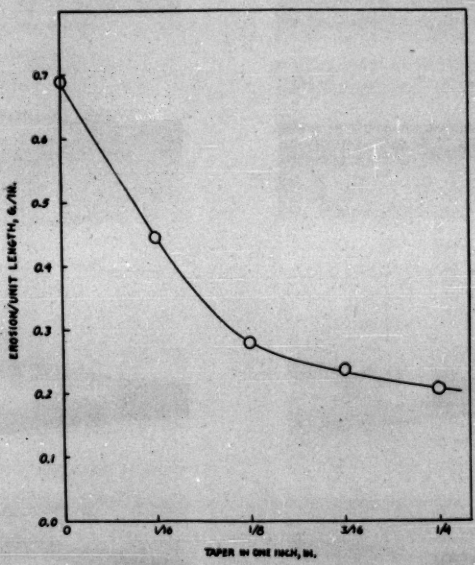

FIG. 21. Effect of expanding taper on the erosion per unit length of the expansion section.

as measured from Fig. 20, the weight per unit length as a function of taper is shown in Fig. 21. Since the weight losses of the two sections preceding the taper were the same as for no taper, it may be concluded that increasing the expansion decreases the total erosion but does not decrease the erosion in the throat itself.

The Chemical Region.

The work on the region above C_0 showed that the erosion there was severe. The erosion produced by charges less than C_0 is much less,

but is appreciable, particularly on repeated firings. The possibility of chemical factors being important in this region was next considered. The work of Mittasch (5) and of Schlect and Naumann (7) indicated that sulphur was a promoter for the reaction between CO and Fe to form iron carbonyl. Then, replacing the 54 grains of black powder in the primer with a material which contains no sulphur should lower the erosion if this chemical mechanism were important. Table VIII gives

TABLE VIII.

Effect of Powder Used in 54 Grain Primer on Erosion in Melting Region.

Wt. of Primer Load, Grains	Powder in Primer	Vent Dia., in.	C_0	$W/(C-C_0)$
54	Al black powder	0.07	14.4	0.052
15.4	60 mm. mortar ignition	0.07	14.6	0.056
54	Al black powder	0.100	15.2	0.048
7.7	Guncotton	0.100	13.2	0.055

the results of using 60 mm. mortar ignition powder and guncotton to replace black powder on the erosion in the melting region. Both of these substitutions have the effect of increasing the rate of melting somewhat, but neither changes the value of C_0 much. It is apparent that the chemical effects of sulphur are slight in the region above C_0. When the mortar ignition powder is used to replace black powder for charges below C_0, however, the results are quite different, as shown by Table IX. While the smallest vent shows the greatest decrease due

TABLE IX.

Effect of Powder Used in Primers on Erosion in the Chemical Region.

Primer	Wt. of Primer Load, Grains	Powder Used in Primer	Charge of Propellant, Grams	Propellant Powder, Lot No.	Dia. of Vent, ins.	Erosion in 10 Shots, Grains
A	54	Al black powder	10	8108	0.14	0.300
A	15.4	60 mm. mortar ignition	10	8108	0.14	0.040
B	150	Al black powder	40	8108	0.625	0.724
B	150	80% KNO_3–20% activated charcoal	40	8108	0.625	0.278
A	54	Al black powder	20	6912	0.500	1.095
A	15.4	60 mm. mortar ignition	20	6912	0.500	0.389

to the elimination of black powder, all of the data indicate a reduction of 60 per cent or more. The results given in Tables VIII and IX lend confirmation to the hypothesis that melting occurs above C_0, but that below C_0 the erosion is chemical in nature.

In obtaining the results given in Table IX, 60 mm. mortar ignition powder could not be used to ignite the Lot 8108 powder with the large

vents because it blew most of the Lot 8108 powder out of the gun before it was ignited. Since this did not happen to as great an extent with black powder, it was felt that a primer powder more closely duplicating the performance of black powder would be required. It was found that an 80–20 mixture of KNO_3 and activated charcoal would work well in a large primer, containing 150 grains of Al black powder, but would not work well in the small 54 grain primer. Results were obtained with the 54 grain primer by using the 60 mm. ignition powder as the main charge as well as in the igniter. The ignition powder ignited so fast that satisfactory burning was obtained.

Further confirmation of the results of Table IX is found in the following table of results for a 0.065 inch hole, 10 grams of 8108 powder, and the 54 grain primer filled as indicated. New vents were used for the second series, which used the mortar powder.

TABLE X.

Chemical Erosion Test on Multiple Vent Assembly With a 0.065 in. Dia. Vent and 10 Grains of Lot 8108.

Rounds	Priming Material in Primer	Block 1	Block 2	Block 3	Block 4
0–10	54 grains Al black powder	0.856	0.546	0.123	0.013
10–20	54 grains Al black powder	330	175	0.034	0.100
20–30	54 grains Al black powder	408	266	0.030	0.016
30–40	54 grains Al black powder	317	0.093	0.017	0.038
0–10	15.4 grains 60 mm. mortar ignition powder Lot 4173	0,028	0.000	0.036 gain	0.051 gain
10–20	15.4 grains 60 mm. mortar ignition powder Lot 4173	0.020	0.068	0.043 gain	0.017 gain

A further set of experiments was performed to determine the effect of taper on the chemical erosion. The results are shown in the following table for a $\frac{3}{16}$ inch diameter hole, with the third section tapering as shown. The primer was the 54 grain type, and the charge was 10 grams of Lot 8108.

TABLE XI.

Chemical Erosion of Tapered Section.

Final Diameter, Inches	Loss During Rounds	Loss in Weight of Blocks, Grains			
		Block 1	Block 2	Block 3	Block 4
$\frac{3}{16}$	0–10	0.302	0.099	0.051	0.019
	10–20	0.051	0.019	0.014	0.000
$\frac{1}{4}$	0–10	0.268	0.076	0.043	0.014
	10–20	0.148	0.041	0.045	0.011
$\frac{5}{16}$	0–10	0.298	0.097	0.028	+0.008 gain
	10–20	0.185	0.055	0.037	0.008
$\frac{3}{8}$	0–10	0.326	0.156	+0.013 gain	+0.004 gain
	10–20	0.164	0.065	0.011	0.036

In connection with the actual erosion in a weapon, one other experiment was performed. An 8–32 screw was placed across the hole of a $\frac{1}{2}$ inch vent and fired with the 54 grain primer and 30 grams of 8108. The threads were all eroded off the upstream side of the screw and the loss in weight of the screw was 0.684 grain. This was repeated using a smooth round taper pin, size $\frac{1}{4}$ inch, and the pin was eroded only 0.028 grain. This indicates that if a surface with small projections is in the path of the gases, these projections are readily eroded even in the chemical region. This would indicate that the balance between the chemical region and the melting region is one of heat transfer as well as the heat required to heat a particular section to its melting point. Thus a design which exposes relatively large area per unit mass of metal will melt at a low value of C_0.

ANALYSIS OF MELTING DATA.

The data taken on the melting region can be analyzed by heat transfer theory as has been shown by Soodak (9). He derived the followed equation.

$$W = \frac{\rho_s f c_p C L}{E r_0}\left[\frac{2}{\gamma(\gamma+1)} \cdot T_0 - T_m\right], \qquad (3)$$

where

W = total weight lost by the vent, g.,
ρ_s = density of the metal, g./cc.,
f = Fanning fraction factor,
c_p = specific heat of the powder gas at constant volume, cal./(g.)(° C.),
C = weight of powder charge, g.,
L = length of vent, cm.,
E = heat required to heat unit volume of metal from ambient temperature to molten state, cal./cc.,
r_0 = radius of vent, cm.,
T_0 = flame temperature of powder gas, ° K.,
T_m = melting point of vent metal, ° K.,
γ = ratio of specific heats of powder gas.

Equation 3 was derived on the assumptions that a steady state of melting has been reached, that the wall of the vent is a plane, i.e., that r_0 is large compared with the thickness of the heated layer, and that there is no heat loss from the powder gases while in the vent. Soodak showed that for the Greaves, Abram, and Rees experiments, the time of discharge was great enough that the steady state assumption was applicable, but that the vent radius was too small (one mm.) for the assumption of a plane wall to apply accurately. The equation did, however, give good general agreement with the Greaves, Abram, and Rees data.

Eq. 3 will be considered in some detail and can be altered slightly for use as follows: We can let $2T_0/\gamma(\gamma + 1)$, the temperature in the throat of the vent, be represented by T', and let the ratio of E/ρ_s be represented by H_m, which is the heat required per unit mass rather than per unit volume. With these substitutions, Eq. 3 becomes

$$W = \frac{fc_pCL(T' - T_m)}{H_m r_0}. \tag{4}$$

This equation indicates that the higher the flame temperature of the powder, the greater will be the erosion. Further the greater the melting point and the heat required to bring the metal to the melting point, the smaller will be the erosion. For a given metal and powder, the erosion should be a function of weight of charge, C, length of vent, L, and radius of vent r_0.

Soodak also considered small chamber work. For this case, the solution was quite difficult as a numerical calculation of the unsteady state equations has to be made for each case. In the case of the unsteady state, the thermal conductivity does become a factor.

The data given in the experimental section of this paper and the data of Greaves, Abram, and Rees indicate that the relations given by Eq. 4 for the interdepencence of W, r_0, C and L do not agree with experiment. It is apparent first, that the term C should be replaced by the term $(C - C_0)$, since the data indicate the melting to be essentially zero at C_0; second, as is evident from Table VI, the erosion does not increase proportionally to L; and third, as r_0 approaches zero, the erosion does not approach infinity as indicated by Eq. 4. It is true that for the Lot 8108 powder and vents of 0.10 in. diameter and greater the data do give good agreement with a straight line of the equation

$$\frac{W}{C - C_0} = \frac{0.005}{d_0}. \tag{5}$$

With regard to the L term, however, it was assumed by Soodak, that no cooling of the gas occurred in the vent. The effect of cooling can be derived as follows:

Eq. 4.2 of Soodak's thesis can be written, for the rate of melting per unit area at a distance along the vent, L, where the gas temperature is T_L:

$$\frac{dw}{dt} = \frac{h(T_1 - T_m)}{E/\rho_s} = \frac{h(T_L - T_m)}{H_m}. \tag{6}$$

Eq. 3.42 of Soodak's thesis gives the rate of change of temperature with distance along the vent as

$$-\frac{dT}{dL} = \frac{f\gamma}{r_0}(T_L - T_m), \tag{7}$$

which may be integrated between the limits of temperature at the throat, T_g, to the temperature at L, T_L,

$$\int_{T_g}^{T_L} \frac{dT_L}{T_L - T_m} = -\int_0^L \frac{f\gamma}{r_0} dL, \tag{8}$$

to give

$$T_L - T_m = \frac{T_g - T_m}{e^{f\gamma L/r_0}}. \tag{9}$$

Substituting from Eq. 9 for $(T_L - T_m)$ in Eq. 6, we get for the weight melted per unit area at distance L from the entrance:

$$w_L = \int_0^{w_L} dw = \frac{1}{H_m e^{f\gamma L/r_0}} \int_0^{t_m} h(T_g - T_m)dt, \tag{10}$$

where the limits of time are from start of melting to the end of melting.

The integral in Eq. 10, has been evaluated by Soodak. In his solution it was assumed that the gas from the whole charge passed through the vent during the time of melting. If we let C_0 be the amount of the charge whose gases went to heat the metal to melting and to final discharge after melting stopped, we get from Soodak's evaluation:

$$w_L = \frac{fc_p(C - C_0)}{2H_m e^{f\gamma L/r_0} A}\left[\frac{2T_0}{\gamma(\gamma + 1)} - T_m\right], \tag{11}$$

where A is the cross sectional area of the throat.

The total weight eroded in the length L is

$$W = 2\pi r_0 w_L dL \tag{12}$$

$$W = \frac{c_v(C - C_0)(T' - T_m)}{H_m} \int_0^L \frac{f\gamma e^{-f\gamma L/r_0} dL}{r_0}. \tag{13}$$

Integrating, we get

$$\frac{W}{(C - C_0)} = \frac{c_v(T' - T_m)}{H_m}(1 - e^{-f\gamma L/r_0}) \tag{14}$$

and by comparison, Eq. 4 can be written, with the use of C_0 as suggested above:

$$\frac{W}{(C - C_0)} = \frac{c_v(T' - T_m)}{H_m} \frac{f\gamma L}{r_0}. \tag{15}$$

Soodak calculated values of f from Eq. 3 for the data of Greaves, Abram, and Rees. His calculations can be modified to allow the use of C_0. For a mild steel, CMS in Table I, $W/(C - C_0) = 0.393$ for a 2 mm. by 25.4 mm. vent in a 1000 cc. vessel. Soodak took $c_p = 0.44$ cal./(° C.)(g.), $H_m = 300$ cal./g., $\gamma = 1.23$, and $T_m = 1800°$ K. The propellant composition as given in Table III was guncotton 65 per cent., nitroglycerin 30 per cent., and mineral jelly 5 per cent, for which

Greaves, Abram and Rees gave an estimated flame temperature of 2900° C. Then in Eq. 15, $c_s(T' - T_m)/H_m$ is $0.36 \times 510/300$ or 0.61. For the calculation of L/r_0, Soodak calculated the average r_0 as 2.7 mm. Then we get

$$f = \frac{0.0393 \times 2.7}{25.4 \times 1.23 \times 0.61} = 0.0056$$

compared to the value of 0.004 calculated by Soodak. These values compare well with values predicted from fluid flow theory for a roughness parameter of about 0.002 mm. This roughness parameter is a measure of the height of the surface irregularities causing roughness.

The value of f as calculated by Soodak depends on the values taken for the other factors. Eq. 14 can be used, however, to determine f from data taken on erosion as a function of length, with γ the only factor dependent on the powder composition. If we consider that data are taken at even multiples of length L_1, then Eq. 14 can be written for the erosion of a length $L = nL_1$:

$$W_n = a(1 - e^{-nb}), \tag{16}$$

where n is an integer and $b = f\gamma L_1/r_0$. Then for the erosion of a unit section, we have

$$W_{n+1} - W_n = a(e^{-nb} - e^{-(n+1)b})$$

$$= ae^{nb}(1 - e^{-b}), \tag{17}$$

$$= e^{-nb}W_1. \tag{18}$$

Then we can write

$$b = \frac{1}{n} \log_e \frac{W_1}{W_{n+1} - W_n} = \frac{f\gamma L_1}{r_0}. \tag{19}$$

Values of f are calculated in Table XII from the data given in Table VI, taking $\gamma = 1.23$. Table XII shows that for a given charge, the value of f is essentially a constant.

Analyzing the data taken for the chemical region, Table X, we find the values of $f\gamma L_1/r_0$ for $n = 1$, 2 and 3 are 0.57, 1.12, and 0.81, respectively, giving values of f of 0.0151, 0.0298, and 0.0215, or an average f of 0.0221. The agreement of the values of f for the melting region and for the chemical region is good, but the chemical region exhibits a greater variation of $f\gamma L_1/r_0$ with length than does the melting region. The indication is that the rate of chemical erosion falls off more rapidly with length than does the rate of melting erosion.

These data indicate values of f higher than that found by Soodak by a factor of three to four. The reason for the discrepancy may lie in the value used for the flame temperature T_0. The values of 2900° C. for the flame temperature of the Greaves, Abram and Rees powder should give a large error if used as the gas temperature; due to cooling of the gases under the conditions of burning in a vented chamber.

For the Lot 8108 powder used in this work, the flame temperature is calculated at about 3120° C., with $c_v = 0.33$ cal./(g.)(° C.). If we take $W/(C - C_0) = 0.044$ for the first section of the multiple vent, and $f\gamma L_1/r_0 = 0.260$ from Table XII, the value of the gas temperature in agreement with these values is 2440° C., or 680° below the flame temperature.

TABLE XII

Calculation of f from Data on Multiple Erosion Vents.

Charge, g.	Average r_0, mm.	$W_{n+1} - W_n$, g.	$\frac{W_1}{W_{n+1} - W_n}$	$\frac{f\gamma L_1}{r_0}$	
22.5	1.677	0.2811	2.022	0.704	0.0377
22.5	1.663	0.1390	3.100	0.567	0.0303
22.5	1.674	0.0907	5.029	0.535	0.0285
22.5	1.644	0.0559*			
30.0	1.692	0.6009	1.737	0.552	0.0299
30.0	1.694	0.3460	1.971	0.340	0.0183
30.0	1.669	0.3049	3.808	0.445	0.0239
30.0	1.669	0.1578*			
37.5	1.773	0.9113	1.305	0.267	0.0151
37.5	1.769	0.6982	1.770	0.286	0.0159
37.5	1.723	0.5149	2.641	0.324	0.0179
37.5	1.724	0.3450*			
45.0	1.763	1.2169*	1.283	0.250	0.0142
45.0	1.774	0.9484	1.691	0.263	0.0150
45.0	1.774	0.7197	2.265	0.273	0.0154
45.0	1.747	0.5372*			
45.0	1.782	1.3221	1.523	0.421	0.0240
45.0	1.767	0.8671	2.005	0.348	0.0195
45.0	1.736	0.6594			

* Since the last section was 1¼ in. long, the weight loss given for the last section in Table VI was divided by 1.375 to give the values for this table.

Eq. 14 may be compared with the data directly by a method shown in Fig. 22. The equation

$$y = a(1 - e^{-bx}), \tag{20}$$

when plotted on log-log paper as log y against log x for different values of the parameters a and b, leads to a series of curves of the same shape. The curves for constant (b) and various values of (a) lie one above

another, and the curves for constant (a) and various values of (b) lie to the right and left of one another. Therefore, if a curve be constructed for $a = 1$, and $b = 1$, this curve can be drawn on tracing paper and moved up and down and to the right and left until it fits the data. The constants are then readily evaluated as Eq. 20 is asymptotic to $y = abx$ for $x \ll 1$ and to $y = a$ for $x \gg 1$.

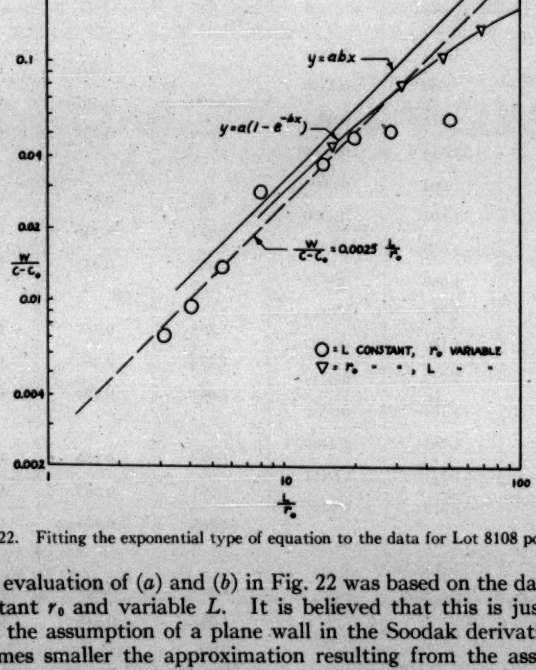

FIG. 22. Fitting the exponential type of equation to the data for Lot 8108 powder.

The evaluation of (a) and (b) in Fig. 22 was based on the data taken at constant r_0 and variable L. It is believed that this is justified in view of the assumption of a plane wall in the Soodak derivation. As r_0 becomes smaller the approximation resulting from the assumption of a plane walled vent becomes worse. Hence the data for a variable r_0 should diverge more from Eq. 20 as r_0 becomes smaller, and this is the case for such data in Fig. 22.

The constants evaluated in Fig. 22 for Eq. 14 give $c_v(T' - T_m)/H_m = 0.22$ and $f\gamma = 0.0143$. These values give $f = 0.0116$ for $\gamma = 1.23$ and the gas temperature as 2740° C. This value of f is somewhat below the minimum f from Table XII. Such values of f require roughness parameters of the order of 0.06 mm., which are not unreasonable in view of the wavy surface of the vents.

The interdependence of friction factor and gas temperature indicates that a study of gas temperatures in vented vessels would be valuable as an independent check on the friction factor. In this connection, it is not only the temperature at $P_{max.}$ that is important, but the gas temperature during the whole melting process. For long duration of escape, the heat loss to the chamber walls will be important.

CONCLUSION.

The experimental results of previous workers and of the author indicate that erosion is of two types, a melting type found above a certain minimum pressure, and a chemical type found below it. This is confirmed by agreement of the data with heat transfer theory for charges above C_0, and with expected performance in the presence of a known active chemical agent for charges below C_0. The equations developed from heat transfer theory agree with the data for all sizes of vents above those of very small diameter, e.g., 0.1 in. For these and smaller, the effect of wall curvature is great enough to require including a term evaluating this factor in the fundamental differential equation.

ACKNOWLEDGMENT.

Able assistance in the experimental work was given by T/5 B. B. Grollman and Cpl. S. Blittman and in the calculations by T/4 G. M. Johnson and T/5 F. H. Friedwald. The drawings and figures were prepared with the assistance of T/4 G. M. Johnson. Criticism and suggestions on this work were given by Mr. Kent and Drs. Ladenberg, Mayer, and Vinti of the Ballistic Research Laboratory. Several powders used were obtained from the duPont Company through the assistance of Dr. W. F. Jackson of the Burnside Laboratory.

The author is indebted to the Ordnance Department, U. S. A., for supporting this work and for permission to publish this paper.

TABLE OF NOMENCLATURE.

A	area of vent, cm².
C	weight of main charge not including igniter, g.
C_0	minimum weight of main charge to start melting, g.
E	heat required to heat unit volume of metal from ambient temperature to molten state, cal./cc.
H_m	heat required to heat unit mass of metal from ambient temperature to molten state, cal./g.
L	length of vent, cm.
L_1	length of first section of multiple vent, cm.
P	pressure, force lb./in².
$P_{max.}$	maximum pressure, force lb./in².
P_0	maximum pressure corresponding to a charge C_0, force lb./in².
T'	$= 2T_0/\gamma(\gamma + 1)$, ° K.
T_g	temperature of gas at throat of vent, ° K.

T_i initial temperature of metal, ° K.
T_L temperature at distance L along vent, ° K.
T_m melting point of the metal, ° K.
T_0 flame temperature of the powder gases, ° K.
V_0 volume of chamber, cc.
W weight of metal eroded, g.
$W_0, W_1, \cdots, W_n$ weight of metal eroded up to distance along vent equal to subscript times length of first unit, g.
a constant.
b constant.
b_{WC} regression coefficient of W on C.
c_p specific heat of powder gas at constant pressure, cal./(g.)(° C.).
c_v specific heat of powder gas at constant volume, cal./(g.)(° C.).
d_0 diameter of the vent, in.
e base of natural logarithms.
f fanning friction factor.
h heat transfer coefficient, cal./(sec.) (cm².) (° C.).
k thermal conductivity of metal, cal./(sec.) (cm.) (° C.).
n integer.
r_0 radius of vent, cm.
t time, sec.
t_m time at which melting ceases, sec.
w weight eroded up to time t per unit area, g./(cm².).
γ ratio of specific heats of gas.
ρ_s density of the metal, g./cc.
Σ summation symbol.

LITERATURE CITED.

1. DEBRUIN, G., "Smokeless Powder and the Erosion of Firearms. Short Historical Outline and Criticism of the Subject." Communiqué de la Ste. Anne "Nederlandsche Springstoffenfabrieken." No. 10, Oct. 1930.
2. DEBRUIN, G. "Smokeless Powder and the Erosion of Firearms. Experimental Part." Ibid., No. 11, Dec. 1931.
3. GREAVES, R. H., ABRAM, H. H., AND REES, S. H., "The Erosion of Guns." *Jour. of the Iron and Steel Inst.*, **117**, 113–177 (1929).
4. KENT, R. H., AND HODGE, A. H., "The Use of the Piezoelectric Gage in the Measurement of Powder Pressures." *Trans. A. S. M. E.*, **61**, 197–204 (1939).
5. MITTASCH, A., *Zeit. für angew. Chem.* **41**, 827 (1928).
6. NOBLE, A., "Artillery and Explosives," pp. 533–6, E. P. Dutton and Co., 1906.
7. SCHLECT, LEO, AND NAUMANN, MAX, "Production of Nickel and Iron Carbonyls," U. S. Patent No. 2,086,881, July 13, 1937.
8. SNAIR, W. H., AND WOOD, W. P., "The White Layer Structure in the Erosion of Machine Gun Barrels." *Trans. Am. Soc. Metals*, **27**, 608–24 (1939).
9. SOODAK, HARRY, "Effects of Heat Transfer between Gases and Solids," Thesis, Duke University, May 1943.
10. STANTON, T. E., "On the Flow of Gases at High Speeds," *Proc. Royal Soc. London*, **A111**, 757–9 (1926).
11. VIEILLE, "Etude sur les Phénomènes d'Erosion, Produit par les Explosifs," *Mémorial des Poudres et Salpêtres*, **11**, 157–210 (1901–2).

THE DYNAMICS OF NUCLEAR REACTIONS.

BY

C. E. MANDEVILLE

Bartol Research Foundation of the Franklin Institute.

ABSTRACT.

The dynamics of nuclear reactions are surveyed on an elemental basis with emphasis upon the c.g. system of coordinate axes. Corrections are given for angular distributions, angular straggling, and thin target straggling.

I. INTRODUCTION.

The elements of nuclear dynamics have been discussed by a number of writers.[1-3] This paper makes no attempt to present any new facts but rather to summarize the ideas of the previous articles and to give some additional information in what is hoped to be a clear and lucid manner. In general, the final expressions have been given in the form which has been standardized by reference (2). When any result has been different from that of reference (2), a footnote has been given. In order to aid visualization of the mechanics of nuclear reactions, free use has been made of simple geometry. The treatment is entirely non-relativistic, and great emphasis has been placed upon thinking in terms of the set of coordinate axes in which the center of gravity of the reaction is at rest.

II. BASIC EQUATIONS.

A nuclear reaction is usually considered to take place as in the self-explanatory diagram of Fig. 1. Let M_1, M_2, M_3, and M_4 refer to the masses of the incident particle, the initial nucleus, the residual nucleus, and the emitted particle. Let E_1, E_2, E_3, and E_4 and p_1, p_2, p_3, and p_4 have the same meaning in kinetic energies and momenta. Remembering the equivalence of mass and energy, the "energy release" of the reaction is defined as

$$Q = (M_1 + M_2) - (M_3 + M_4) = E_3 + E_4 - E_1. \qquad (1)$$

In practice, it is generally true that $E_2 = 0$.

If momentum is to be conserved, the momenta of the various particles will form the closed triangle of Fig. 2.[4] It follows immediately

[1] H. W. Newson, *Phys. Rev.*, **48**: 790 (1935).

[2] M. S. Livingston and H. A. Bethe, *Rev. Mod. Phys.*, **9**: 245 (1937).

[3] N. N. Das Gupta and S. K. Ghosh, *Rev. Mod. Phys.*, **18**: 225 (1946).

[4] The equations deduced from Fig. 2 and the succeeding equations are valid for mass numbers and energies in Mev. Only when computing Q directly from mass differences must accurate masses in mass units be used.

that

$$p_3^2 = p_1^2 + p_4^2 - 2p_1p_4 \cos \varphi, \quad (2)$$

$$M_3E_3 = M_1E_1 + M_4E_4 - 2(M_1M_4E_1E_4)^{\frac{1}{2}} \cos \varphi, \quad (3)$$

$$M_3(Q + E_1 - E_4) = M_1E_1 + M_4E_4 - 2(M_1M_4E_1E_4)^{\frac{1}{2}} \cos \varphi. \quad (4)$$

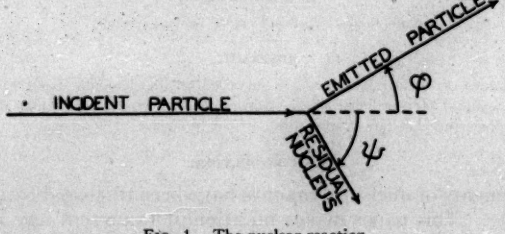

FIG. 1. The nuclear reaction.

Letting $M_3 + M_4 = M_1 + M_2 = M$, (4) becomes

$$E_4 + E_1(M_1 - M_3)/M - M_3Q/M - [2(M_1M_4E_1E_4)^{\frac{1}{2}} \cos \varphi]/M = 0. \quad (5)$$

The solution of this quadratic in $E_4^{\frac{1}{2}}$ is

$$E_4^{\frac{1}{2}} = [M_1M_4E_1]^{\frac{1}{2}}[\cos \varphi]/M \pm \left(\frac{1}{M}\right)(M_1M_4E_1 \cos^2 \varphi - M[E_1M_1 - E_1M_3 - M_3Q])^{\frac{1}{2}}, \quad (6)$$

$$E_4^{\frac{1}{2}} = \left(\frac{1}{M}\right)[M_1M_4E_1]^{\frac{1}{2}}[\cos \varphi] \pm \left(\frac{1}{M}\right)(MM_3Q - M_1M_4E_1 \sin^2 \varphi + E_1M_3M_2)^{\frac{1}{2}}. \quad (7)$$

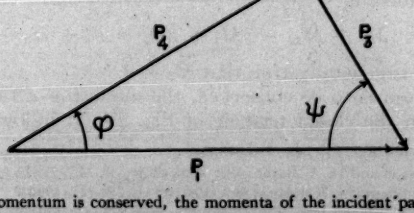

FIG. 2. If momentum is conserved, the momenta of the incident particle, the emitted particle, and the residual nucleus will form a closed triangle from which the energy of the emitted particle, a function of the angle of observation, is deduced.

Thus if E_4 is measured at some given value of φ, Q may be obtained. The significance of the fact that $E_4^{\frac{1}{2}}$ is a double value function of φ will be discussed with reference to the system of coordinates in which the center of gravity of the interacting particles is at rest (c.g. system). If subscripts (3) and (4) are interchanged, the recoil energy of the residual nucleus is obtained.

$$E_3^{\frac{1}{2}} = \left(\frac{1}{M}\right)[M_1M_3E_1]^{\frac{1}{2}}(\cos\psi) \pm \left(\frac{1}{M}\right)(MM_4Q - M_1M_3E_1\sin^2\psi + E_1M_4M_2)^{\frac{1}{2}}. \quad (8)$$

Referring the reaction to the c.g. system of coordinate axes, conservation of momentum and energy require that the following equations hold:[5]

$$\begin{aligned} &\text{(a)}\ M_1V_1^{cg} = M_2V_2^{cg}, \\ &\text{(b)}\ M_3V_3^{cg} = M_4V_4^{cg}, \\ &\text{(c)}\ (E_3^{cg} + E_4^{cg}) - (E_1^{cg} + E_2^{cg}) = Q. \end{aligned} \quad (9)$$

Also,

$$\begin{aligned} &\text{(a)}\ V_1 = V_2^{cg} + V_1^{cg}, \\ &\text{(b)}\ V_1^{cg} = (V_1M_2)/M, \\ &\text{(c)}\ V_2^{cg} = (V_1M_1)/M = (2E_1M_1)^{\frac{1}{2}}/M. \end{aligned} \quad (10)$$

Since the initial nucleus is at rest in laboratory coordinates,

$$\text{(d)}\ V_2^{cg} = V_{cgs}$$

where V_{cgs} is the velocity of the origin of the c.g. system in laboratory coordinates. From the equations above,

$$\text{(e)}\ E_1^{cg} = E_1M_2^2/M^2; \qquad E_2^{cg} = \frac{E_1M_1M_2}{M^2}; \qquad E_3^{cg} = \frac{M_4E_4}{M_3}.$$

Substitution of these values in II(9c) leads to

$$\text{(f)}\ E_4^{cg}(1 + M_4/M_3) - E_1M_2/M = Q$$

or

$$\text{(g)}\ E_4^{cg} = \left(Q + \frac{E_1M_2}{M}\right)\frac{M_3}{M},$$

the energy of the emitted particle in the c.g. system. Interchanging subscripts (3) and (4), the recoil energy of the residual nucleus in the c.g. system is found to be

$$\text{(h)}\ E_3^{cg} = \left(Q + \frac{E_1M_2}{M}\right)\frac{M_4}{M}.$$

[5] Equations II(9) and II(10) relate to the *magnitudes* of the velocities concerned.

From equations II(10g) and II(10h), the magnitudes of V_3^{cg} and V_4^{cg} are immediately obtained.

Suppose now that the velocity of the emitted particle in the c.g. system is less than the velocity of the origin of the c.g. system in laboratory coordinates. From equations II(10c), II(10g), and II(10h), it is clear that

$$\frac{MM_3}{M_4}\left(Q+\frac{E_1M_2}{M}\right) < E_1M_1, \qquad V_4^{cg}/V_{cgs} < 1, \tag{11}$$

$$\frac{MM_4}{M_3}\left(Q+\frac{E_1M_2}{M}\right) < E_1M_1, \qquad V_3^{cg}/V_{cgs} < 1. \tag{12}$$

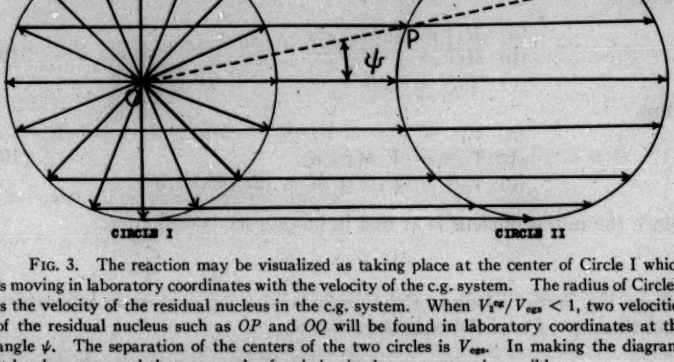

FIG. 3. The reaction may be visualized as taking place at the center of Circle I which is moving in laboratory coordinates with the velocity of the c.g. system. The radius of Circle I is the velocity of the residual nucleus in the c.g. system. When $V_3^{cg}/V_{cgs} < 1$, two velocities of the residual nucleus such as OP and OQ will be found in laboratory coordinates at the angle ψ. The separation of the centers of the two circles is V_{cgs}. In making the diagram, it has been assumed that any angle of emission in the c.g. system is possible.

It is obvious that this condition arises more frequently when the residual nucleus is under consideration. The vector diagram of Fig. 3 applies to that situation. The radius of circle I of Fig. 3 is V_3^{cg}, the velocity of the recoil nucleus in the c.g. system. To this randomly oriented radius vector is added V_{cgs}. The distance of separation of the centers of circles I and II is obviously V_{cgs}. The resultants, which will terminate on the circumference of circle II, are the various values of V_3, the velocity of the residual nucleus in laboratory coordinates. Two of the resultants, OP and OQ, are drawn in Fig. 3. Thus two resultant velocities of differing magnitudes are found at the same angle ψ in laboratory coordinates. OQ corresponds to the plus sign before the radical of equation II(8), whereas OP corresponds to the minus sign.

Consider the radius vectors OM and ON in Fig. 4, where the two circles are redrawn. OM and ON rotating in clockwise and counter-

clockwise directions, respectively, will coincide at some position OD where ψ takes on its maximum value ψ_{max}, and the discriminant of equation II(8) vanishes. From Fig. 4,

$$\sin \psi_{max} = V_3^{cg}/V_{cgs}. \tag{13}$$

No recoil nuclei will be found beyond ψ_{max}, and all of them, corresponding to both plus and minus sign before the radical of II(8), will be found in a cone about the forward direction having a half-angle ψ_{max}. Assuming an isotropic distribution of recoil nuclei in the c.g. system (which may or may not be the case), the fraction of the particles in the cone corresponding to the minus sign before the radical would be

$$\frac{1}{4\pi}\int_0^{\pi-\beta_0} 2\pi \sin\beta \, d\beta \quad \text{where} \quad \sin(\pi - \beta_0) = \frac{V_3 \psi_{max}}{V_3^{cg}} \sin \psi_{max}$$

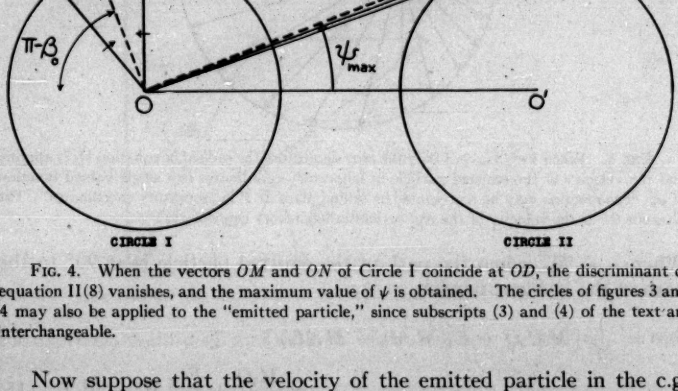

FIG. 4. When the vectors OM and ON of Circle I coincide at OD, the discriminant of equation II(8) vanishes, and the maximum value of ψ is obtained. The circles of figures 3 and 4 may also be applied to the "emitted particle," since subscripts (3) and (4) of the text are interchangeable.

Now suppose that the velocity of the emitted particle in the c.g. system is greater than or equal to the velocity of the c.g. system in laboratory coordinates. This condition does not often apply to the residual nucleus, unless Q is large and E_1 is small. In Fig. 5, V_{cgs} corresponds to the separation of the two points O and P in the circle. The vectors giving the various magnitudes of V_4 and the related values of φ now emanate from P and terminate on the circumference of the circle. The velocity of the emitted particle is thus seen to be a single value function of φ, and the energy of the emitted particle is obtained by taking only the plus sign of equation II(7). The preceding discus-

[6] β is taken positive counterclockwise from OO'. The radial vectors corresponding to the minus sign before the radical then lie in a cone of half-angle $\pi - \beta_0$ in the c.g. system.

sions obviously apply to the emitted particle and the residual nucleus interchangeably. From Fig. 5 it is also clear that only when $V_4^{cg} \geq V_{cg}$, is emission at 90° to the incident beam possible. When II(7) is squared,

$$E_4 = \frac{1}{M^2}[M_1M_4E_1\cos^2\varphi \pm 2[(E_1QMM_1M_3M_4 + E_1M_1M_2M_3M_4 - (M_1M_4E_1)^2\sin^2\varphi)^{\frac{1}{2}}\cos\varphi] + MM_3Q + E_1M_3M_2 - M_1M_4E_1\sin^2\varphi]. \quad (14)$$

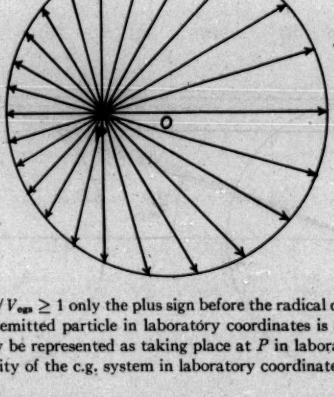

FIG. 5. When $V_4^{cg}/V_{cg} \geq 1$ only the plus sign before the radical of equation II(7) applies, and the velocity of the emitted particle in laboratory coordinates is a single valued function of φ. The reaction may be represented as taking place at P in laboratory coordinates. The distance OP is the velocity of the c.g. system in laboratory coordinates.

When $\varphi = 90°$, when the path of the emitted particle is at 90° to the path of the incident particle,

$$E_4^{90} = \frac{1}{M^2}[MM_3Q + E_1(M_3M_2 - M_1M_4)] = \frac{M_3Q}{M} + \frac{E_1}{M}(M_3 - M_1). \quad (15)$$

For φ differing only slightly from 90°.

$$E_4 = \frac{2\cos\varphi}{M}(M_1M_4E_1E_4^{90}) + E_4^{90}. \quad (16)$$

Denoting the angle between the perpendicular to the path of the incident particle and the path of the emitted particle by θ so that $\theta = \frac{\pi}{2} - \varphi$, for small values of θ,

$$E_4 = \frac{2\theta}{M}(M_1M_4E_1E_4^{90}) + E_4^{90}. \quad (17)$$

EXAMPLE: Suppose that Li^8 is produced by the reaction $Li^7 + D \rightarrow Li^8 + H^1 - 0.26$ Mev at a bombarding energy of 1 Mev. From II (13),

$$\sin \psi_{max} = \left(\frac{2}{8}\frac{1}{9}\left[-0.26 + \frac{7}{9}\right]\right)^{\frac{1}{2}} \times \frac{9}{(2 \times 2)^{\frac{1}{2}}} = 0.54,$$

$$\psi_{max} = 32.7°.$$

At $\psi = 20°$, the two energies of the recoiling Li^8 are found from II (8) to be 0.053 Mev and 0.36 Mev.

Experiments to determine the angular distribution of the disintegration products are frequently performed. The data must then be transformed to the c.g. system for theoretical interpretation.

Let the number of particles emitted per unit solid angle in laboratory coordinates be $N(\varphi)$. Then

$$N(\varphi) \sin \varphi \, d\varphi = N(\beta) \sin \beta \, d\beta, \tag{18}$$

where β and φ are clearly defined by Fig. 6 as the angles of emission in the c.g. system and the laboratory system. A relation exists between

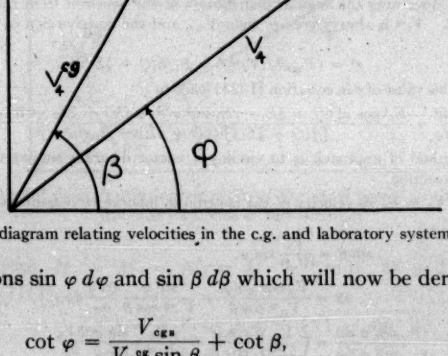

FIG. 6. Vector diagram relating velocities in the c.g. and laboratory systems of coordinates.

the expressions $\sin \varphi \, d\varphi$ and $\sin \beta \, d\beta$ which will now be derived. From Fig. 6,

$$\cot \varphi = \frac{V_{cgs}}{V_4^{cg} \sin \beta} + \cot \beta, \tag{19}$$

$$\cot \varphi = \frac{r + \cos \beta}{\sqrt{1 - \cos^2 \beta}}, \qquad r = V_{cgs}/V_4^{cg}. \tag{20}$$

This gives a quadratic in $\cos \beta$.

$$\csc^2 \varphi \cos^2 \beta + 2r \cos \beta + r^2 - \cot^2 \varphi = 0, \tag{21}$$

$$\text{(a)} \quad \cos \beta = \frac{-r \pm \sqrt{r^2 - \csc^2 \varphi \, (r^2 - \cot^2 \varphi)}}{\csc^2 \varphi}, \tag{22}$$

$$\text{(b)} \quad \cos \beta = -r \sin^2 \varphi \pm \cos \varphi \sqrt{1 - r^2 \sin^2 \varphi}.$$

Consider the case of $V_4^{cg}/V_{cg_3} \geqslant 1$. Taking the plus sign before the radical, since $\cos\beta$ is a single valued function of φ in this case, we have on differentiating

$$\frac{\sin\beta\, d\beta}{\sin\varphi\, d\varphi} = 2r\cos\varphi + \sqrt{1 - r^2\sin^2\varphi} + \frac{r^2\cos^2\varphi}{\sqrt{1 - r^2\sin^2\varphi}}. \qquad (23)^7$$

Then if $N(\varphi)$ is observed, $N(\beta)$ may be calculated.

Now suppose that $V_4^{cg}/V_{cg_3} < 1$. In this case, $\cos\beta$ is a double valued function of φ. Denoting all values of β lying within the cone of half-angle $\pi - \beta_0$ by β_1 and all values of β exterior to the cone by β_2,

$$N(\varphi) = N(\beta)\left\{\frac{\sin\beta_1\, d\beta_1}{\sin\varphi\, d\varphi} + \frac{\sin\beta_2\, d\beta_2}{\sin\varphi\, d\varphi}\right\}, \qquad (24)$$

$$N(\varphi) = \frac{2N(\beta)[1 - r^2\sin^2\varphi + r^2\cos^2\varphi]}{\sqrt{1 - r^2\sin^2\varphi}}. \qquad (25)^8$$

The minus sign before the radical of equation II(22b) relates to β_1, the plus sign to β_2.

EXAMPLE: Concerning the angular distribution of the neutrons from the reaction $D + D \rightarrow He^3 + n + Q$. V_4^{cg} is always greater than V_{cg_3}, and the positive sign of equation II(22b) applies.

$$r^2 = (V_{cg_3})^2/(V_4^{cg})^2 = E_1/6(Q + \tfrac{1}{2}E_1).$$

Substitution of this value of r in equation II (23) leads to

$$\frac{\sin\beta\, d\beta}{\sin\varphi\, d\varphi} = \frac{E_1^{\frac{1}{2}}\cos\varphi[6Q + 3E_1 - E_1\sin^2\varphi]^{\frac{1}{2}} + (3Q + 2E_1 - E_1\sin^2\varphi)}{[\frac{1}{3}(Q + \frac{1}{2}E_1)]^{\frac{1}{2}}[6Q + 3E_1 - E_1\sin^2\varphi]^{\frac{1}{2}}}.$$

An alternate method of approach is to employ a vector diagram similar to that of Fig. 6. For the $D + D$ reaction,

$V_4 = V_n$ = velocity of the neutron in laboratory coordinates.

From Fig. 6,

$$\sin\beta = \frac{V_n}{V_n^{cg}}\sin\varphi,$$

$$d\beta = \frac{V_n\cos\varphi\, d\varphi}{V_n^{cg}\cos\beta} + \frac{\sin\varphi}{V_n^{cg}\cos\beta}\frac{\partial V_n}{\partial\varphi}d\varphi,$$

$$\frac{\sin\beta\, d\beta}{\sin\varphi\, d\varphi} = \left(\frac{V_n}{V_n^{cg}}\right)\frac{\cos\varphi}{\cos\beta} + \frac{V_n}{(V_n^{cg})^2}\frac{\sin\varphi}{\cos\beta}\frac{\partial V_n}{\partial\varphi},$$

where

$$\cos\beta = \frac{(\cos\varphi)\sqrt{2E_n} - \frac{1}{2}E_1^{\frac{1}{2}}}{[\frac{1}{3}(Q + \frac{1}{2}E_n)]^{\frac{1}{2}}}.$$

V_n and $\frac{\partial V_n}{\partial\varphi}$ are obtained from equation II(7).

III. n–p SCATTERING.

The collision of a neutron with a proton is depicted in the vector diagram of Fig. 7. For this reaction, the magnitudes of the velocities

[7] Compare reference (2), equation 784a.

[8] Compare reference (2), equation 784b.

satisfy the equation

$$V_4^{cg} = V_3^{cg} = V_{cg}, \qquad \text{and} \qquad \beta = 2\varphi. \tag{1}$$

If it is assumed that the scattering is spherically symmetrical in the c.g. system,

$$N(\varphi) = \frac{\sin \beta \, d\beta}{\sin \varphi \, d\varphi} = \frac{\sin 2\varphi \, 2d\varphi}{\sin \varphi \, d\varphi}. \tag{2}$$

The total number of particles to be found in laboratory coordinates between φ and $\varphi + d\varphi$, would be

$$N_T(\varphi) \, d\varphi = N(\varphi) \, 2\pi \sin \varphi \, d\varphi = 8\pi \sin \varphi \cos \varphi \, d\varphi. \tag{3}$$

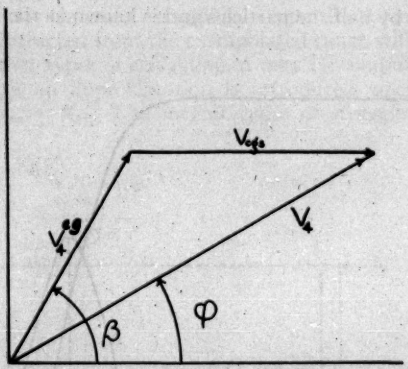

FIG. 7. Vector diagram relating velocities of the recoil proton in the c.g. and laboratory systems of coordinates.

For this reaction, $M_1 = M_2 = M_3 = M_4 = 1$ m.u., $M = 2$ m.u., $Q = 0$. By equation II(7),

$$2E_4^{\frac{1}{2}} = E_1^{\frac{1}{2}} \cos \varphi + E_1^{\frac{1}{2}} \sqrt{1 - \sin^2 \varphi}, \tag{4}$$

$$E_4 = E_1 \cos^2 \varphi, \tag{5}$$

$$dE_4 = -2E_1 \sin \varphi \cos \varphi \, d\varphi, \tag{6}$$

$$N(E_4) \, dE_4 = -N_T(\varphi) \, d\varphi = 4\pi/E_1. \tag{7}$$

The number of scattered particles per unit range of energy in the laboratory system is constant.

IV. GEOMETRIC CORRECTIONS.

There are several types of straggling which must be considered when the emitted particles of nuclear reactions are observed. Among these

are:

(*a*) Range straggling,
(*b*) Angular straggling,
(*c*) Straggling arising from target thickness.

It has long been known from experiment that range straggling obeys the well known Gaussian distribution; that is,

$$N(R)dR \cong \frac{\alpha}{\sqrt{\pi}} e^{-\alpha^2(R-R_0)^2} dR, \tag{1}$$

where $N(R)dR$ is the probability that the charged particle come to rest at a distance between R and $R + dR$ from the starting point. R_0 is the range exceeded by half the particles and is known as the mean range.

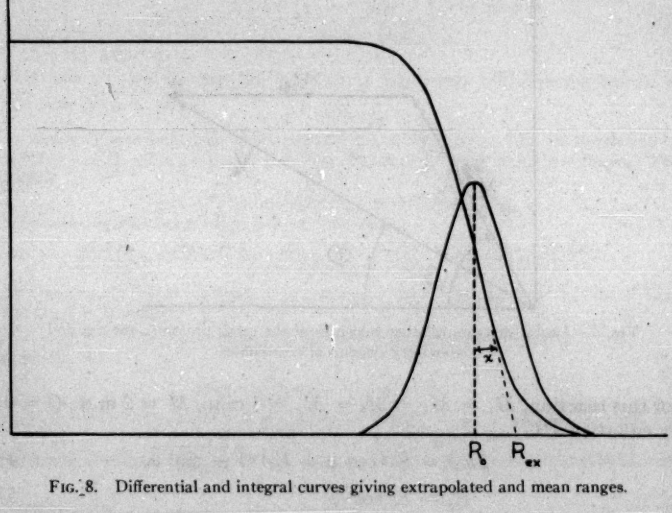

FIG. 8. Differential and integral curves giving extrapolated and mean ranges.

The average value of the mean square deviation $\overline{(R - R_0)^2}$ of the range of the particles from the mean range is given by

$$\overline{(R - R_0)^2} = \int_{-\infty}^{+\infty} \frac{\alpha}{\sqrt{\pi}} e^{-\alpha^2(R-R_0)^2} (R - R_0)^2 dR = \frac{1}{2\alpha^2}. \tag{2}$$

When experiments are performed, the mean range of the emitted particle is the sought after quantity. This mean range is usually obtained by subtracting an appropriate correction from the extrapolated range. The extrapolated range is determined by extrapolation of the

point of maximum slope of the integral curve. Differential curves are often converted to integral curves for the purpose of this convenient extrapolation. These curves are illustrated in Fig. 8. The other types of straggling simply increase the distance between R_0 and R_{ex} already introduced by normal range straggling. At $R = R_0$, the height of the integral curve is one-half its initial value. From Fig. 8,

$$2(R_0 - R_{ex}) = \tan x = -\sqrt{\pi}/\alpha,$$
$$R_{ex} - R_0 = \sqrt{\pi}/2\alpha = \Delta.$$

From IV(2),

$$\Delta^2 = \frac{\pi}{2}\overline{(R - R_0)^2}. \tag{3}$$

It is clear that, for Gaussian straggling, a quantity Δ may be computed which when subtracted from the extrapolated range will give the mean range. For other types of straggling, Δ may be computed in the same manner, though an approximation is introduced when the result is taken to be $R_{ex} - R_0$. The several types of straggling will now be considered.

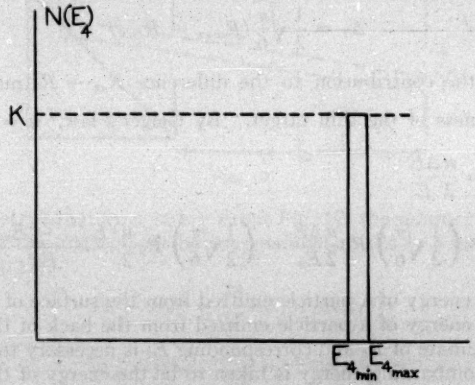

FIG. 9. $N(E_4)$ as a function of E_4 when the particles are emitted from a "thin" target.

THIN TARGET CORRECTION.

When a thin target is bombarded, the emitted particle will emerge from various depths in the target material. Assuming that the yield function of the reaction under study is constant over an energy interval as large as the thickness of the target, the number of particles produced at any given depth and thus the number of emitted particles produced per unit range interval will be constant. For small intervals of energy, for intervals of energy comparable to the thickness of the thin target, the range-energy relation may be regarded as linear so that a rectangular

function similar to $N(R)$ will describe $N(E)$. The function $N(E)$ is plotted in Fig. 9. Let $\overline{(R-R_0)^2_T}$ equal the average square value of the fluctuation of R about R_0 arising from the finite thickness of the thin target. Then,

$$\overline{(R-R_0)^2_T} = \frac{\int_{R_{min}}^{R_{max}} (R-R_0)^2 N(R)dR}{\int_{R_{min}}^{R_{max}} N(R)dR} = \frac{\int_{R_{min}}^{R_{max}} (R-R_0)^2 K dR}{\int_{R_{min}}^{R_{max}} K dR},$$

K = constant,

$$\overline{(R-R_0)^2_T} = \frac{\frac{1}{3}(R-R_0)^3\Big]_{R_{min}}^{R_{max}}}{R_{max}-R_{min}} = \frac{(R_{max}-R_{min})^2}{12},$$

remembering that $R_0 = (R_{min} + R_{max})/2$. Then

$$\Delta^2_T = \frac{\pi}{24}(R_{max}-R_{min})^2,$$

$$\Delta_T = \frac{1}{2}\sqrt{\frac{\pi}{6}}(R_{max}-R_{min}) \qquad (4)$$

and Δ_T is the contribution to the difference $R_{ex} - R_0$ made by the finite thickness of the thin target. By Geiger's law,[9] $n = \dfrac{2d(\log R)}{d(\log E)}$.

Then, $\dfrac{\Delta R}{R} = \dfrac{n}{2}\dfrac{\Delta E}{E}$,

$$\Delta_T = \left(\frac{1}{2}\sqrt{\frac{\pi}{6}}\right) R_0 \frac{n}{2}\frac{\Delta E}{E_0} = \left(\frac{1}{2}\sqrt{\frac{\pi}{6}}\right) R_0 \frac{n}{2}\frac{(E_{max}-E_{min})}{E_0} \qquad (5)$$

E_{max} is the energy of a particle emitted from the surface of the target. E_{min} is the energy of a particle emitted from the back of the target.[10] A rough estimate of R_0 and corresponding E_0 is necessary to determine Δ_T. The bombarding energy is taken to be the energy of the incident particle at the center of the thin target.

ANGULAR STRAGGLING.

Observation of the emitted particle is usually made at 90° to the incident bombarding beam in the laboratory system. However, a

[9] For values of n for this differential form of Geiger's law, see reference 2.

[10] $E_{max} - E_{min}$ is usually determined by the thickness which the thin target presents to the emitted particle. However, if the energy of the emitted particle varies rapidly with bombarding energy, and if the thin target is sufficiently thick to make that variation appreciable, an additional correction for the difference between the bombarding energy at the surface and back of the target must be made.

finite solid angle is subtended at the target by the detecting apparatus, and a spread in energy and thus in range of the emitted particle is intercepted by the detector. Since the experiment is not performed at exactly 90°, a correction must be made. Most experiments are now performed only with "good geometry" as defined by Livingston and Bethe.[2] The angular straggling of emitted particles, collimated by two square apertures of side $2a$ and separation b, will now be computed for

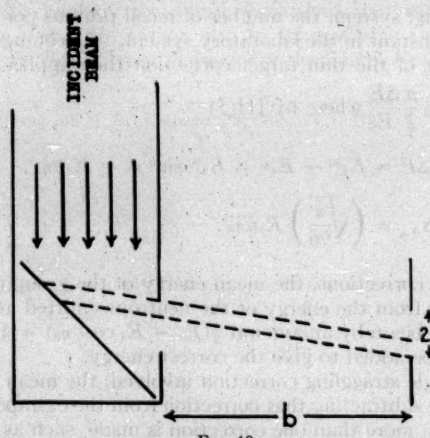

FIG. 10.

good geometry; that is, $a \ll b$. From Fig. 10, the number of particles detected at the angle θ will be proportional to $(2a - b \tan \theta)$. From equation II(17),

$$E_4 - E_4^{90} = \frac{2\theta}{M}(M_1M_4E_1E_4^{90})^{\frac{1}{2}} \tag{6}$$

and by Geiger's law,

$$\frac{R_4 - R_4^{90}}{R_4^{90}} = \frac{n}{2}\left(\frac{E_4 - E_4^{90}}{E_4^{90}}\right). \tag{7}$$

Then,

$$\overline{(R_4 - R_4^{90})^2} = \frac{\int_0^{2a/b}\left[\left(\frac{nR_4^{90}\theta}{M}\right)\left(\frac{M_1M_4E_1}{E_4^{90}}\right)^{\frac{1}{2}}\right]^2 (2a - b\tan\theta)d\theta}{\int_0^{2a/b}(2a - b\tan\theta)d\theta} \tag{8}$$

$$\overline{(R_4 - R_4^{90})^2} = \frac{2}{3}\frac{a^2}{b^2}\frac{n^2}{M^2}(R_4^{90})^2\left(\frac{M_1M_4E_1}{E_4^{90}}\right), \tag{9}$$

$$\Delta_A = \sqrt{\frac{\pi}{3}}\frac{n}{M}\frac{a}{b}R_4^{90}\left(\frac{M_1M_4E_1}{E_4^{90}}\right)^{\frac{1}{2}}. \tag{10}$$

RECOIL PROTONS.

As has long been known, the most precise method of observing neutron energies is simply the measurement of the proton's recoil energy arising from a head-on collision with the neutron. In order to obtain sufficient intensity, proton recoils making an angle as great as some arbitrary limit η_0 are usually accepted. The straggling of the neutrons is then increased. By III(7), it is seen that assuming spherical symmetry in the c.g. system, the number of recoil protons per unit interval of energy is constant in the laboratory system. A rectangular function similar to that of the thin target correction then applies. By IV(5), $\Delta_{A_n} = \frac{1}{2}\sqrt{\frac{\pi}{6}} R_0 \frac{n}{2} \frac{\Delta E}{E_0}$ where by III(5)

$$\Delta E = E_4^{90} - E_4^{\eta_0} = E_4^{90} \sin^2 \eta_0 = E_4^{90} \eta_0^2, \tag{11}$$

$$\Delta_{A_n} = \left(\sqrt{\frac{\pi}{96}}\right) R_0 n \eta_0^2. \tag{12}$$[11]

After all other corrections, the mean energy of the group of recoil protons will differ from the energy of the neutrons emitted at exactly 90° to the incident beam by an amount $\frac{1}{2}(E_4 - E_4 \cos^2 \eta_0) = \frac{1}{2} E_4 \eta_0^2$. This amount must be added to give the correct energy.

Were a single straggling correction involved, the mean range would be obtained by subtracting that correction from the extrapolated range. However, when more than one correction is made, such as range straggling, straggling arising from target thickness, and angular straggling, the corrections are combined so that

$$\Delta = \sqrt{\Delta_R^2 + \Delta_A^2 + \Delta_T^2 + \cdots}. \tag{13}$$

For corrections for normal range straggling and the range energy relation, see references (2) and (12).

EXAMPLE: The observed extrapolated range of the alpha particles from the reaction $F^{19} + H^1 \rightarrow O^{16} + He^4$ was found to be 6.03 cm. of standard air at a bombarding energy of 0.85 Mev. The target thickness was estimated to be 30 Kev for the incident protons and 67 Kev for 7 Mev alpha particles. The beam was defined by two rectangular slits having a width of 0.3 cm. and a separation of 3 cm.; $n = 3.18$ (Fig. 35, reference 2), the range correction, 1.12 per cent. (Fig. 37, reference 2). From equation IV(10), the angular straggling correction is given by

$$\frac{\Delta_A}{R_4^{90}} = \sqrt{\frac{\pi}{3}} \frac{n}{M} \frac{a}{b} \left(\frac{M_1 M_4 E_1}{E_4^{90}}\right)^{\frac{1}{2}} = 1.02 \left(\frac{3.18}{20}\right)\left(\frac{0.15}{3}\right)\left(\frac{4 \times 0.835}{7.1}\right)^{\frac{1}{2}} = 0.56\%.$$

By equation IV(5),

$$\frac{\Delta_T}{R_4^{90}} = \frac{1}{2}\sqrt{\frac{\pi}{6}} \frac{n}{2} \frac{E_{max} - E_{min}}{E_0} = 0.36 \left(\frac{3.18}{2}\right)\left(\frac{0.067 + \frac{1}{4}(0.03)}{7.1}\right) = 0.6\%.$$

[11] Compare reference (2), equation 809.

The final percentage to be subtracted from the observed extrapolated range is

$$\sqrt{(1.12)^2 + (0.56)^2 + (0.6)^2} = 1.38\%.$$

The mean range of the alpha particles is then 5.95 cm. From the range-energy relation[2,12] and equation II(15), Q is readily determined.

ACKNOWLEDGMENTS.

The writer wishes to thank professor W. E. Bennett of the Illinois Institute of Technology for many discussions and suggestions with regard to the text. He wishes also to acknowledge the interest and advice of Dr. W. F. G. Swann, Director of the Bartol Research Foundation.

[12] M. G. Holloway and M. S. Livingston, Phys Rev. **54**, 18 (1938).

Machinery vs. Jobs.—An editorial in *Compressed Air Magazine*, Vol. 52, No. 4, states: "Untold millions of words and hours have been spent in arguing whether machinery makes more or fewer jobs. The man who has just lost a job through the introduction of labor-saving machinery is naturally hard to convince that technologic advances create employment. Yet that same man would hardly advocate that his city should junk its snow-handling equipment and return to shoveling snow into horse-drawn wagons. Nor does he go home and tell his wife to throw out her washing machine, vacuum cleaner, and other mechanical aids that do much to make life easier for her. Neither can we conceive that, if he were suddenly to acquire a factory, he would attempt to run it without the best machinery obtainable. We also feel certain that his office force would use typewriters and other modern business machines.

"The point we desire to make is that there is more to the argument than whether machinery increases or decreases employment. The subject has many ramifications, one of which is that technology has brought about better living conditions in this country and, consequently, made our lot more enjoyable. During the depression, armies of men worked with picks, shovels, rakes, and other implements. They were employed, but they weren't very happy.

"The best pay and the most leisure come when people can multiply their productiveness through machinery. In the United States, industry now has an investment for each worker of around $6,000, and a good part of it is in machinery. There is more than 6 hp. available for each shop employee. A hundred years ago, when well nigh everything depended upon muscular effort, the average annual industrial wage was $248. In the last prewar 'normal' year of 1939 it was $1,150, and workers had 40 per cent. more time to themselves than their forefathers of a century ago."

R. H. O.

Inert Gas Filled Synchronous Motors.—Two special 300-hp., 240-r.p.m. inert-gas-filled synchronous motors now being built by the General Electric Company for use in an inflammable atmosphere incorporate all necessary features into one simple, smooth design. The enclosure has built-in coolers and a sealed chamber which is filled with a noncombustible gas. The gas is under sufficient pressure so that any leakage will be outward and no air or inflammable gas will get into the motor.

By removing only one access cover, the field leads, stator leads, terminal boards, and bridge resistors for the temperature relay are all within easy reach. There are no bumpy terminal boxes to mar the smooth external lines of the motors.

The inert gas follows unrestricted flow lines in the cooler, which is located over the motor, to give efficient heat transfer. The cooler can be removed for inspection or maintenance.

Resistance temperature detectors are imbedded in the stator windings. They are used with a temperature relay to remove the motor from the line in the event that the maintenance man forgets to turn on the cooling water, or if the temperature of the stator windings becomes excessive for any other reason.

R. H. O.

NOTES FROM THE NATIONAL BUREAU OF STANDARDS.*

THE MASS SPECTROMETER IN GAS ANALYSIS.

The mass spectrometer, one of the newer analytical instruments, has shown itself to be a remarkably useful apparatus in the analysis of gases and complex mixtures of gases. Many industries, such as gas, petroleum, chemicals, and rubber, rely heavily on gas analysis, and any improvement in methods or apparatus is of far-reaching importance. Although established chemical methods have long yielded valuable information concerning compositions of gases, they have serious limitations. The mass spectrometer offers an entirely new and different instrument for this type of analysis. It can in one operation resolve a very complex mixture of gases in a few moments of instrument time, although subsequent computing may require hours or even days, depending upon the complexity of the mixture and the method of computation employed.

The nearest approach to a real qualitative and quantitative system of gas analysis that has yet been devised is offered by the mass spectrometer. Gas analysis is in some respects the most curious branch of analytical chemistry. No other kind of analysis of equal importance is so totally devoid of a definite system. When a mineral is analyzed, there is a qualitative system for discovering the elements and radicals present, and a quantitative system for determining the amounts of each. But when a gas mixture is analyzed by the conventional volumetric chemical methods, the kinds of gas present are deduced from typical reactions which themselves are designed to disclose the amounts of these gases. In many cases the identifying reaction is not sufficiently specific to resolve the mixture to its actual components. Thus combustion methods are incapable of identifying or estimating more than 2 hydrocarbons of a related series in any one sample.

The mass spectrometer separates various gases on the basis of the actual weight of the ions characteristically produced on dissociating each molecular species by electron bombardment. In many instances such a separation affords a clear-cut identification of each component of the mixture. Usually the quantitative resolution of the mixture may be achieved by the proper mathematical treatment of the spectrometer data; and often the qualitative and quantitative processes are simultaneously conducted as in the case of the older chemical methods.

* Communicated by the Director.

Both the mass spectrometer and the conventional volumetric chemical methods have recently been used by a group of cooperating laboratories in the analysis of a standard sample of natural gas. Twenty laboratories possessing a total of 21 spectrometers participated in the spectrometric tests, and 30 laboratories in the chemical tests. This represents one phase of study of existing methods of gas analysis by means of a nation-wide cooperative analysis of standard samples, which the National Bureau of Standards is making in cooperation with a subcommittee of the American Society for Testing Materials. (These samples are not to be confused with the regular standard samples issued by the Bureau for purchase, but are carefully prepared gas samples furnished to cooperating laboratories.) Reports of this cooperative analysis [1] give for the first time a picture of the actual state of gas analysis in this country with respect to 2 of the 3 most important methods of analysis, the third method being fractional distillation.

All analytical data, together with the average values derived from each series of analyses, have been translated from extensive tabular form to a set of frequency-distribution tests which reveal at a glance the entire story both in general and in essential detail. Each circle appearing on the frequency-distribution plots represents a value derived from a single analysis. The circles are plotted equidistant on the ordinate corresponding to their value. Thus the abscissas are values derived from the analyses, and the ordinates indicate the frequency with which these values occur. This manner of plotting shows clearly the distribution of all the results and forms a basis of a probability curve, of which the maxima are the most probable values. These graphical pictures not only save hours of study of the tabulated data, but actually make the significance of the data so self-evident that lengthy and detailed explanation of each plot is unnecessary.

In general the results are scattered considerably more than had been expected. The lack of reproducibility between laboratories clearly demonstrates for the first time the real need for standardization of analytical methods and procedure in the field of gas analysis. Although the spectrometric values show better reproductivity and closer agreement with the known composition than do the chemical values, further improvement is believed possible. As the method is new and has not yet been subject to great variations of apparatus and procedure, efforts are being made to establish a standard procedure that will lead to even better results with the mass spectrometer.

---

[1] Martin Shepherd, "Analysis of a Standard Sample of Natural Gas by Laboratories Cooperating with the American Society for Testing Materials," *J. Research NBS*, **38**: 19 (1947), RP 1759; Martin Shepherd, "Cooperative Analysis of a Standard Sample of Natural Gas with the Mass Spectrometer," *J. Research NBS*, **38**: 491 (1947), RP 1789.

PRECISION OF TELESCOPE POINTING.

The accuracy and precision of measurements made with optical instruments—whether by the surveyor determining boundaries, the gunner locating a target, the astronomer mapping the stars, or the physicist in the laboratory—depend upon the errors introduced when sighting through the telescope portion of the instrument. These errors fall into two main classes. One large group of errors arises basically because of imperfections of the mechanical mounts by which the telescope is directed, errors of the graduated circles serving as accessories to the telescope, and improper kinaesthetic relations between the type of slow movement and the reactions of the observer. Errors of this class can continually be reduced as the art of the instrument designer improves. There is also a more subtle class of errors which arise because of the limitations of the observer's eye and the fact that observations are usually made through a column of air, a turbid medium that is optically imperfect. With this group of errors the instrument designer can do little, but such errors can be profitably studied in order to determine the choice of conditions that will render their effects least unfavorable.

The latter class of errors has been comprehensively investigated by Dr. Francis E. Washer and his associates of the optical instruments laboratory at the National Bureau of Standards. Their investigations fall generally into three classifications:

(a) A study of the variation in the probable error of pointing as a function of the distance to the target. This is a direct evaluation of the manner in which the optical imperfections of the air affect the precision of pointing.

(b) A measure of the probable error of pointing, as governed by the choice of magnification, both in the laboratory where the effect of the short column of air is unimportant and for long air paths.

(c) An experiment designed to show that the difference in the precision achieved in laboratory and outdoor pointing is in fact due to the effect of the atmosphere.

To eliminate the effects of mechanical error, the telescope is mounted rigidly and left undisturbed during the course of a series of observations. The image of the target is moved with respect to the cross-hairs by means of a weak prism, placed in front of the objective and capable of rotation about its vertical axis. To make an observation, the prism is oscillated about this axis causing the image of the target to sweep from right to left of the cross-hairs. The amplitude of oscillation is successively decreased until the image of the target appears to coincide with the cross-hairs in the telescope eyepiece. The position of the prism is then noted with an auxiliary telescope and scale. The probable error, PE_s, is determined from a series of ten such observations.

The quantity, PE_s, that is determined in these experiments for the combination of telescope and observer is the probable error of a single pointing about the instantaneous "true" pointing at the time at which it is made. It is a measure of the error of a single pointing determined from a number of pointings taken rapidly, and does not contain any appreciable effect of drift.

To study the effect of range on the precision of pointing, fifteen outdoor test objects were used. These objects, readily discernible from the laboratory, were at accurately known distances 100 to 13,600 meters from the point of observation. Several series of observations were made on each target by each of two observers for a variety of outdoor weather conditions. For such outdoor pointing, no appreciable difference between observers was found. The probable errors fluctuate considerably from day to day, depending on weather conditions. However, when all values for each target were averaged, the following relation between the probable error, PE_s (expressed in seconds), and range, d (meters), was derived:

$$PE_s = \pm (0.064d^{\frac{1}{2}} \pm 0.19).$$

For practical purposes, the variation of PE_s with range can be neglected and the value

$$PE_s = \pm (0.62 \pm 0.01)$$

taken as the average for all distances and weather conditions.

In some of the experiments, a red filter was used, but no improvement in precision resulted as compared with that attained without the filter. In addition, a peculiar effect indicating a real difference between right- and left-eye pointing was noted; that is, observers tend to point more to one side of the target with one eye than with the other. In some cases this effect, found also in indoor pointing, amounts to as much as one second.

As control of conditions for outdoor pointing is not practicable, and as experience has shown that low and consistent values of PE_s are obtained indoors, the study of the effect of magnification was made on indoor targets using a special arrangement of a telescope, prism, and collimater. For these experiments the magnification was varied from 6 to 414 diameters with the brightness of the target background maintained at a level compatible with easy vision. The probable error of a single pointing, PE_s, is found to vary with the magnification, M, as indicated in the following equation:

$$PE_s = \frac{4.96}{M} + 0.07.$$

The value 4.96 seconds is the vernier acuity of the observer's eye and consequently different values for different observers may be an-

ticipated. In fact, it is possible that an arrangement of this sort used under proper conditions might prove to be a convenient means for measuring the vernier acuity of the eye.

The values of PE_s found in the work with indoor targets are very much lower than are found for the same magnification with outdoor targets. It seems probable that turbulence of the air column intervening between target and observer is the chief cause of this discrepancy. This was corroborated by a study wherein the effect of the air column could be introduced or eliminated at will. To do this a special target was placed on the tower of the Soldiers' Home, 4,710 meters from the observer at the National Bureau of Standards. The target consisted of two diagonals intersecting to form a cross. A swinging arm fastened to the top of the target could be moved into coincidence with the center of the cross (under direction of the observer) and successive settings read with the aid of a scale located at the bottom of the target.

As the image-forming light from both the intersection of the diagonals and the swinging arm traversed the same column of air to arrive at the viewing telescope, and as the setting was made with no reference to the cross-hairs in the telescope, the setting was considered to be independent of the air column. Following a series of observations of this kind, several settings were made by the observer at the telescope, using the weak prism and the cross-hairs in the telescope. The values of PE_s found by the "air-column-eliminated" method are very much lower than those found by the "air-column-present" method. They agree closely with the values for pointings with the indoor target at the same magnification.

Results of the investigations at the National Bureau of Standards prove conclusively that the influence of the air column limits the ultimate precision obtained by telescope pointing for outdoor targets. From a study of data on pointing, it is evident that there is little gain in pointing accuracy as a result of increasing the magnification above 20 diameters although high magnification may still be used to advantage for distinguishing detail.

DDT Makes Playgrounds Safer. The dog tick that spreads the Rocky Mountain spotted fever is another of the many pests for which DDT is proving a practical and inexpensive control. This is good news for mothers who have worried over the possibility of ticks attaching to children even when they were playing safely in the back yard or on the school or community playground. A light dusting with 10 per cent. DDT powder at the rate of one ounce to 1,000 square feet of area covered with grass, weeds, or shrubs, is recommended by the U. S. Department of Agriculture as a simple and effective way of killing the ticks. One dusting will usually protect for the tick season.

The light dusting, says Dr. E. F. Knipling of the Bureau of Entomology and Plant Quarantine, will not be dangerous to children and pets. It will make safer the play areas where children should be protected as well as possible during the tick season.

In towns and in rural areas such a dusting, or spraying with a DDT spray, along the edges of paths and roadways, also reduces the tick hazard. Bureau studies of the habits of the ticks show that the pests tend to crawl toward paths and roadways, probably attracted by the scent of passing animals, including human beings. A DDT treatment for a few feet on each side of a path or road will kill the ticks that have concentrated there and the long time effect of DDT treatment is waiting for ticks that crawl into the treated zone later.

Rocky Mountain spotted fever is a disease that rightly causes concern to mothers. Many systematically follow the advice of the entomologists to look over the children carefully before bedtime to make sure of removing ticks picked up during the day. A tick does not ordinarily transmit the disease until it has been attached for several hours, but overnight attachment allows ample time if the tick is carrying the disease. The entomologists caution persons handling ticks, because they may get the disease in this manner. Just pick the ticks off with tweezers, and avoid crushing them on the skin.

R. H. O.

THE FRANKLIN INSTITUTE.

STATED MONTHLY MEETING, WEDNESDAY, OCTOBER 15, 1947.

The stated monthly meeting of The Franklin Institute was held on Wednesday, October 15th, at 8:15 P.M. The meeting was called to order by Mr. Richard T. Nalle, President. There were approximately 250 persons in attendance.

The minutes of the May meeting, which were printed in the June issue of the JOURNAL, were not read but were approved as printed.

The Secretary then gave his report on membership for the summer months up to and including September, which is as follows:

Honorary	0
Sustaining	1
Active	151
Associate	81
Student	47
Total membership as of September 30th	5426

The Secretary then announced that the Board of Managers of The Franklin Institute at its meeting on September 17th, 1947, unanimously resolved that General George C. Marshall be nominated for Honorary Membership in the Institute for action by the Membership at its next meeting.

> "In recognition of his outstanding ability as a military leader and statesman: of his valuable guidance as a member of the policy committee of the Office of Scientific Research and Development for Atomic Studies by American and British scientists: of his vision and understanding that many of the principles of foreign policy advocated by Benjamin Franklin are applicable today."

The Secretary then stated that the By-Laws provide that election should be made by 4/5 of the votes of active members present at any stated meeting and therefore invited all active voting members of the Institute present in favor of the election to signify by saying "Aye". The vote was unanimous and General George C. Marshall was declared elected to honorary membership in The Franklin Institute.

The President then introduced the speaker of the evening, Dr. L. O. Grondahl. Dr. Grondahl is the director of Research and Engineering at the Union Switch and Signal Company in Swissvale, Pennsylvania, and on two occasions he was a recipient of medals awarded by The Franklin Institute.

Dr. Grondahl spoke on Guided Missiles in World War II including the story of the research and development of the Azon which is controllable in azimuth only. It was the only guided missile used in combat in World War II. The Razon, controllable in both range and azimuth, was also described. Dr. Grondahl showed motion pictures depicting their construction and use both experimentally and in war theaters.

After Dr. Grondahl's talk, the Active Members of The Franklin Institute were requested to remain to vote on the proposed changes in the By-Laws as printed in the September issue of the JOURNAL. The proposed changes were voted upon and unanimously approved.

HENRY B. ALLEN, *Secretary.*

LIBRARY NOTES.

The Committee on Library desires to add to the collections any technical works that members would wish to contribute. Contributions will be gratefully acknowledged and placed in the library. Duplicates received will be transferred to other libraries as gifts of the donor.

Photostat Service. Photostat prints of any material in the collections can be supplied on request. Orders received in the morning are filled the same day. The average cost for a print 9 × 14 inches is thirty-five cents.

The Library and reading room are open on Mondays, Tuesdays, Fridays and Saturdays from 9 A.M. until 5 P.M., Wednesdays and Thursdays from 2 P.M. until 10 P.M.

RECENT ADDITIONS.

ARCHITECTURE AND BUILDING.

AMERICAN INSTITUTE OF STEEL CONSTRUCTION. Steel Construction, Fifth Edition. 1947.
BROWN, G., C. HOYER, AND R. BIERWIRTH. Theory and Application of Radio Frequency Heating. 1947.

BIOGRAPHIES.

MORTON, ELEANOR. Josiah White, Prince of Pioneers. 1946.

BOTANY.

STILES, WALTER. Trace Elements in Plants and Animals. 1946.

CHEMISTRY AND CHEMICAL TECHNOLOGY.

CHEVALIER, AUGUSTE, AND JEAN LEBRAS. Le Caoutchouc. 1945.
FARADAY, JOSEPH E. Encyclopedia of Hydrocarbon Compounds C_6 and C_7. 1947.
HARRY, RALPH G. Modern Cosmeticology. Volume 1. 1946.
SWANSON, CHARLES OSCAR. Physical Properties of Dough. 1946.
YOST, D. M., H. RUSSELL, AND C. GARNER. The Rare-Earth Elements and Their Compounds. 1947.

DICTIONARIES.

REGEN, B. R., AND R. R. REGEN. German-English Dictionary for Electronics Engineers. 1946.

ELECTRICITY AND ELECTRICAL ENGINEERING.

LOEB, LEONHARD BENEDICT. Fundamentals of Electricity and Magnetism. Second Edition. 1938.
RIDENOUR, LOUIS N., ed. Radar System Engineering. 1947.
SANDERLIN, WALTERS. The Great National Project. 1946.
WALKER, RONALD CLAUDE. Electronic Equipment and Accessories. 1946.

GEOLOGY.

COTTON, CHARLES ANDREW. Geomorphology. n.d.
WAHLSTROM, ERNEST E. Igneous Minerals and Rock. 1947.

MECHANICAL ENGINEERING.

MILLER, JOHN A. Men and Volts at War. 1947.
NOCK, O. S. The Locomotives of Sir Nigel Gresley. 1946.
TURKISH, MICHAEL C. Valve Gear Design. 1946.

METALLURGY.

HOLLOMON, J. H., AND L. D. JAFFE. Ferrous Metallurgical Design. 1947.

MINERALOGY.

DEMILLE, JOHN B. Strategic Minerals. 1947.

MINING ENGINEERING.

ROMEUF, JEAN. Le Charbon. 1946.

PETROLEUM.

FANNING, LEONARD M. American Oil Operations Abroad. 1947.

PHARMACY AND HYGIENE.

BERNHEIM, FREDERICK. The Interaction of Drugs and Cell Catalysts. 1946.
UMBREIT, WAYNE W., AND OTHERS. Manometric Techniques. 1945.
WADSWORTH, AUGUSTUS B. Standard Methods of the Division of Laboratories and Research of New York Department of Health. 1947.

PHYSICS.

HOFFMAN, BANESH. The Strange Story of the Quantum. 1947.

RAILROADS.

HARLOW, ALVIN FAY. The Road of the Century. 1947.

SCIENCE.

SIMON, LESLIE E. German Research in World War II. 1947.

TEXTILES.

JACKSON, LLOYD H. Yarn and Cloth. Calculations. 1947.
TEPLITZ, IRVING. Principles of Textile Converting. 1947.

NOTES FROM THE BIOCHEMICAL RESEARCH FOUNDATION.

Monochromatic Light Absorption by Chicken Erythrocytes. A Correction.—J. O. ELY AND M. H. ROSS. The authors reported in a previous paper (1) that the maximum absorption of monochromatic light, obtained from a quartz-mercury-vapor lamp, by the nuclei of chicken erythrocytes was at 2808 Å. Re-investigation has shown that that report was erroneous and that, of the various spectral bands of the quartz-mercury-vapor light, the greatest absorption by chicken erythrocytes was found to be at 2654 Å. Table I shows the extinction coefficients of several samples of chicken erythrocytes for the wave lengths 2483 Å, 2535 Å, 2654 Å, and 2808 Å.

TABLE I.

Monochromatic Light Absorption by the Nuclei of Chicken Erythrocytes.

Sample No.	Extinction Coefficients			
	2483 Å	2535 Å	2654 Å	2808 Å
1	0.360	0.405	0.463	0.262
2	0.439	0.517	0.588	0.318
3	0.389	0.560	0.597	0.385
4	0.327	0.448	0.485	—
5	0.424	0.543	0.565	0.410
6	0.425	0.530	0.605	0.461
Average	0.394	0.501	0.551	0.367

It may be seen in Table I that the maximum absorption was at 2654 Å rather than at 2808 Å as previously reported.

REFERENCE.

(1) ELY, J. O., AND ROSS, M. H., *J. Franklin Inst.*, **242**:85 (1946).

BOOK REVIEWS.

BIBLIOGRAPHY OF THE PLATINUM METALS, 1918–1930, by James Lewis Howe and Staff of Baker & Co., Inc. 138 pages, 19 × 29 cms. Newark, N. J., Baker & Co., Inc., 1947. Price $5.00.

This bibliography of the platinum metals supplements the standard work on the subject covering the years 1748–1917. The previous work was compiled by Mr. Howe and issued as Bulletin 694 of the U. S. Geological Survey in 1919, while the present publication was prepared with the cooperation of the staff of Baker & Co., Inc. The new compilation follows the same basic arrangement as the earlier volume—the references are arranged alphabetically according to author for each year.

Despite the inclusion of over four thousand references this is not a complete bibliography, for the compilers have purposely omitted certain types of material. These are listed in the preface in detail, and include principally articles of ephemeral interest, those dealing with prices, those describing minor discoveries of deposits, and articles on uses in the jewelry field. Important patents have been included although no attempt has been made to list every patent mentioning the platinum metals.

Each entry gives the author, title, citation of original publication and citation of an abstract where possible, preference being given to *Chemical Abstracts* and second choice to *Chemische Zentralblatt.* A subject index is included.

There are over 100 entries prior to 1918 to serve as an addendum to the earlier volume. One notes with interest that it is expected a similar volume for 1931–1940 will appear next year, with decennial compilations contemplated thereafter. This promise of future volumes enhances the value of the present work and makes it a must for those working in the field of the platinum metals.

G. E. PETTENGILL.

EXAMINATION OF INDUSTRIAL MEASUREMENTS, by John W. Dudley, Jr. 113 pages, tables, 14 × 21 cms. New York, McGraw-Hill Book Company, 1946. Price $2.00.

The usefulness of the Statistical Method in industrial work is no longer doubted for it has proved itself many times in the more recent past. The practical application, however, is not so clear, especially to engineers who often might assume that if a certain mathematical model was said to represent a law of error then any set of data, however small, which appeared to fit the model would provide adequate assurance as to future sets of similar data. This only leads to confusion and delay in accepting the Statistical Method.

This little book is designed to introduce to the engineer adaptable statistical techniques that will be valuable in themselves and provide a good background for understanding. At the outset variations in the types of data are discussed pointing out their sources and characteristics, the importance of order, the reasons for and methods of presenting data. This section brings out the reasoning of the statistician which is invaluable as a practical asset. The probability curve, quality control chart and the median normal curve are next taken up in logical order. Examinations of data directed toward the kinds and frequency of errors are done in the latter part of the book where such subjects as unknown order of differences between sets of measurements, and correlation and curve fitting are given adequate treatment.

The book is a practical means for engineers to become acquainted with statistical procedures to collect data and actually use it or present it in such a manner that it can be subjected to a more elaborate analysis when necessary.

R. H. OPPERMANN.

MATRIX AND TENSOR CALCULUS, by Aristotle D. Machal. 132 pages, drawings, 15 × 24 cms. New York, John Wiley & Sons, Inc., 1947. Price $3.00.

The two parts of this book indicated by the title are separate and distinct. The matrix calculus is a purely analytic and algebraic subject, whereas the tensor calculus is geometric, being connected with transformations of coordinates and other geometric concepts.

There are eight chapters in the 41 pages of Part I. Beginning with algebraic preliminaries the progression is through differential and integral calculus of matrices, and matrix methods in problems of small oscillations leading up to a group of phenomena known under the caption of "flutter" by aeronautical engineers. The vibrations taking place in flutter phenomena can often lead to loss of control or even to structural failure in such aircraft parts as wing, aileron, and tail. The treatment of the subject in this book gives the matric form for the equations of motion and brief mention about the approximate solutions with the aid of matrix iteration methods. The last chapter of this part is introductory and suggestive on matrix methods in elastic deformation theory.

Part II contains 68 pages of text divided into ten chapters on tensor calculus and its applications pointing out that a detailed study of the classical differential calculus along a certain direction demands the introduction of the tensor calculus. The treatment is concerned with Euclidean tensor calculus although a small part is devoted to curved tensor calculus in connection with the fundamentals of classical mechanics and fluid mechanics. Of particular interest in this part is the application of the tensor calculus to the deformation media, elastic or otherwise.

The work is a well connected logical progression of interest to engineers generally who have need of this type of mathematics and especially to aeronautical engineers.

R. H. OPPERMANN.

MATERIALS OF INDUSTRY, Their Distribution and Production, by the late Samuel F. Mersereau. Fourth edition, Revised by Calvin G. Reen and Kenneth L. Holderman. 623 pages, illustrations, 15 × 21 cms. New York and London, McGraw-Hill Book Company, Inc., 1947.

This standard text book for high schools on the various industrial materials now appears in a fourth revised edition. Various changes have been made to bring it up to date and considerable new material has been added on modern products. The teaching aids of glossaries, questions and bibliography have been augmented by the listing of suggested visual aids—motion pictures and film strips.

The revisers have made a special effort to retain the pattern developed by Mr. Mersereau in the original text. All in all the volume merits the consideration of any teacher giving a course in industrial materials.

G. E. P.

GUIDE TO THE LITERATURE OF MATHEMATICS AND PHYSICS, Including Related Works on Engineering Sciences, by Nathan Green Parke III. 205 pages, 16 × 23 cms. New York and London, McGraw-Hill Book Co., Inc., 1947. Price $5.00.

Although for some time there have been three helpful guides to the literature of chemistry, there has been nothing comparable for the literature of mathematics and physics. Mr. Parke has made a successful attempt at remedying this deficiency. His approach considers two main aspects of the problem with a resultant division of the book into two parts, general considerations on the use of the literature and a listing of the principal titles.

In the first section he offers some stimulating thoughts on the principles of reading and study and follows these with comments on self-directed education. The chapter on "Literature Search" suggests some basic principles, treats of the different kinds of reference works and discusses catalogues and indexes. In this latter part Mr. Parke describes briefly library cataloging and shows the relationship between classification and subject headings. A final chapter mentions problems dealing with periodicals and their use.

The major part of the volume is devoted to a bibliography of the literature of mathematics and physics. This is extended to include selected titles in the allied engineering fields such as aeronautics and radio. The entries are arranged alphabetically by subject and then by author. Each subject is introduced by a brief paragraph delineating the subject and often singling out particular titles for a brief characterization. The range of the bibliography is broad, including both foreign language and nineteenth century works. *Reviews of Modern Physics* has been indexed for the first seventeen volumes. To facilitate access to the entries an author index has been provided as well as a classified arrangement of the subject headings.

Mr. Parke indicates that the list has been developed under working conditions and, when supplemented by the periodical literature, should be adequate for scholarly purposes. Unfortunately any such work as this is out of date before it can be published and consequently must always be used with that reservation. Nonetheless individuals and libraries may well be grateful for this filling of a gap and can well use it as a basic starting point for some years to come.

G. E. PETTENGILL.

BOISSIÈRE'S PYTHAGOREAN GAME, by John F. C. Richards. Pages 177–217. 17 × 25 cms. New York, Scripta Mathematica, 1946. Price $.50 paper bound.

Mr. Richards offers a translation from the original Latin of Boissière's description of the "very noble and ancient Pythagorean game called Rythmomachia." The original book was published in Paris in 1556. The game employs a board divided into squares, and pieces in the shape of circles, triangles, squares and pyramids. First divided into odds and evens, the pieces are then marked on their surface with numbers which bear a definite mathematical relationship to one another. Boissière describes the method of arriving at these numbers and then gives the rules of play, which likewise involve mathematical relationships. The terms used to describe the moves are warlike, being encounter, rally, ambush and siege.

The translation of this interesting mathematical game originally appeared in *Scripta Mathematica* for September 1946 and has been reprinted to make it more widely available.

G. E. PETTENGILL.

PUBLICATIONS RECEIVED.

Chemical Process Principles, Part III: Kinetics and Catalysis, by Olaf A. Hougen and Kenneth M. Watson. 1107 pages, tables and drawings, 14 × 22 cms. New York: John Wiley & Sons, Inc.; London: Chapman and Hall, Limited, 1947. Price $4.50.

Wind Tunnel Testing, by Alan Pope. 316 pages, drawings and illustrations, 15 × 22 cms. New York: John Wiley & Sons, Inc.; London: Chapman & Hall, Limited, 1947. Price $5.00.

Power System Stability, by Selden B. Crary. Volume II, Transient Stability. 329 pages, drawings and illustrations, 15 × 22 cms. New York: John Wiley & Sons, Inc.; London: Chapman & Hall, Ltd., 1947. Price $6.00.

Fundamentals of Electricity and Magnetism, by Leonard B. Loeb. Third Edition. 669 pages, drawings, 15 × 24 cms. New York: John Wiley & Sons, Inc.; London: Chapman & Hall, Ltd., 1947. Price $6.00.

Vat Dyestuffs and Vat Dyeing, by M. R. Fox. 323 pages, drawings and illustrations, 14 × 22 cms. New York: John Wiley & Sons, Inc., 1947. Price $5.50.

Elementary Nuclear Theory, by H. A. Bethe. 147 pages, drawings, 14 × 22 cms. New York: John Wiley & Sons, Inc., 1947. Price $2.50.

Sunspots in Action, by Harlan True Stetson. 252 pages, drawings and illustrations. 15 × 22 cms. New York: The Ronald Press Company, 1947. Price $3.50.

Electric Motor Maintenance, by W. W. McCollough. 126 pages, illustrations, 15 × 22 cms. New York: John Wiley & Sons, Inc., 1947. Price $2.00.

The Chemistry of Organic Cyanogen Compounds, by Vartkes Migrdichian. American Chemical Society Monograph Series. 460 pages, tables, 16 × 23 cms. New York: Reinhold Publishing Corporation, 1947. Price $12.00.

The Naming of the Telescope, by Edward Rosen. 110 pages, illustrations, 13 × 19 cms. New York: Henry Schuman, 1947. Price $2.50.

The Selected Writings of Benjamin Rush, edited by Dagobert D. Runes. 433 pages, 14 × 21 cms. New York: Philosophical Library, 1947. Price $5.00.

Chemical Process Principles, Part II, Thermodynamics, by Olaf A. Hougen and Kenneth M. Watson. 805 pages. New York: John Wiley & Son, Inc., 1947. Price $5.00.

Industrial Management, by William R. Spriegel. Fourth Edition. 656 pages, illustrations, 15 × 24 cms. New York: John Wiley & Sons, Inc., 1947. Price $5.00.